0031-6997/85/3701-0081$02.00/0
PHARMACOLOGICAL REVIEWS

Vol. 37, No. 1
Printed in U.S.A.

The Biophysical Pharmacology of Calcium-Dependent Acetylcholine Secretion

EUGENE M. SILINSKY

Department of Pharmacology, Northwestern University Medical School, Chicago, Illinois

I. Introduction

Something there is that doesn't love a wall,
That sends the frozen-ground-swell under it,
And spills the upper boulders in the sun;
And makes gaps even two can pass abreast.
The Mending Wall; Robert Frost (1914)

IN A COLD London laboratory, in the year 1808, Humphrey Davy passed electric currents through a series of molten metallic substances and in this fashion isolated the alkaline earth metal (Me) ions Ca, Sr, Ba, and Mg (7). Two of these four divalent cations, Ca and Mg, were subsequently found to be essential cofactors for most biological processes (225, 226). In the years that followed Davy's discovery, physical chemists provided a wealth of additional information on the specific properties of the Me group; this knowledge helped to fracture many walls of ignorance about the ionic control of biological behavior. For example, differences in the effects of the four related Me species at excitable cell membranes have guided biophysicists in their studies of the forces by which Ca and Mg regulate ion permeation though membrane barriers (71, 105, 111). Such comparative biophys-

ical studies are analogous to investigations of structure-activity relationships in receptor pharmacology, whereby differences in biological activity of a series of structurally related drug congeners are used to study the forces that regulate the microscopic domain of the receptor (252, 253).

The secretion of neurotransmitter substances in response to membrane depolarization is particularly sensitive to changes in the concentration of Ca in the extracellular fluid (122, 74, 114, 240). Consequently, the involvement of the Me series in neurotransmitter secretion has been the subject of intensive study by investigators in both biophysics and in membrane pharmacology. Despite similarities in the experimental techniques and in the mathematical formulations used in these two fields of inquiry (51, 178, 179, 236–238, 240, 241, 248, 249, 253, 261), there exists an intangible impedance to the exchange of ideas across the experimental disciplines. It is my intent to describe the various theories of Ca-dependent transmitter release in the hope of favoring communication among secretionists from different scientific backgrounds.

This review is principally concerned with the release of the neurotransmitter, acetylcholine (ACh) as detected by electrophysiological recordings at the skeletal neuromuscular junction. As an overture to the subsequent discussion of the secretory process, the electrophysiologal methods and the inorganic chemistry of the Me series will be outlined in section II. Then, after describing the various models for Me-dependent ACh release (section III), a discussion of the intracellular physical forces that initiate secretion (section IV) and the depressive and facilitatory processes that ensue after secretion (section V) will be presented. The review concludes with a summary (section VI) and the inevitable speculative incursion, for which I beg the reader's indulgence. Two appendices have also been included for the convenience of the newcomer to quantitative presynaptic electrophysiology. Appendix A provides complete derivations of the salient equations of biophysical pharmacology. Appendix B provides a description of the effects of cations other than the alkaline earth series on ACh release. For the reader concerned predominantly with recent developments in the field, a perusal of sections III *A*, VI, and tables 2 to 4 should prove sufficient.

II. Experimental Observations

A. Methods in Synaptic Electrophysiology

Prior to electrophysiological recordings of synaptic events, evoked ACh release was measured by stimulating cholinergic nerve trunks at high frequency for several minutes and then bioassaying the effluent by using other tissues sensitized to ACh (61). The advent of the intracellular recording electrode allowed subtle, millisecond to millisecond variations in ACh secretion to be detected (87, 122) and helped to clarify some of the paradoxical results obtained by the earlier methods (86). The electrophysiological approach to the study of ACh release at the skeletal neuromuscular junction is illustrated in figure 1. In figure 1A, a glass pipette microelectrode (1), filled with concentrated KCl, is positioned over a muscle fiber at the region of innervation. The electrode is then introduced into the interior of the muscle fiber (with varying degrees of dexterity depending upon the investigator) and a resting potential (V) generally of 70 to 90 mV, negative inside, is recorded. Once impaled, the innervated region of the muscle reveals esthetically pleasing deflections, some of which occur spontaneously and yet others appear when an electrical stimulus is applied to the motor nerve. The innervated region of muscle is termed the end-plate region (114, 122) and thus the spontaneous potentials are known as miniature end-plate potentials (MEPPs) (Figure 1A). The MEPPs are random events of fairly constant size and may be mimicked by the local application of small droplets of ACh to the muscle surface. When a sequence of electrical stimuli is delivered to the nerve, a series of evoked responses termed end-plate potentials (EPPs) appears at a fixed latency after the nerve impulse. As the concentration of Ca in the bathing fluid is lowered, the EPPs fluctuate, not in a smoothly graded fashion, but rather as integral multiples (1 to 5, figure 1A) of the MEPP. Experiments such as those shown in figure 1A led Katz and Castillo to suggest the *quantal theory* of synaptic transmission (67) as follows. The MEPP represents the fundamental quantum of secretion, and the nerve impulse serves to unify the individual quanta into a synchronous burst of secretion detectable as the EPP. Quantal events have been observed wherever electrophysiological recordings of spontaneous synaptic potentials are technically feasible (122, 167, 171).

The MEPP is not produced by an individual ACh molecule; rather it is generated by the concerted action of several thousand ACh molecules (114, 122, 205). How then is the constancy of the quantum maintained? Based upon evidence from morphological studies that revealed the presence of small 40 to 50-nm synaptic vesicles in the nerve terminal (figure 1B, v), Castillo and Katz (69) suggested that the vesicle represents the morphological counterpart of the ACh quantum (the *vesicle hypothesis*). Vesicles at cholinergic nerve terminals have been found to contain high concentrations of ACh [approaching molar (272)] and to be docked near the nerve terminal membrane at *active zones* of release [az, figure 1B (41, 131)]. By the vesicle hypothesis, the MEPP is produced by the all-or-none discharge of the ACh contents of one synaptic vesicle. An EPP consisting of a mean of five quanta ($M = 5$; ideally an EPP with amplitude five times the mean MEPP amplitude e.g. Fig 1A) would be produced when nerve stimulation provokes the nearly synchronous release of the entire ACh complement of five synaptic vesicles (see figure 1B, M = 5). Note that the EPP occurs only in response to depolarization (figure

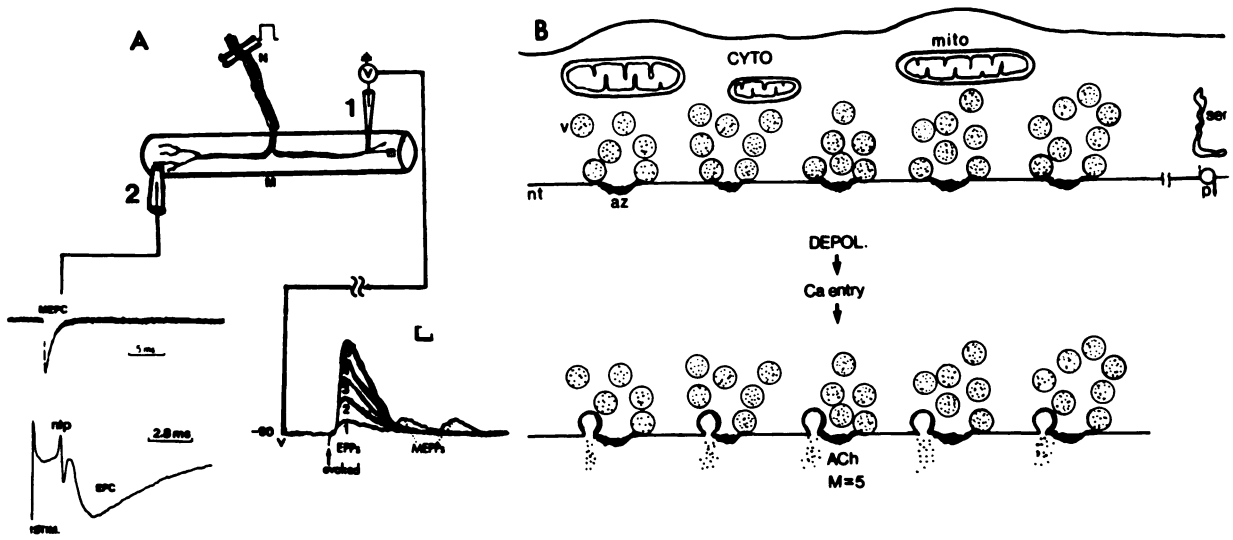

FIG. 1. Electrophysiological and structural observations on acetylcholine (ACh) release. A, the electrophysiological methodology. *N*-nerve, *M*-muscle. The innervated region of a frog skeletal muscle fiber is impaled intracellularly with a microelectrode in A 1, producing a recorded resting potential (V) of 90 mv (negative inside). A series of stimuli delivered to the nerve supply (arrow shows the stimulus artifact, which marks the moment of stimulation) produces a series of evoked responses (end-plate potentials, EPPs) which fluctuate as integral multiples (1 to 5) of the spontaneous potentials (MEPPs). The mean number of ACh packets released synchronously (*M*) is the ratio of the EPP/MEPP under the conditions shown in A. Calibration bars: 1 mV, 1 msec. In A 2, focal extracellular microelectrode recordings are shown. Note the spontaneous miniature end-plate current (MEPC). Stimulation under these focal recording conditions (STIM) produces a nerve terminal action potentials (ntp) and an end-plate current (EPC). This record is the averaged response to 128 stimuli (Biomac computer of average transients). The average amplitude of the EPC was approximately 0.2 mv. Several theories as to the significance of the two phases of the ntp have been proposed; for precise details see refs. 160, 37. The electrophysiological records in A were made in low Ca solutions containing Mg. All experimental records shown in figures 1 to 4 were obtained from end-plates in frog cutaneous pectoris nerve-muscle preparations. B, the morphological correlates of the intracellular microelectrode recordings presented in A 1. Synaptic vesicles (v) containing ACh are docked at active zones (az's), which occur at regular intervals (approximately 1 μ) along the nerve terminal (nt). (For further details of the structure of the az, see figure 7, A). Depolarization (DEPOL.) opens Ca channels allowing Ca entry into the nerve ending cytoplasm (CYTO). Once in the cytoplasm, Ca promotes the exocytotic discharge of ACh from the vesicle. The release of the ACh contents of five synaptic vesicles (B) is equivalent to an EPP of five times the MEPP amplitude (A 1). Structures likely to clear Ca and other cations from the nerve terminal cytoplasm are sketched in B; these include plasma membrane pumps (p), smooth endoplasmic reticulum (ser), and mitochondria (mito).

1B, DEPOL.), which is normally provided by the action potential and requires Ca entry to unify the vesicles at spatially distributed active zones into a coincident secretory event. The vesicle hypothesis is such an attractive explanation for the electrophysiological quantum that it is likely that vesicles would have been postulated, even if they had not been observed morphologically (80). Although some opposition to this view has been voiced (257a), powerful supportive evidence for the vesicle hypothesis has recently been provided at cholinergic nerve endings (109, 206).

After release, ACh diffuses rapidly across the narrow synaptic cleft (25 nm) and interacts with receptors on the postsynaptic membrane. These postsynaptic processes have been reviewed in detail recently (15, 98, 254, 205). Briefly, ACh receptors are found at the rims of flexible funnel-like structures that span the postsynaptic membrane. When ACh is bound to the receptor, the conformation of the attached funnel is changed from a closed, pinched state to an open state which allows essentially unrestricted cation permeation. The net inward movement of sodium ions supplied by the ACh-operated ion channels and the outward restorative current through the neighboring postsynaptic membrane produces the MEPPs and EPPs at the skeletal neuromuscular junction.

Under normal conditions, the EPP is so large as to reach threshold for a muscle action potential; the propagating action potential then produces a twitch of the skeletal muscle. To prevent the dislodging of electrodes by muscle twitches, the synaptic electrophysiologist generally maintains the EPP at a subthreshold level either presynaptically by altering the extracellular divalent cation environment, or postsynaptically by the use of a nicotinic receptor blocker such as curare. Under these conditions, with certain qualifications, the EPP may be used as a linear, moment-to-moment assay for the release of ACh (see legend to figures 1 and 2 for more details).

Following the chemical reaction between ACh and the receptor, ACh is hydrolyzed by acetylcholinesterase (15, 98) and the choline liberated by this process is then transported into the nerve ending by a choline carrier (33). Choline acetyltransferase, associated with the synaptic vesicle (33), reacetylates choline into ACh; this newly synthesized transmitter appears to be preferentially released (33, 114) (for further details see section V

A and appendix B 1 a). Synaptic vesicles have been shown to recycle locally after secretion (41, 114).

Electrophysiological events at nicotinic cholinergic synapses where the receiving cell is a neuron are similar to those just described for the skeletal neuromuscular junction (15, 28, 81, 170, 171, 278). Thus, there are spontaneous potentials (miniature excitatory postsynaptic potentials, MEPSPs) and evoked potentials (excitatory postsynaptic potentials, EPSPs) that produce action potentials if the threshold for excitation of the receiving neuron is reached. In this review, the impulsive physiologically functional form of ACh release reflected as the EPP or the EPSP will be referred to as *synchronous release* or the mean number of ACh quanta (*M*) released synchronously (237, 178, 248). *M* has also been referred to as phasic release (183, 170) and as mean quantal content (an unfortunate term since it does not refer to the number of ACh molecules in a quantum but rather to the number of quanta contributing to an evoked response).

B. Specific Effects of the Alkaline Earth Metals (Me's): Ca, Sr, Ba, and Mg as Activators (Agonists) and Antagonists of Acetylcholine Release

The synchronous release of ACh in response to a nerve impulse (*M*) is steeply dependent on the Ca concentration in the extracellular fluid. Figure 2A (circles) illustrates a typical log [Ca]-*M* curve to saturation at the frog neuromuscular junction; the maximal response in this fiber was approximately 1000 quanta, achieved at Ca concentrations between 5.0 and 7.0 mM; in normal (1.8 mM) Ca, *M* was approximately 400 quanta. Experiments on giant non-cholinergic nerve endings in the squid, where Ca currents may be measured directly (see e.g. 147, 148, 122, 8), led Katz and his colleagues to propose the *Ca hypothesis* (122, 124) as an explanation for the dependency of evoked transmitter release on extracellular Ca. Specifically, it was suggested that depolarization of the nerve terminal opens Ca channels at localized regions in the nerve ending; Ca then enters the cytoplasm down its electrochemical gradient through these voltage-sensitive channels (for reviews see refs. 122, 114, 147). Once inside the nerve ending, Ca reduces an energy barrier between nerve terminal and vesicular membranes at the active zone, allowing the membranes to fuse. The fused membranes then perforate and the synaptic vesicles discharge their transmitter quanta by exocytosis (e.g., figure 1B). For evoked ACh release to occur, Ca is virtually the only ion required in the bathing fluid as focal depolarizing pulses applied to the motor nerve terminal in isotonic $CaCl_2$ (with a trace of KCl) produce synchronous ACh release (127). The timing of Ca action is critical for evoked ACh release, however, as the external surface of the nerve ending must be exposed to Ca prior to depolarization to support *M* (125). Spontaneous ACh release is relatively insensitive to extracellular Ca (see section III B 2).

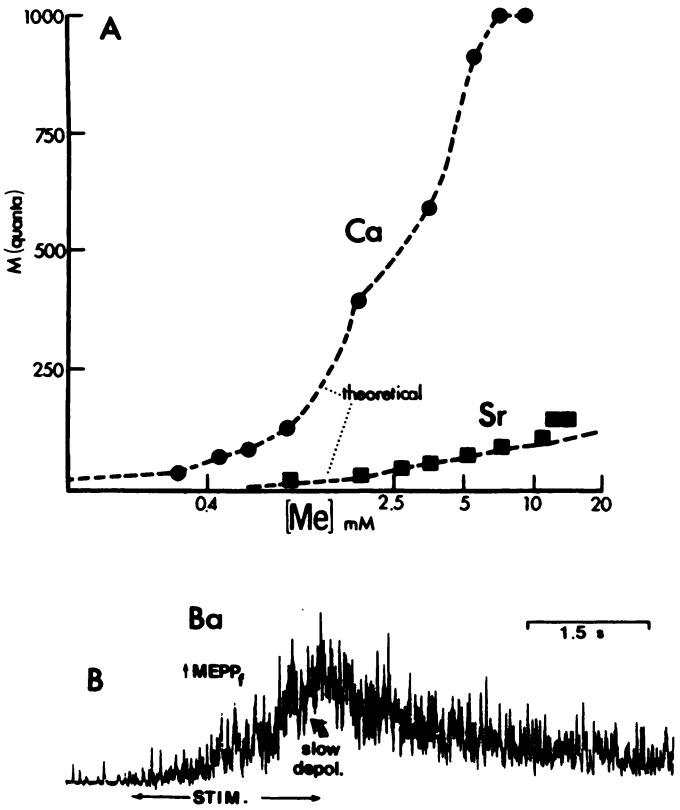

FIG. 2. ACh release in different alkaline earth metal (Me) environments. A shows curves of log [Ca]-*M* and [Sr]-*M* made from the continuous impalement of a single muscle fiber (reprinted with permission from ref. 240). These high levels of *M* were measured in a curarized preparation by dividing the EPP in curare by the MEPP amplitude in the absence of curare and then multiplying by a correction factor related to the affinity of curare for the postsynaptic ACh receptor (see eqn 2, ref. 240). The theoretical curve (dashed line) will be discussed in section III A 3. B shows that nerve stimulation in Ba solutions, while not producing EPPs, generates a large increase in MEPP frequency (MEPPf). The MEPPf in B was approximately 700/sec at the end of stimulation as determined from the amplitude of the underlying slow depolarization (slow depol.) associated with this asynchronous release process. The slow depolarization (5 mV) when divided by the product of the MEPP time constant and MEPP amplitude provides an estimate of MEPPf (see eqns 2 and 3, ref. 237). In B, the stimulation frequency was 30 Hz; solution contained 0.7 mM Ba and 6 mM Mg. When EPPs or slow depolarizations are a substantial fraction of the membrane potential, corrections for non-linear summation of the individual quantal events must be made (refs. 165, 172, 187). For further details, see text.

The low levels of ACh release illustrated in figure 1A (1) occurs in reduced extracellular Ca solutions (e.g. 0.1 mM) or in normal Ca (1.8 mM) Ringer when Mg is added at an order of magnitude higher concentration than Ca. The equivalence of these different solutions is a consequence of the role of Mg as a *competitive inhibitor* of evoked ACh release (120). Specifically, by occluding an external membrane site associated with Ca channels, Mg competitively inhibits the entry of Ca into the nerve terminal (133, 167). A variety of other cations share this effect with Mg (see appendix B).

One other Me species, Sr, is capable of supporting the synchronous release of ACh from discrete releasing sites

along the nerve ending, but is substantially less efficient than Ca in the process (181, 73, 175, 240). This is illustrated in figure 2B, where the maximum *M* in Sr is only 150 quanta as compared to maximal *M* of approximately 1000 produced by Ca in the same fiber. As Ca and Sr move through the same channel to support release (8, 248), the reduced maximal response in Sr, which pharmacologists term a reduced *efficacy* (252), makes Sr a *partial agonist* when compared to the naturally occurring *full agonist*, Ca.

In addition to synchronous release, associated with the impulsive delivery of Ca or Sr to the cytoplasm, increases in quantal ACh secretion may be observed as an acceleration of the ongoing MEPP frequency (MEPPf) when a steady Ca translocation occurs from distant loci to strategic intracellular regions associated with the secretory process (134, 250, 208, 213, 178). Thus, a prolonged depolarizing pulse applied to the nerve terminal (68, 54, 55) or an increase in the extracellular potassium concentration (56) will cause a steady Ca movement through Ca channels and increase MEPPf. In the absence of extracellular Ca, increases in MEPPf may be produced by agents which cause Ca to leak from cellular storage sites such as smooth endoplasmic reticulum and mitochondria (e.g., caffeine, uncouplers of oxidative phosphorylation, etc., see refs. 243, 101).

With respect to the last of Sir Humphrey Davy's Me species, namely Ba, the earlier literature on the effects of Ba on ACh secretion proved enigmatic to the electrophysiologist. Specifically, when Ba is substituted for Ca in equimolar amounts at cholinergic nerve endings, neurally evoked ACh release is at least as great in Ba solutions as in Ca solutions *when ACh release is assayed by biochemical or bioassay techniques* (76). All of the electrophysiological studies have demonstrated, however, that Ba cannot support the multiquantal EPP or EPSP in response to a single nerve impulse (181, 235, 170). What then is the electrophysiological correlate of the ACh release detected in the effluent of stimulated nerves? Figure 2B shows that, although no EPPs are produced, repetitive nerve stimulation (STIM.) produces a slowly developing avalanche of MEPPs. The stimulation-induced MEPPs occur at such a high frequency that they produce an underlying slow depolarization (figure 2B, slow depol.) of the postsynaptic membrane. This slow depolarization is produced by the continuous entry of Ba into the cell in response to repetitive high frequency nerve stimulation and is linearly related to the frequency of MEPPs (see legend, figure 2). Although in the low Ba concentrations of figure 2B, the MEPPf at the peak of stimulation is approximately 700/sec, under other conditions (e.g. 3.6 mM Ba, 4 Hz stimulation) less than 10 stimuli are sufficient to elevate MEPPf from resting levels of 1/sec to 7000/sec in Ba solutions (see figure 2 in ref. 237). It is apparent, then, that increases in MEPPf represent the electrophysiological correlate of ACh release into the perfusion fluid of stimulated preparations bathed in Ba solutions (170, 235, 237). Despite the enormous absolute efficiency of Ba in supporting quantal release, however, the absence of temporal harmony between each nerve impulse and each electrophysiological event makes this ion an inappropriate teleological choice as the normal physiological mediator of evoked transmitter secretion. In fact, electrophysiological records such as shown in figure 2B are similar to those produced when cholinergic nerves are exposed to black widow spider venom (150). The record in figure 2B also shows that the elevated MEPPf in Ba decays only very slowly after the cessation of nerve stimulation (the EPP decay would appear as a sharp spike on the time scale of figure 2B). This long-lived effect of Ba is reminiscent of facilitatory processes that well outlast the stimulation period at cholinergic nerve endings (see section V B 3).

In this review, the term *asynchronous release* (235, 237, 238, 178) will be used for evoked increases in MEPPf (e.g. figure 2B). The terms tonic release and delayed release have also been used to describe this process of secretion (183, 170). Although asynchronous release appears most prominently in Ba solutions (248), Sr and Ca are also capable of supporting increases in MEPPf in response to nerve impulses. The *extracellular* Me potency sequence for evoked asynchronous release, Ba > Sr > Ca, however, is the opposite of the potency sequence in supporting *M*, Ca > Sr > Ba (248).

All of the Me effects are on the processes that couple depolarization to ACh release and not on the depolarization process itself. This may be demonstrated experimentally as shown in figure 1A (2). If a relatively low resistance microelectrode is placed extracellularly at a "hot spot" of nerve-muscle activity, miniature end-plate currents (MEPCs, which are extracellular reflections of MEPPs) may be recorded in the absence of nerve stimulation. When the nerve is stimulated (stim.), the action potential is initiated and propagates near to the nerve terminal (ntp). Subsequent to the ntp, Ca channels are opened, Ca enters the nerve ending, ACh is released and the released ACh produces the end-plate current (EPC, an extracellular manifestation of the EPP). Although high concentrations of Me species ($\gg$ 10 mM) may reduce the ntp, maximal effects of the various Me species on EPCs and *M* have been achieved in the majority of experiments without any concomitant change in the size or configuration of the computer-averaged ntp (240).

In summary, it appears that Ca, Sr, and Ba all support the quantal release of ACh in response to nerve impulses, albeit with different absolute efficiencies and temporal proclivities. In contrast, extracellular Mg is a competitive inhibitor of evoked ACh release. Some of the chemical properties of the Me species that might be responsible for these differences are outlined in the next section.

C. *Inorganic Chemistry of the Me Series*

Table 1 summarizes the important properties of the alkaline earth cations (the group IIa metals in the pe-

TABLE 1

*Inorganic chemistry of the alkaline earth metal (Me) cations**

Ion	Ionic radius (r in Å)	Ionic potential (charge/r)	Hydration properties		Coordination number
			Dehydration rate	Free energy (kcal/mole)	
Mg	0.78	2.6	0.0004	455.5	6
Ca	1.06	1.9	1	380.8	Variable(6–8)
Sr	1.27	1.6	2	345.9	—
Ba	1.43	1.4	5.6	315.1	8

* The atomic radii are those determined by Goldschmidt from oxide crystals (see ref. 222, table 1) and appear to be the most pertinent values to biological membranes. As the charge of all the Me species is +2, the ionic potential is 2 divided by the radius of each species. The dehydration rate refers to the rate of substitution of inner sphere water molecules relative to the value for Ca, which = $3 \cdot 10^8$ sec^{-1} (72). Free energies of hydration were determined from electrode potential measurements (222). The coordination number (94, 273) refers to the number of coordinate bonds the ion can form and is directly related to the size of the ion, i.e., a larger ion can coordinate with more nearest neighbor molecules (for further discussion, see text and sections III, VI, and appendix B).

riodic table). It will be observed that the radius of the naked, unhydrated ion increases with atomic weight in the order Mg < Ca < Sr < Ba. As these ions are all divalent, the ratio of charge to radius, termed the ionic potential, follows the reverse sequence: Mg > Ca > Sr > Ba. The ionic potential is probably the most useful characteristic on which to focus as it determines the strength of the ionic bonds that the Me species may form. The table indicates that Ba forms relatively weak bonds while those of Mg are quite strong. Mg binds so tightly in certain instances that it actually immobilizes a measurable fraction of the water molecules in its inner sphere of influence; this high affinity of Mg for water is reflected in the low rate constant of dehydration (column 4). Indeed, if dehydration is required for an Me species to activate a particular biological process, then Mg might be expected to have meager agonist effects on that process. Other properties listed in table 1 will be described as this review proceeds. For the present purposes, the data in table 1, column 3, and the electrophysiological experiments discussed in the preceding section suggest that if the ionic potential is less than 2, then the ion is capable of supporting evoked ACh release but if the ionic potential is greater than 2, it acts as an inhibitor of evoked release. In this regard, the divalent cation Co has an ionic potential of 2.7 and is a very potent inhibitor of Me-dependent ACh release (267, 58).

III. Quantitative Models for the Involvement of Alkaline Earth Cations in ACh Release

A. *Binding and Screening Models*

1. The General Scheme. The traditional approach to synchronous ACh release has been to apply the law of mass action to the interaction of extracellular alkaline earth cations with some hypothetical site, X, on or in the nerve terminal membrane as follows:

$$\mathrm{Me} + X \underset{}{\overset{K_{ME}}{\rightleftarrows}} \mathrm{Me}X \downarrow \xrightarrow[e_{ME}]{\text{Depolarization}} ?—?—?—?—?—?—?—? \rightarrow$$

Synchronous ACh Release (M)

In this scheme, the extracellular Me binds reversibly to X and forms an MeX complex. When the membrane is depolarized, the MeX may then proceed through a series of largely unknown reactions (?) to harmonize the individual quantal events into a synchronous burst of ACh release detectable electrophysiologically as the EPP (M). The ability of the MeX complex to support M, once the membrane is depolarized, is termed the efficacy (e_{ME}). Ca, the full agonist, has high efficacy and consequently even a low [CaX] would produce large M. Sr, the partial agonist, has low efficacy as is reflected by the much smaller maximal M observed in Sr solutions (figure 2A); a high [SrX] is thus required to produce even moderate M. Mg is a competitive inhibitor of M and has zero efficacy; MgX is unable to support M, however high its concentration is raised.

Applying the law of mass action to first reaction in the above sequence, under equilibrium conditions, produces eqn 1:

$$y_{ME} = \frac{K_{ME}[\mathrm{Me}]}{1 + K_{ME}[\mathrm{Me}]} \qquad \text{eqn 1}$$

where y_{ME} is the fraction of total number of Me receptors occupied at [Me], and K_{ME} is the equilibrium *affinity* constant of Me for site X.

The law of mass action states that the rate of a chemical reaction is proportional to the 'active mass', i.e., concentration, of the reactants. Considering only the first reaction in the scheme, the binding of Me to X: the rate of formation of MeX = k_{+1}[Me][X] where k_{+1} is the association rate constant (in mM^{-1} s^{-1}) and the rate of dissociation of MeX = k_{-1} [MeX] where k_{-1} is the dissociation rate constant (in s^{-1}). At equilibrium, under conditions where there is no reaction subsequent to MeX (e.g. if the membrane is not depolarized or if Me = Mg), the rate of formation is equal to the rate of dissociation. Thus,

$$k_{+1}[\mathrm{Me}][X] = k_{-1}[\mathrm{Me}X] \qquad \text{eqn 1a}$$

Rearranging

$$\frac{k_{+1}}{k_{-1}} = \frac{[\mathrm{Me}X]}{[\mathrm{Me}][X]} = K_{ME} \qquad \text{eqn 1b}$$

The ratio of the forward to the backward rate constant is defined as the equilibrium affinity constant, K_{ME}; K_{ME} is the reciprocal of the equilibrium dissociation constant, K_d.

Generally, it is preferable to determine the fraction of total Me receptors occupied, y_{ME}, also termed the occupancy (253).

$$y_{ME} = [MeX]/X_T \qquad \text{eqn 1c}$$

where X_T is the total X concentration. Dividing both sides of eqn 1a by X_T: $k_{+1}[Me][X]/X_T = k_{-1}[MeX]/X_T$. Now as $[X]/X_T$ = fraction of free receptors = $1 - y_{ME}$, substituting y_{ME} and $1\text{-}y_{ME}$ into eqn 1a and rearranging: $k_{+1}[Me](1 - y_{ME}) = k_{-1}y_{ME}$, or

$$\frac{y_{ME}}{1 - y_{ME}} = [Me]K_{ME} \qquad \text{eqn 1d}$$

Finally, solving for y_{ME} by adding the numerator to the denominator on each side of the equation:

$$y_{ME} = \frac{K_{ME}[Me]}{1 + K_{ME}[Me]} \qquad \text{eqn 1}$$

Eqn 1 is one of the most widely used mathematical expressions in the physical and biological sciences. It represents a rectangular hyperbola and has been used to describe the adsorption of gases onto light bulb filaments [the *adsorption isotherm* of Langmuir (143)] and the kinetics of enzyme-substrate reactions [the Henri-Michaelis Menten equation (233)]. This equation first appeared, however, as an unnumbered expression in a paper by A. V. Hill (110) who was studying the relative importance of physical and chemical forces at the ACh receptor. There is no reason to doubt the validity of eqn 1 when the membrane is not depolarized, or when Me is a competitive inhibitor, i.e., when $e_{ME} = 0$ and no reaction takes place subsequent to binding. Accordingly, the most conclusive experimental results have been obtained by studying competitive inhibition at motor nerve terminals.

2. Me Species as Competitive Antagonists of Evoked ACh Release. A. METHOD FOR DETERMINING THE EQUILIBRIUM CONSTANT OF MG AND OTHER COMPETITIVE INHIBITORS. The roots of synaptic Me pharmacology may be traced to a study by Jenkinson (120) published in 1957, who showed that Ca and Mg compete for the membrane receptor, X, that controls ACh release. Rather than making unwarranted assumptions about the unknown relationship between binding of Ca to X and the subsequent biological response, Jenkinson compared *equal levels of synchronous release* in the presence and absence of Mg, and made the plausible assumption that *equal M values reflect equal concentrations of CaX*. Thus the only effect of Mg as a competitive inhibitor would be to exclude Ca from X and thereby reduce the CaX concentration; by increasing the Ca concentration in the presence of Mg, CaX may be restored to the same concentration as that present in the absence of Mg. The expression for y_{CA} in the presence of Mg is:

$$y_{CA} = \frac{[Ca]K_{CA}}{1 + [Ca]K_{CA} + [Mg]K_{MG}} \qquad \text{eqn 2e}$$

(see appendix A 1). This corresponds to a parallel shift to the right of the log [agonist]-response curve in the presence of antagonist without a change in maximum (253).

On the assumption that equal values of M produced by a low concentration of Ca ($[Ca_L]$) and by a higher concentration of Ca in the presence of Mg, ($[Ca_H]$) are produced by equal y_{CA}, then eqn 2e becomes;

$$\frac{[Ca_H]}{[Ca_L]} - 1 = [Mg]K_{MG} \qquad \text{eqn 2}$$

where the ratio of the two concentrations of agonist that produce matching responses was called the DOSE RATIO by Gaddum (91). Thus,

$$\text{DOSE RATIO} - 1 = [Mg]K_{MG} \qquad \text{eqn 2}$$

Eqn 2 is generally known as the *Schild equation* (6, 229). As the derivation in appendix A 1 shows, eqn 2 is independent of: the affinity constant of the agonist, the fraction of receptors occupied by the agonist, the shape of the log [Ca]-M curve (which can be quite complex), and the particular agonist as long as the agonist acts at the same receptor as Ca. Finally, any competitive inhibitor should obey eqn 2, as long as it acts at site X. It is thus possible to state eqn 2 in a more general sense at receptor X as follows;

$$\text{DOSE RATIO FOR AGONIST} - 1 = [Me]K_{ME} \qquad \text{eqn 2}$$

where Me in eqn 2 is a competitive inhibitor at site X. When K_{ME} remains constant over a range of dose ratios, then it is highly probably that Me is a competitive inhibitor at the same site as the agonist (253). In the simplest sense, however, the ability to surmount the inhibition by increasing the agonist concentration suggests the presence of a competitive relationship between agonist and antagonist (51). Eqn 2 has in fact been used independently by physical chemists to describe the competition of gases for adsorptive surfaces (258).

At the frog neuromuscular junction, Jenkinson (120) examined log[Ca]-M curves in various concentrations of Mg. He found that Mg was a competitive inhibitor of Ca, with a mean $K_{MG} = 0.25$ mM^{-1}; this value for Ca/Mg competition has been confirmed in subsequent experiments (see table 2). Another conventional Ca antagonist, the divalent cation Co, is a competitive inhibitor of Ca at site X, but has a much higher affinity than Mg; the mean reported K_{CO} as an inhibitor of M ranged from 10 mM^{-1} (267) to 14.3 mM^{-1} (58) at frog motor nerve endings.

B. APPLICATIONS TO THE EXTERNAL SURFACE OF THE NERVE TERMINAL. **i. Are differences between synchronous and asynchronous release due to different ion channels?** It has been suggested that the Ca channels which mediate the synchronous impulsive release of ACh (M) may differ in pharmacological specificity from those which mediate increases in MEPPf in

TABLE 2

*Me equilibrium constants at nerve endings**

Ion	K_{ME} (mM^{-1}) {K_d mM}	Method (Reference)
Mg	0.25 {4}	Antagonist of *M* in Ca (eqn 2) (120)
Mg	0.34 {2.97 ± 0.27, *n* = 8}	Antagonist of *M* in Ca (eqn 2) (74)
Mg	0.23 {4.4}	Antagonist of *M* in Ca (eqn 2) (58)
Mg	0.22 {4.6 ± 0.2, *n* = 4}	Antagonist of evoked MEPPf in Ca (eqn 2) (249)
Mg	0.19 {5.4 ± 0.7, *n* = 4}	Antagonist of evoked MEPPf in Ba (eqn 2) (237)
Mg	0.27 {3.7 ± 0.3, *n* = 4}	Antagonist of evoked MEPPf in Sr (eqn 2) (179)
Mg	0.30 {3.3 ± 0.5, *n* = 4}	Antagonist, Ca fluxes into synaptosomes (191)†
Ca	8.3 {0.12 ± 0.02, *n* = 5}	Antagonist of evoked MEPPf in Ba (eqn 2) (236)‡
Ca	4.2 {0.24 ± 0.04, *n* = 7}	Antagonist of evoked MEPPf in Sr (eqn 2) (178)‡
Ca	6.7 {0.15 ± 0.01, *n* = 4}	Antagonist, Ca fluxes into synaptosomes (191)†
Ca	7.7 {0.13}	Agonist, extrapolation of probability of release from latency-frequency histograms (21)§
Ca	0.9 {1.1 ± 0.19, *n* = 8}	Agonist, extrapolation (eqn 8d) (74)
Ca	0.02–0.06 {16.7-50}	Agonist, after block by La (eqn 14) (240)
Sr	0.27 (± 0.02, *n* = 6) {3.7}	Antagonist of *M* in Ca (eqn 2) (240)
Sr	0.26 (± 0.03, *n* = 4) {3.8}	Partial agonist compared to Ca (eqn 10c, spare receptor assumption) (240)
Sr	0.24 (± 0.01, *n* = 6) {4.2}	Partial agonist, Ca compared with Ca + Sr, (eqn 13, spare receptor assumption) (240)
Sr	0.65 {1.55 ± 0.15, *n* = 6}	Agonist, extrapolation of reciprocal plots (eqn 96) (175)
Ba	1.1 (± 0.4, *n* = 8) {0.9}	Antagonist of *M* in Ca (eqn 2) (238)
Ba	0.64 {1.56 ± 0.08, *n* = 4}	Antagonist, Ca fluxes into synaptosomes (191)†

* The mean equilibrium affinity constant (K_{ME}) or equilibrium dissociation constant (K_d) is presented ± 1 S.E.M. where possible.

† These are apparent K_{ME} values as determined from concentrations of Me that inhibit the influx of ^{45}Ca into K-depolarized synaptosomes by 50% (191); the transmitter here is likely to be dopamine and not ACh (79). All other K_{ME}'s were obtained from studies on frog end-plates.

‡ These values may differ because of the different stimulation conditions or because the differences in efficacies between Ca and Sr for asynchronous release are not great enough to provide an accurate value for K_{CA} using Sr as the agonist.

§ The method involved examining latency-frequency histograms at different [Ca]. Specifically, an equation similar to the alpha function (eqn 28) was combined with the gamma (eqn 29) and binomial (eqn 26) distributions and the resulting equation [eqn 11 of Bennett et al. (21)] plotted on double reciprocal coordinates; extrapolation to the abscissal intersect provided an estimate of K_{CA}. Although a first power relationship was observed, thus minimizing the errors inherent in extrapolating reciprocal plots, the assumption of simple binomial statistics may be invalid. This was discussed by Bennett and Lavidis in a subsequent paper (22).

response to nerve stimulation (118, 170). These suggestions are based, in part, upon the observations that Mg supports increases in MEPPf produced by *prolonged* high frequency stimulation (97, 118, 249). Implicit in this interpretation is that the inhibitors of *M*, e.g., Mg and Co, should not inhibit asynchronous ACh release. The experimental results, however, are not in accord with this suggestion. Figure 3, panel I shows that the slow depolarization associated with asynchronous release in 1.8 mM Ba (A) is inhibited by 10 mM Mg (B) and this inhibition may be fully overcome by increasing the extracellular Ba concentration to 5.8 mM in the presence of 10 mM Mg (C). On the assumption that this surmountable relationship reflects a competitive relationship between Ba and Mg, then the Schild equation predicts that K_{MG} = (DOSE RATIO for Ba − 1)/[Mg]. With the values in figure 3, K_{MG} = [(5.8/1.8) − 1]/10 mM = 0.22 mM^{-1} (237), a value statistically indistinguishable from that found by others for Mg as an antagonist of Ca-dependent *M* (see table 2). Co inhibits Ba-dependent asynchronous release but with much higher affinity than Mg; the mean affinity constant for Co as antagonist of Ba dependent asynchronous release [14.3 mM^{-1} (237)] is equal to that found in the same tissue for Co as an antagonist of Ca-dependent synchronous release (58). The simplest interpretation is that Ba mediates asynchronous ACh release by entering the nerve terminal through the same channel normally traversed by the natural agonist, Ca, in supporting *M*. Asynchronous release mediated by Sr or Ca and synchronous release mediated by Sr are also blocked by Mg or Co with the same respective antagonist affinity described above (see table 2 for results with Mg). The site of antagonism is near the external surface of the Ca channel as Mg and Co delivered to the cytoplasm of the cholinergic nerve do not inhibit evoked release (133, 60). It thus appears that both synchronous and asynchronous release are initiated through the conventional Ca channel in the motor nerve ending, regardless of the activating cation.

These results suggest that the Schild equation provides a powerful method for the detection of an external receptor site that controls ion entry. The force of this equation

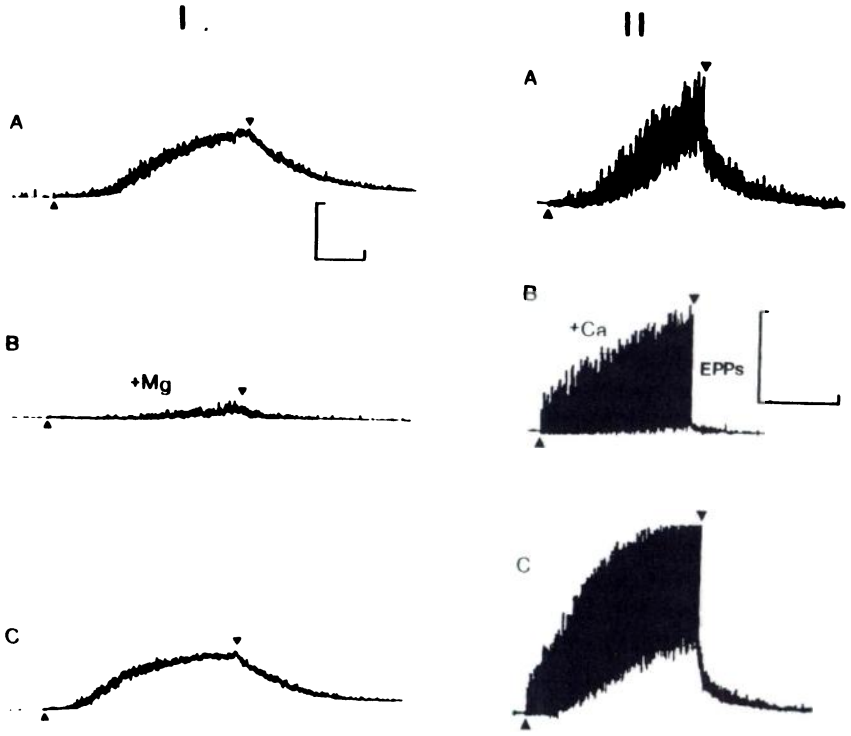

FIG. 3. Interactions of Ba with Mg (panel I) and Ca (panel II) at cholinergic nerve endings. Panel I: Asynchronous release in 1.8 mM Ba (A) is antagonized by Mg (B, 1.8 mM Ba + 10 mM Mg); this antagonism was overcome by raising the concentration of Ba (C, 5.8 mM Ba + 10 mM Mg). Nerve stimulation was delivered for 8 sec (between arrows) at a frequency of 15 Hz. Calibrations: 6 mv, 2 sec. [Reprinted with permission from Silinsky (237).] Panel II: Asynchronous release in 0.25 mM Ba (A) is antagonized by Ca (B, 0.25 mM Ba + 0.25 mM Ca); this antagonism was overcome by raising the concentration of Ba (C, 0.75 mM Ba + 0.25 mM Ca). Note EPPs in Ca solution. Stimulation frequency—25 Hz. Calibrations, 8 mv, 3 sec. Reprinted with permission from Silinsky (236).

lies in the fact that competitive inhibitors do not proceed past the binding step (efficacy = 0); the K_{ME} values are thus not confounded by a conformational change of the Me*X* complex into another state.

ii. Determination of the equilibrium affinity constants for Ca, Sr, and Ba. In a variety of experimental conditions in which extracellular Ba and Sr are capable of supporting neurally evoked increases in MEPPf, Ca cannot support asynchronous release. As full agonists, partial agonists, and competitive antgonists represent a continum of decreasing efficacy (253), if the paucity of effects of Ca on this release process is due to a very low efficacy, then Ca might be a competitive inhibitor of asynchronous release. figure 3, panel II shows this to be the case. In this figure, the slow depolarization associated with asynchronous release in 0.25 mM Ba (panel II, A) is inhibited completely by a low concentration of Ca (B, 0.25 mM Ba + 0.25 mM Ca; note the EPPs produced by Ca). This relationship appears competitive. An increase in the concentration of Ba to 0.75 mM in the presence of 0.25 mM Ca produces a slow depolarization (C) that matches the control observed in 0.25 mM Ba alone. From the Schild equation, the K_{CA} for Ca as an antagonist of the agonist, Ba: K_{CA} = (DOSE RATIO for Ba-1)/[Ca] = $\{(0.75/0.25) - 1\}/0.25\text{mM} = 8\ \text{mM}^{-1}$ (236). Similar values were found in other experiments (see table 2). It thus appears that Ca has over 40-fold higher affinity as an antagonist than Mg for a membrane site that controls depolarization-secretion coupling. Ca also antagonizes Sr-dependent asynchronous ACh release (figure 4). Nerve stimulation in 1.5 mM Sr solutions produces EPPs (shown as regular spikes in figure 4) and an increase in MEPPf over control during and after the period of stimulation (figure 4A). Addition of 0.25 mM Ca to the Sr solution (figure 4B) increases *M* (shown as a decreased fluctuation of the EPP on the pen record) and antagonizes asynchronous release. Increasing the concentration of Sr to 3.0 mM in the presence of Ca (figure 4C) increased both forms of ACh release to greater than the control level. The mean K_{CA} value for Ca as an antagonist of Sr is shown in table 2; this affinity for Ca is of the same order as that calculated with Ba as the agonist.

What is the locus of the high affinity for Ca? Based upon circumstantial evidence, the site was suggested to be near the external surface of Ca channels (236). Direct evidence was provided by the use of Ca-containing lipid vesicles (Ca liposomes) to deliver Ca to the nerve terminal cytoplasm (figure 4, D and E). Specifically, synchronous release mediated by Sr (D) was increased by Ca liposomes (E) without an antagonism of asynchronous ACh release; antagonism by Ca must thus be at a site accessible from the extracellular fluid but not the cytoplasm (236, 178). As the conventional Ca channel blockers Co and Mg block Ca-dependent ACh release only at

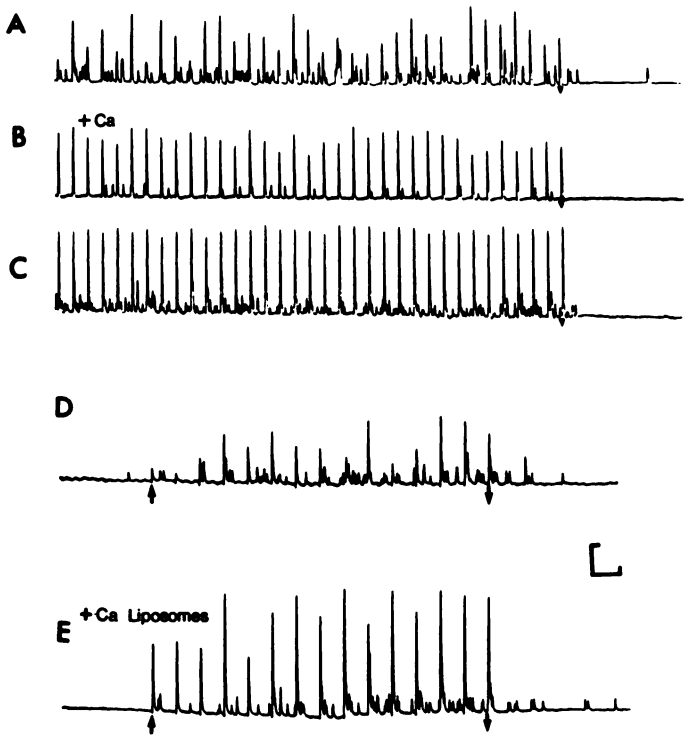

FIG. 4. Extracellular (A–C) and intracellular (B, D) interactions between Sr and Ca. Unstimulated MEPPf approximately 0.3/sec. A, synchronous release (EPPs appearing as regular spikes) and evoked MEPPs in 1.5 mM Sr; evoked MEPPf 16/sec). B, evoked MEPPs are antagonized by 0.25 mM extracellular Ca (B, 1.5 mM Sr + 0.25 mM Ca, evoked MEPPf = 4/sec) while synchronous release is increased (this is shown by the decreased fluctuations on the pen record). C, increasing the [Sr] overcomes the inhibition by extracellular Ca of asynchronous release (C, 3.0 mM Sr + 0.25 mM Ca, evoked MEPPf = 21/sec) and further increases synchronous release. Stimulation frequency 7 Hz (stimulation terminated at the arrow), MEPP amplitude approximately 1 mv. In D and E, evoked MEPPs in control Sr Ringer (D, 1.3 mM Sr + 1.0 mM Mg, evoked MEPPf = 13/sec) are not antagonized by intracellular Ca (E, control Ringer + 80 mM Ca-containing liposomes, evoked MEPPf = 14/sec). Note increase in synchronous release produced by Ca-containing liposomes (nerve stimulation delivered at a frequency of 3 Hz between the arrows). Calibrations for D and E, 2 mv, 500 msec. Reprinted with permission from Mellow et al. (178). For further details, see text.

an external membrane site (133), it appears that Ca controls Me dependent ACh release by binding with high affinity to that same site.

With respect to synchronous release, the Me species which interact at Ca channels but have low efficacy (Sr) or zero efficacy (Ba) for M should act as competitive inhibitors of Ca in this release process. This prediction was borne out; both Ba and Sr competitively inhibited Ca-dependent M. Values for the K_{SR} and K_{BA} as antagonists of Ca-dependent M as calculated by the Schild equation are presented in table 2. These results will be discussed more fully in subsequent sections of this review.

In the past, the Schild equation has provided useful insights into the competition of gases at solid surfaces (258) and the competition of drugs with neurotransmitters at receptors on the postsynaptic membrane (51, 52, 98). From the preceding discussion, it appears that eqn 2 may also be used to explore the membrane events by which alkaline earth cations regulate the secretory process.

iii. Do Me species bind to the nerve terminals? In the early 1970s, results obtained by extrapolation showed that Ca, Sr, and Mg had essentially the same affinity for the X site associated with ACh release (74, 175). Studies in biophysics have suggested that membrane events which display equal apparent affinity for cations of the same valency are likely to be mediated by non-selective screening of fixed negative membrane surface charges (34, 62, 173). Screening occurs without dehydration and is independent of the specific properties of the ion, apart from valency and concentration, while binding requires removal of the surrounding water molecules and is dependent upon the specific chemical characteristics of the ion. Figure 5A shows an Me species with its surrounding envelope of water. Note that the water in the immediate neighborhood of the divalent cation (the primary or inner hydration sphere) is highly structured, i.e. it is bound and immobilized in a radial direction due to the force of the ion's electric field on the water dipole. In the secondary region of hydration, the water is less ordered than in its usual structure, which is regained in the bulk solution away from the influence of the ion.

The mathematical formalism of the screening process is known as the Gouy-Chapman theory of the diffuse double layer (102, 43, 103, 34). Diffuse double-layer theory was applied to the motor nerve ending by Muller and Finkelstein in 1974 (190) in an attempt to describe the mechanism by which Mg inhibits Ca-dependent ACh release; the following is a qualitative description of the theory.

Biological membranes have fixed negative surface charges produced by acidic proteins and phospholipids (e.g., sialic acid residues). These negative surface charges constitute the first of the two layers in double-layer theory (figure 5B, 1.) The second layer (figure 5B, 2) refers to the oppositely charged ions (concentric circles) in solution near the membrane (MEMB.), the distribution of cations near the membrane being determined by the electrical potential (ψ) produced by the fixed attractive negative charges at the membrane surface. Specifically, the cations will be concentrated near the membrane and will decrease in concentration exponentially with distance. Finally, at a sufficient distance from the membrane surface (the bulk solution), no further influence of surface potential on ion concentration will be observed. At this distant region, only thermal forces would control cation distribution.

Quantitatively, the surface potential (ψ_0) determines the concentration of Me near the membrane ([Me_0]) in accordance with a Boltzmann distribution (eqn 3):

$$[Me_0] = [Me]\exp\{-\psi_0/25\} \qquad \text{eqn 3}$$

Thus the more negative the surface potential, the greater

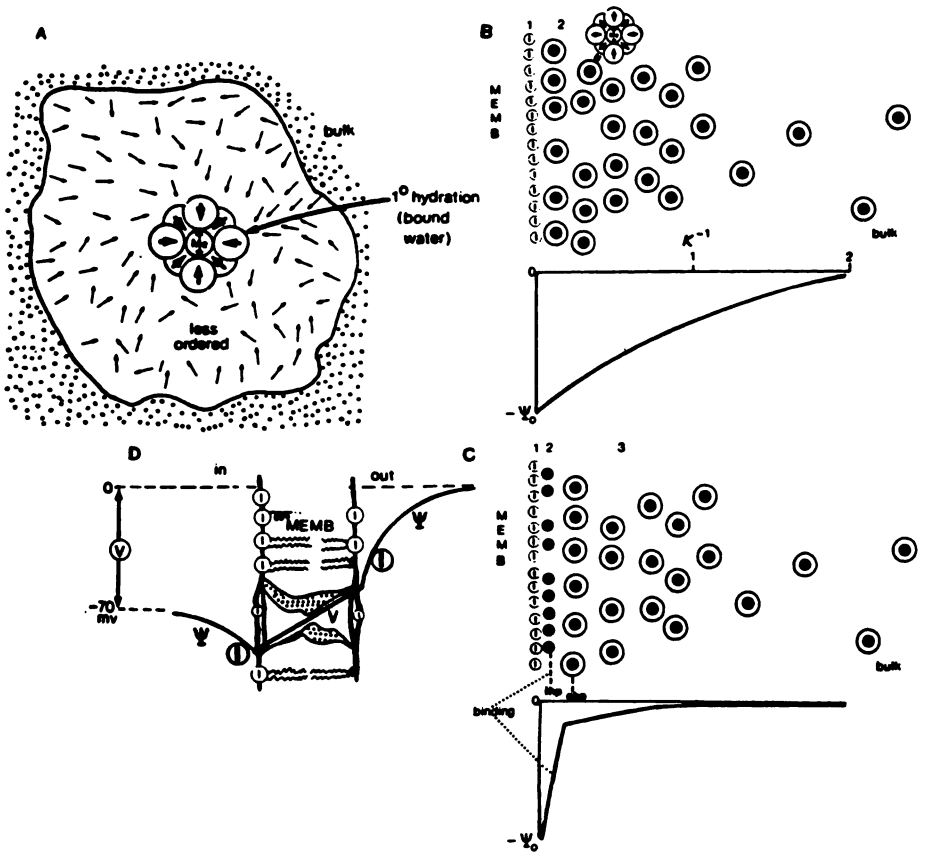

FIG. 5. Aspects of cation behavior in aqueous media (A) and in the vicinity of membrane (MEMB) fixed negative charges (B–D). A shows an Me species coordinated with eight water molecules; note the bound water is radially oriented in the primary hydration sphere (the arrow tip is dipped into the 0 atom of the H-O-H dipole). The coordination of eight neighboring water molecules (coordination number = 8; see table 1) would be characteristic of Ba, and under some conditions, Ca as well (see section VI). Immediately surrounding the region of bound water, there is a region of water less ordered than the usual bulk solution. (Drawn after refs. 137, 34, 112). B shows some of the predictions of diffuse double-layer theory in the absence of ion binding (MEMB = membrane). The first layer (1) is the membrane fixed negative charges. The second layer (2) consists of the cations (dark circles) enclosed in a primary hydration sheath (the outer circle). Note the decay of the negative surface potential at the membrane (ψ_o) with distance from the membrane follows an approximately exponential curve for small potentials; the distance to which it decays to 1/e = the Debye length, κ^{-1} (the reciprocal Debye constant). The concentration of Me species also decays exponentially with distance and with the same length, κ^{-1}. Concentration of Me at the membrane is also related to the surface potential exponentially (see text for further details). C shows the influence of binding on ion concentration and the decay of surface potential with distance. Binding creates a triple layer of (1) fixed membrane charges, (2) bound dehydrated ions, and (3) diffuse hydrated charges. Binding is really a superequivalent adsorption in which the bound charge density may be greater than the membrane fixed charge density, with gross electroneutrality being maintained by the anions in the diffuse layer. Binding is also called specific adsorption to conceal the fact that it is not well-understood. Note the decay of surface potential with distance is very steep and linear in the region of binding. For convenience neither hydration of the membrane nor counter-ions (anions) are shown. The region of binding is referred to as the Stern layer and is further subdivided into: the inner Helmholz plane (ihp), where the ions are bound, and the outer Helmholz plane (ohp) which marks the beginning of the diffuse layer (2, 34). Intermediate forms present between these planes (e.g. partially hydrated ions) are not shown. The original approach to surfaces by Helmholz and Perrin envisaged the double layer as a simple capacitor with almost all the surface potential concentrated at the membrane surface between the fixed membrane charges and opposite charged ions tightly adhering to the membrane. It was Stern who fused the Helmholz-Perrin view with Gouy-Chapman theory (C, see refs. 2, 34). The treatment of diffuse double-layer theory in B and C and in the text assumes that the anions are also divalent. If positive and negative ions of differing valency are present, then a series of Gouy-Chapman expressions is required to describe the interactions of these ionic species with the fixed membrane surface charges (103, 111, 190). D shows the distinction between surface potentials (ψ) at the external and internal faces of the cell membrane—these are produced by the fixed charges at the respective membrane surfaces—and the membrane potential (V), which is produced by small charge movements through ion channels (stippled) and the very small subsequent difference in charge storage on the membrane capacitance. Note that normal positivity of V on the outside of the membrane (the true V is shown as a dashed line) is made more negative than its true level by the fixed negative charges on the outside surface of the membrane. In contrast, the normal internal negativity associated with the resting membrane potential (approximately a Nernst potential for potassium is made more negative by fixed internal surface charges. The measured membrane potential (V = −70 mv) reflects the potential difference between *bulk* internal and external solutions.

the concentration of Me_0. If the surface negativity is reduced in some fashion, then the concentration of Me near the membrane would decrease relative to the bulk concentration. The first property to consider with respect to diffuse double-layer theory, therefore, is the way surface potential influences ion distribution; accordingly, the Boltzmann distribution is an inherent part of the Gouy-Chapman equation. The second concern of diffuse

double-layer theory is the decay of surface potential as a function of distance from the membrane. As a general rule, the surface potential (at low surface potentials in the absence of binding) decays exponentially with distance to 1/e of its membrane surface value at one Debye length (κ^{-1}, figure 5B). It should be noted that, at any given surface potential, the same constant κ^{-1} also describes the exponential decay of ion concentration with distance from the membrane, the [Me] falling to 1/e of its membrane value at one Debye length.

Although the surface potential modifies the distribution of ions, ions also modify the surface potential. The Gouy-Chapman equation relates the electrical potential at the surface of the membrane (ψ_0 in mV) to the density of membrane surface charges (σ in charges/Å^2) and the distant *bulk* concentration of cation, C, as follows:

$$\frac{\exp\{zF\psi_0/2RT\} - \exp\{-zF\psi_0/2RT\}}{2} = \frac{136\,\sigma}{C^{1/2}} \qquad \text{eqn 4}$$

where z is the valency, R is the gas constant (8.314 joules^{-1}mole^{-1}), F is the Faraday (96,500 coulombs/mole), and T is the absolute temperature (in degrees Kelvin). As the left hand side of eqn 4 is the hyperbolic sine function, sinh, then

$$\sinh(zF\psi_0/2RT) = 136\,\sigma/C^{1/2} \qquad \text{eqn 4a}$$

Making the simplification for illustrative purposes that when $x \ll 1$, $\sinh x = x$, and whereas $z = 2$ for Me species, and at 22°C, RT/F = 25, then eqn. 4a becomes

$$z\psi_0/50 = 136\,\sigma/[\text{Me}]^{1/2}.$$

Solving for ψ_0

$$\psi_0 = 3400\,\sigma/[\text{Me}]^{1/2} \qquad \text{eqn 4b}$$

(This treatment assumes for simplicity that the anions in solution are also divalent; see figure legend). From eqn 4b, it is apparent that as the surface charge density (σ) increases, the surface potential increases; as the bulk concentration of Me increases, then the surface potential decreases. The decrease in the negative surface potential by increasing concentrations of Me may be viewed as a shielding or screening of the negative surface potential by positively charged Me species. This effect occurs to an equal degree regardless of the chemical properties of the divalent species; such non-selectivity serves as the practical definition of screening.*

For example, if Mg is added to the extracellular fluid, then by eqn 4b, the surface potential would be reduced. Such a reduction in surface potential will reduce the concentration of Ca near the surface of the membrane relative to the bulk solution in accordance with the Boltzmann expression (eqn 3). This is the view of Muller and Finkelstein (190), namely that antagonism of M is produced by a decrease in the surface potential due to screening by the Me antagonist. This in turn decreases the concentration of Me agonist near the membrane and reduces the availability of Me agonist for entry through Ca channels. Choosing conditions whereby [Ca_0] is linearly related to the bulk Ca concentration [Ca], these authors found that the curve for inhibition by Mg (0.5 M to 4 mM) of Ca-dependent M ([Ca] = 0.4 mM) predicted from diffuse double layer theory agreed with the previously published experimental results on the inhibition of M by Mg (74). Muller and Finkelstein had to assume a value of σ (1/54 Å^2) to fit the model and they used a modified version of eqn 4 to account for the effects of monovalent as well as divalent cations (103). Subsequent work has shown that the theory of the diffuse double layer predicts changes in M produced by alterations in the extracellular monovalent cation concentrations (184).

Application of the Gouy-Chapman equation to motor nerve terminals reflected an innovative interpretation of the secretory process, especially in view of the belief at the time that all Me species had equal apparent affinity for the nerve terminal. There are several difficulties with this approach, however. First, it would indeed be surprising if permeant ions—which must dehydrate and bind to sites near the Ca channel, and then traverse the membrane through these channels—behaved in accordance with a model which assumes that Me species interact with a single extracellular site only in the hydrated state. Next, eqn 4 assumes that the fixed charges are smeared uniformly over the surface of the nerve terminal; this common assumption is difficult to relate to the structure of the nerve terminal, where Ca channels have been observed morphologically at discretely localized active zones (e.g. figure 7A). Finally, in the words of Muller and Finkelstein (190): "... simple electrostatic screening, which quantitatively accounts for the action of Mg, is not sufficient to explain entirely the effects of other multivalent cations." Perhaps it is most relevant to enquire whether the Gouy-Chapman theory explains the effects of Ca at the external surface of the nerve ending, i.e., do Ca and Mg have equal affinity at the external surface of Ca channels? The answer to this has already been provided in the preceding section, namely Ca has over 40-fold higher affinity than Mg at this site. These results are thus not consistent with the simple theory of the diffuse double layer but suggest that if alkaline earth cations do interact with fixed membrane surface charges, then binding is more important than screening at these charged sites.

In simple membrane systems where fixed membrane charges are more easily studied experimentally, a modi-

* Although derivation of eqn 4 is beyond the scope of the review, it may be noted here that eqn 3 is a direct consequence of Coulomb's law and of the Boltzmann distribution. Coulomb's law states that the force of attraction between two charged "points" increases as the magnitude of the charges increases and decreases as the inverse square of the distance between the charges. Modification of Coulomb's law for solid surfaces leads to Gauss's law and the differential form of Gauss's law is the Poisson equation. The Gouy-Chapman equation is a combination of the Poisson and Boltzmann expressions (173). The reader desiring a more rigorous treatment may see reference 34.

fication of diffuse double-layer theory known as the Stern equation (2, 34, 173) is used to account for the binding of ions. The Stern equation assumes a triple layer (figure 5C) near the surface of the membrane: (1) the fixed-membrane charges, (2) the dehydrated Me bound to the membrane, and, (3) the diffuse layer of hydrated cations in solution. The bound Me is extremely effective in reducing surface potential; ψ_0 thus drops off very rapidly with distance in the region of binding (figure 5C). The Stern equation envisages binding as a reduction in surface charge density, σ. Specifically, the reduction in surface charge density by a given concentration of Me, $\Delta\sigma$, as a fraction of maximal reduction in σ ($\Delta\sigma_{max}$) is equal to: $[Me_M]\ K_{ME}$.

$$\frac{\Delta\sigma}{\Delta\sigma_{max}} = \frac{[Me_0]\ K_{ME}}{1 + [Me_0]\ K_{ME}} \qquad \text{eqn 1e}$$

which is eqn 1, the rectangular hyperbola! As eqn 1 was essentially developed as a tool to explain the varied behavior of substrates of different binding constants, i.e. different K_{ME}'s, then it appears that alkaline earth cation binding is the simplest *single* approach to the extracellular surface of the nerve terminal. These results certainly do not rule out a minor component of cation screening at the nerve terminal. Indeed, it will be shown later that screening of fixed negative *internal* surface charges appears to be the best explanation for the action of intracellular Me species in promoting asynchronous ACh release (248, 178). At the external surface of the nerve terminal, theoretical considerations have shown, however, that as σ is decreased from the level appropriate to artificial lipid membranes and crayfish nerve (1/60 Å^2) to those postulated for the external surface of vertebrate nerve (1/100 to 1/140 Å^2), Me behavior changes from a predominantly screening situation to binding (62).

It should be stressed at this juncture that the Gouy-Chapman equation refers to the surface potential, which is not equivalent to the potential across the cell membrane (e.g. figure 5D). The amount of charge movement (mostly potassium) necessary to produce the resting transmembrane potential (figure 5 D–V) is so small (in the range of one electronic charge 10,000 Å^2) that it does not contribute to the potential at the membrane surface (173). Figure 5 B–D illustrates additional details not described in the text as well as some of the assumptions made in this simplified description of membrane surfaces (see figure legend). The left hand side of figure 5D serves as a prelude to the subsequent discussion of the surface potential in the cytoplasm near the *internal* face of the membrane (section IV).

In summary, the different affinities of the Me species suggest that Me species bind to negatively charged receptors at the external surface of the nerve ending. It thus appears that more detailed information about nerve terminal function may be obtained by relating the biological behavior to the specific physical properties of the ion. This is discussed in the next section.

iv. Selectivity sequences and the physical properties of the Me cations. Physical chemists interested in the ion selectivity of glass membranes have developed a theoretical approach to Me selectivity in biological membranes based on Eisenmann's original model of monovalent ion selectivity (82, 71). The model, as applied to Me species, may be described as follows:

From thermodynamic considerations, under standard conditions the free energy of the Me binding reaction to X (ΔG_0) is related to the K_{ME} by

$$\Delta G_0 = -RT \ln K_{ME} \qquad \text{eqn 5}$$

Thus, the higher the equilibrium affinity constant, the more negative the free energy and the more favored the reaction. The overall ΔG_0 consists of two components, however, the free energy of the MeX reaction (ΔG_{ME-X}) and the free energy of hydration (ΔG_{HY}), i.e.

$$\Delta G_0 = \Delta G_{ME-X} - \Delta G_{HY} \qquad \text{eqn 6}$$

The more highly negative the free energy of hydration, the less negative the overall free energy ΔG_0 and the less favored the Me-site interaction. This is because, in order to bind, the ion must lose all or at least part of its hydration sphere and the more negative the ΔG_{HY}, the more tightly the ion holds onto its surrounding water. Values of ΔG_{HY} are obtained from electrode potentials measurements and are listed in table 1.

The electrostatic MeX interactions at the membrane are described by Coulomb's law, which for a divalent cation in this situation may be approximated by eqn 7 (see ref. 62):

$$\Delta G_{ME-X} = 664\ q_x/(r_{ME} + r_x) \qquad \text{eqn 7}$$

where q_x is the charge of the negative membrane site X (in electronic charges) and the r's reflect the crystal radius of the Me species and the radius of site X. (Me crystal radii are shown in table 1.) Thus the smallest naked ion, Mg, by eqn 7 has the most negative free energy of interaction with site X because Mg can enter into the most intense coulombic interaction with site X once its water shell is removed.

The importance of Me-X interactions relative to dehydration may be deduced from the equilibrium selectivity sequence of affinity constants generated by the Eisenmann theory (82, 71). This theory was originally proposed to account for the fact that only 11 selectivity sequences of the 120 possible permutations (5! = 120) were observed for the five monovalent alkali cations. For the four Me species, instead of 24 possible sequences (4! = 24), only seven sequences are predicted as follows (71):

I Ba > Sr > Ca > Mg
II Ba > Ca > Sr > Mg
III Ca > Ba > Sr > Mg
IV Ca > Ba > Mg > Sr
V Ca > Mg > Ba > Sr
VI Ca > Mg > Sr > Ba
VII Mg > Ca > Sr > Ba

Sequence I reflects the order of decreasing crystal radii (see table 1) and increasingly negative free energies of hydration. If Me species were found to obey sequence I, then the relative ease by which the Me species loses its hydration shell is likely to determine the order of Me selectivity. At the other extreme, the sequence of increasing atomic radii (VII) appears when an electrostatic interaction between Me and membrane site X is the primary determinant of selectivity.

Under what conditions might the membrane site X determine selectivity at cholinergic nerve endings? The answer depends on the equivalent coulombic strength of site X; if X has a small radius or is highly charged, then by Coulomb's law, it has a high strength (for further details see ref. 62). At high site strength, eqn 7 would dominate the overall free energy term and the sequence of Me species would follow VII. At low strength, the coulombic Me-X force will be unimportant and the free energy of hydration will determine selectivity (sequence I). At intermediate site strength, both hydration and ion-site interactions would determine selectivity (sequences II to VI). Indeed, as the strength of site X is increased, one Me species changes its relative position in each sequence as that ion's hydration force succumbs to the coulombic MeX force as the major determinant of its free energy.

At the motor nerve ending the equilibrium affinity constants of the Me species for X as calculated by the Schild equation (table 2) decrease in the order: Ca > Ba > Sr ≅ Mg, which is sequence III or IV. It thus appears that site X possesses moderate negative electrostatic strength and that both hydration and Me-X interactions determine the behavior of alkaline earth cations at the external surface of the nerve ending. This sequence suggests that, although some generalizations may be made with respect to ionic potential and biological behavior of the group IIa metals, a more precise picture requires consideration of the Me interaction with the biological membrane. This becomes more apparent if the divalent cation Cd is considered. Cd has essentially the same ionic potential and dehydration kinetics as Ca (72,222), yet Cd is a potent inhibitor of synchronous ACh release (228, 57).

In summary, the results in this section suggest that the use of mass action principles as applied to the binding of competitive inhibitors (the Schild equation, eqn 2) can provide helpful insights into the properties of ions at the external surface of secretory cells. At the motor nerve endings, alkaline earth cations bind with predictable equilibrium selectivity to an external membrane site of moderate electrostatic field strength prior to influencing transmitter release. The next section shows, however, that attempts to quantify the behavior of Me species as agonists have been much less fruitful, with considerable variability in the experimental results leading to a welter of different theories of evoked ACh secretion.

3. Models for the Action of Me Agonists. There is little reason to doubt the validity of eqn 1 for competitive antagonists or for the binding step in the reaction scheme for agonists. For Me agonists, however, the membrane and intracellular reactions subsequent to binding to X are largely unknown. This makes the precise interpretation of the quantitative results dependent on the physical theory favored by the investigator. It is evident from the shapes of the log [Ca]-M and log [Sr]-M curves (figure 2A) that the binding-response relationship is complex. The various theories differ as to the loci of action for Ca, Sr, Ba, and Mg and as to the precise mechanisms responsible for the complex, cooperative behavior of alkaline earth cation agonists.

A. THE FOURTH POWER MODEL OF RAHAMIMOFF AND COLLEAGUES. The simplest relationship between binding and synchronous ACh release is one in which M at any particular [Ca] or [Sr] as a fraction of the maximal M of the nerve terminal (i.e., the fraction of the maximal synchronous ACh release = $y_{RELEASE}$) is directly proportional to the fraction of Me receptors occupied, (y_{ME}) as follows:

$$y_{RELEASE} = e_{ME} y_{ME} \qquad \text{eqn 8}$$

where the proportionality constant is the efficacy (e_{ME}), namely, the effectiveness of the ion, once bound to X, in supporting M. (For the assumptions inherent in this approach, see appendix A 1 and A 6.) At low levels of release, the experimental results at the frog neuromuscular junction could be fitted by such an expression but only if the right hand side of eqn 8 was raised to a power, N (eqn 8a).

$$y_{RELEASE} = \{e_{ME} y_{ME}\}^N \qquad \text{eqn 8a}$$

As the limiting slope of the log [Ca]-log M relationship was found to equal 4 (see appendix A 8 for details), it was suggested that four and only four Ca ions (74) cooperate in some fashion to produce the release of a quantum of ACh (i.e., $N = 4$ in eqn 8a).

For simplicity, on the assumption that $e = 1$ for the full agonist Ca, an assumption consistent with earlier theories of receptor phenomena (5), then

$$y_{RELEASE} = y_{ME}^4 \qquad \text{eqn 8b}$$

To determine the K_{CA} as an agonist, eqn 1 was substituted into eqn 8a and rearranged by taking the fourth root of both sides as follows:

$$y_{RELEASE}^{1/4} = \frac{[Ca]K_{CA}}{1 + [Ca]K_{CA}} \qquad \text{eqn 8c}$$

Taking the reciprocals of both sides produces an expression suitable for Lineweaver-Burk linearization (146):

$$\frac{1}{y_{RELEASE}^{1/4}} = \frac{1}{K_{CA}[Ca]} + 1 \qquad \text{eqn 8d}$$

The equation is one of a straight line when the reciprocal of the calcium concentration is plotted on the abcissa

and the reciprocal of the fourth root of $y_{RELEASE}$ is plotted on the ordinate. When the left hand side of eqn 8d is set = 0, then $1/[Ca] = -K_{CA}$. Thus by extrapolation to the intercept on the ordinate, the affinity constant for Ca as an agonist can be estimated. The mean K_{CA} determined by this method was 0.9 mM^{-1} (74); this represented the first published value for the apparent affinity of Ca in the process of evoked ACh release. The fourth power model for Ca action was confirmed by others but only at low levels of M at the frog neuromuscular junction (4, 104, 267); ACh release from sympathetic ganglia appears to follow the simpler relationship described in eqn 8 (170) while ACh release from mammalian neuromuscular junctions and frog neuromuscular junctions at more normal M appears more complex than eqn 8b (see below).

In a most significant publication in 1971, Meiri and Rahamimoff (175) found that Sr supported M but was less effective than Ca in the process; the agonist effect of Sr was inhibited by Mg. These authors also observed that depending upon the [Ca] concentration, Sr could either inhibit M (at normal [Ca]) increase M (at very low [Ca]) or have no effect on M (in Ca + Mg solutions). These results provided evidence that Sr was a partial agonist for the same process shared by the full agonist, Ca. The results with Sr and synchronous ACh release were subsequently confirmed and extended at several cholinergic synapses (170, 240). The low efficacy of the partial agonist Sr was described by the constant β, which is roughly equivalent to e. Thus using eqn 8c for Sr

$$y_{RELEASE} = \{\beta y_{SR}\}^4 \qquad \text{eqn 9a}$$

The authors felt that four Sr must "cooperate" to release a quantum of ACh but were cautious in this interpretation; technical difficulties prevented a determination of the initial slope of the log [Sr]-log M plot. Rearranging eqn 9a into the form of eqn 8d

$$\frac{1}{y_{RELEASE}^{1/4}} = \frac{1}{\beta K_{SR}[Sr]} + \frac{1}{\beta} \qquad \text{eqn 9b}$$

When the left hand side of eqn 9b is set = 0, then the β's cancel and as before: $1/[Sr] = -K_{SR}$. The mean extrapolated K_{SR} was 0.645 mM^{-1} (table 2). Values for β of Sr were very much lower than the $\beta = 1$ assumed for the full agonist Ca; β for Sr ranged from 0.3 to 0.5 (for specific details, see eqns 12a in appendix A 5).

The results reported by Rahamimoff and his colleagues demonstrate that when K_{ME}'s are estimated by extrapolation of fourth root reciprocal plots, Sr and Ca have about the same apparent affinity, but differ remarkably in the efficacy of the ion for M. These papers also demonstrated quantitatively that the dose-response curves for the agonists Ca and Sr do not fit the simple rectangular hyperbola of eqn 1, confirming an observation originally made by Jenkinson in his paper on Mg (120). The absence of a simple rectangular hyperbolic relationship is the working definition of cooperativity (see appendix A 8 and A 9) and the apparent limiting slope (N) of 4 in the log [Ca]-log M curve (appendix A 8) led to the suggestion of the cooperative action of four Ca ions in the ACh release process. Unfortunately, the sites and mechanisms responsible for the observed cooperativity as well as the precise cooperative number N remain a matter of conjecture to this day (see section VI).

In their 1971 paper, Meiri and Rahamimoff (175) speculated on the structural correlates of affinity and efficacy. Specifically, it was suggested that the X site is the Ca channel and equal affinity reflects equal probability of occupying a channel. Efficacy was thought to be related to mobility in the channel, with Sr having a lower efficacy than Ca because the heavier naked Sr moved more slowly through the channel. This view will be examined in more detail in the next section.

B. THE CA RECEPTOR MODEL (SILINSKY). **i. Overview.** Despite the reproducibility of the fourth power model at low levels of M frog muscle, the model does not apply when M becomes much greater than 10 (4, 104, 240). As normal levels of ACh release are generally, M = 200 to 500, it appears that an alternative model is needed to describe the entire [Me]-M relationship to saturation for Ca and Sr. From a teleological point of view, it would be surprising if the fourth power relationship did hold over the entire range of [Ca] as it would reflect the behavior of a very inefficient secretory system. For example, if half of the X sites are occupied (i.e. $y_{ME} = 0.5$), then $y_{RELEASE}$ would be $(0.5)^4$ or 0.06; that is, occupation of half the Ca binding sites would produce a response that is only about 6% of the maximum. Nature, however, has usually preferred the opposite behavior for full agonists. In the vast majority of receptor-effector systems with the complexity of the [Ca]-M relationship, maximal biological responses are produced by using a very small proportion of the receptor sites, in turn leaving the majority of the sites spare (194, 252) or reserve. If X represents a Ca receptor near the external orifice of the Ca channel, then it is possible that maximal M could be produced by using a small proportion of the total complement of Ca channels, in turn leaving the majority of the channels spare. For example, if the maximal M is limited by the number of available synaptic vesicles or active zones, then there is no *a priori* reason that maximal M would require maximal Ca entry. The results to be described below suggest that spare Ca channels exist on cholinergic motor nerve terminals (240, 142a) as well as on presynaptic terminals in the mammalian brain (77–79).

Spare Ca receptors have been demonstrated at motor nerve endings by using irreversible antagonists of depolarization secretion-coupling. If in the face of an irreversible occlusion of a proportion of the Ca binding sites, increasing the concentration of Ca can overcome the inhibition and restore maximal M, spare Ca receptors are suggested (89, 253). The trivalent La is a potent Ca channel blocker (182) and an irreversible inhibitor of

evoked ACh release (65, 240). It has been found that inhibition of *M* in Ca solutions by La can be overcome by increasing the [Ca] (240), suggesting the presence of spare Ca channels. It is perhaps best to envisage treatment with La as a physical dissection of Ca channels from the nerve endings, in effect, removing them from further participation in the Ca entry process. If the majority of Ca channels are spare, then despite removal of some of the Ca channels by La, increasing the Ca concentration, by mass action, will allow Ca to occupy and traverse the additional channels. Spare receptors are only observed for agonists of high efficacy, i.e agonists that are extremely effective at activating a limiting substrate beyond the receptor. For *M* mediated by the partial agonist (Sr), it has been observed that inhibition by La cannot be overcome be increasing the [Sr] (240). This result is to be expected as Sr, with low efficacy, requires all of its receptors to produce maximal *M* an order of magnitude lower than maximal *M* in Ca. Removal of receptors by La thus denies Sr the possiblity of restoring a maximal response, however high its extracellular concentration is elevated. The notion of spare Ca channels has been confirmed recently using antibodies to Ca channels at mammalian motor nerve endings; after destruction of a significant proportion of Ca channels by antibody, the log [Ca]-*M* curve is shifted to the right without a change in slope (142a).

Spare Ca channels have been also been demonstrated in the mammalian brain by comparing Ca fluxes and secretion at different extracellular Ca concentrations (77–79). For example, in response to membrane depolarization, the secretion of vasopressin from neurosecretory terminals was maximal at Ca concentrations as low as 1.1 to 2 mM but Ca entry continued to increase as Ca was raised near 10 mM (77, 78). Evidently, far less than maximal Ca entry is required to produce maximal secretion in this system as well.

ii. Determination of affinities and efficacies for Ca and Sr. The basic axiom of receptor theory has been presented earlier in the discussion of antagonism (IIIA, 2), namely that quantification *must* be made by comparing equal biological responses (see refs. 51, 253, 266). Thus the Schild equation was used to calculate K_{ME} for an antagonist by comparing equal *M* in the presence and absence of the antagonist. It is also possible, however, to obtain information about K_{ME} and e_{ME} for agonists by comparing matching *M* produced by the full agonist (Ca) and the partial agonist (Sr) or matching *M* produced by Ca in the presence and absence of an irreversible inhibitor such as La. To determine K_{CA}, K_{SR}, e_{CA}, and e_{SR} by comparing equivalent responses, it is convenient to introduce a parameter that R. P. Stephenson called the stimulus, *S* (252). *S*, in effect, represents a physical blow to the tissue by an aggressive pharmacological or physical force, in this instance, the Me agonist. The response to this blow (*M*), is a function of the complexity of the responding tissue. The stimulus is defined as the product of *e* and *y*, thus,

$$S_{ME} = e_{ME}y_{ME} \qquad \text{eqn 10}$$

Much as two aggressive physical blows may have the same momentum even if one blow is delivered slowly by a large, lumbering individual and the other struck rapidly by a small, wiry individual, an activator of low *e* and high *y* (Sr) may produce the same stimulus as an activator of high *e* and low *y* (Ca). The only assumption that is made is *equal responses (M) are produced by equal stimuli (S)*, regardless of the activating cation. As the response to a physical blow may vary depending upon the recipient in a complex fashion, the secretory response of a tissue may behave in a complex fashion with respect to the stimulus as well. The assumption that equal responses reflect equal stimuli is roughly equivalent to suggesting that blows of equal momentum, regardless of the size of the aggressor, will produce the same physical effect.

As a corollary of eqn 10, which assumes a linear relationship between *S* and *y*, cooperativity in the [Me]-*M* relationship is ascribed to events beyond binding at the receptor and beyond efficacy, i.e., cooperativity is due to the complex relationship between *S* and *M*. Support for this assumption may be obtained from studies of Ca currents in which Ca entry has been shown to be a linear function of extracellular Ca occupancy (38, 106, 148, 191).

With respect to Ca and Sr, if *M* produced in a certain [Ca] is matched by a certain [Sr], as $M_{CA} = M_{SR}$; then $S_{CA} = S_{SR}$; and thus by eqn 10, $e_{CA}y_{CA} = e_{SR}y_{SR}$, and by eqn 1

$$\frac{e_{CA}[Ca]K_{CA}}{1+[Ca]K_{CA}} = \frac{e_{SR}[Sr]K_{SR}}{1+[Sr]K_{SR}} \qquad \text{eqn 10a}$$

Simplification of this equation, as will be described below, may be used to obtain quantitative information about the properties of the Ca receptor.

In using receptor theory at the nerve ending, it was my intention to provide a quantitative description of the entire [Me]-*M* relationship for both Ca and Sr with minimal assumptions, and to evaluate the assumptions that were made. Ultimately, the most rigorous test of the theory centers on how accurately the determined values of e_{ME} and K_{ME} for Ca and Sr predict the log [Me]-*M* relationships observed experimentally. The specific approach taken was as follows. First, the K_{SR} values calculated by the Schild equation (eqn 2) were compared with the values of K_{SR} calculated by methods in which Sr is used as an agonist and which assume that the majority of Ca receptors are spare. If the values are in good agreement, then the presence of spare Ca receptors would be suggested quantitatively. Next, K_{CA} and e_{ME} values were determined and used to generate theoretical log [Me]-curves; these curves were then compared to

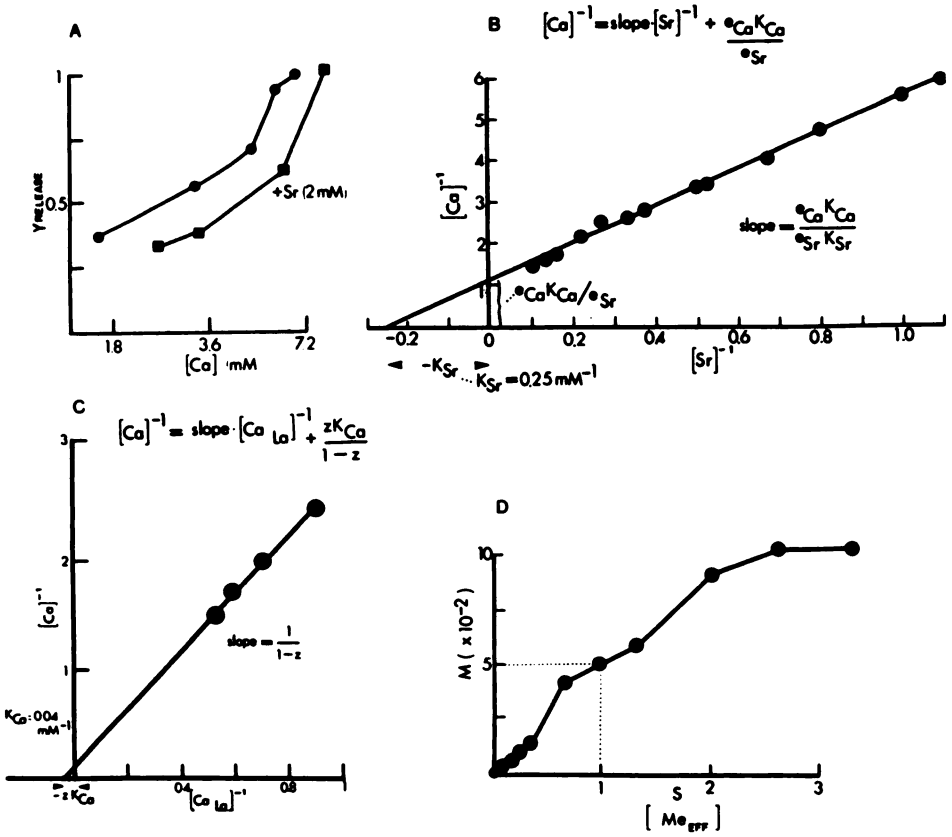

FIG. 6. Mathematical equations of receptor theory as applied to Ca and Sr. A, Sr as a competitive inhibitor of Ca in synchronous ACh release. B compares concentrations of Ca and Sr that produce equal M. C compares concentrations of Ca in the presence and absence of La that produce equal M (see text for further details). D shows a decoder curve that links stimulus ($S_{ME} = e_{ME}\, y_{ME}$) to response (M). It was created for Ca on the spare receptor assumption as follows. $S = 1$ is arbitrarily defined at the concentration of Ca that produces a half-maximal response [Ca_{50}]. S = 0.5, 2 or 3 is thus 0.5 [Ca_{50}], 2 [Ca_{50}], or 3 [Ca_{50}], respectively, (as on the spare receptor assumption, the denominator of the y_{CA} expression reduces to 1 and e_{CA} and K_{CA} are constants). Next, each [Ca] was converted into a value for S using eqn 10 and S was then plotted against the experimentally measured M in that [Ca]. S may also be viewed as the intracellular effective concentration of Ca or Sr ([Me_{EFF}]) at synchronous release sites. For further details, see text and ref. 240, p. 424. Reprinted with permission from Silinsky (240, 241).

those observed experimentally. Finally, the theoretical curves based on the mathematical framework of receptor theory were reconsidered in accordance with the known properties of Ca binding proteins and the thermodynamic equations of sequential biochemical reactions.

To use the Schild equation properly for Sr as a competitive inhibitor, it is first necessary to reduce the efficacy of Sr to 0 (see 90, 51, 253); this was accomplished by pretreatment with the irreversible Me antagonist La. Figure 6A shows the competitive inhibition of Ca dependent M by Sr, reflected as a parallel shift to the right of the log [Ca]-$y_{RELEASE}$ curve in the presence of Sr. The K_{SR} calculated by the Schild equation was 0.27 mM^{-1} (table 2).

There are several methods to calculate the K_{SR} as a partial agonist on the spare receptor assumption. Basically, these equations, and all equations used by the receptor pharmacologist to study *physiological events*, are derived from the same single assumption demonstrated in eqn 10a, namely, equal stimuli produce equal responses. After incorporating the spare receptor assumption, the equations are then rearranged in the form of a straight line to obtain estimates of K_{ME} and e_{ME} (figures 6B and C).*

For example, using the spare receptor assumption on eqn 10a (see also appendix A 2) produces:

$$\frac{1}{[Ca]} = \frac{e_{CA}K_{CA}}{e_{SR}K_{SR}[Sr]} + \frac{e_{CA}K_{CA}}{e_{SR}} \qquad \text{eqn 10c}$$

Eqn 10c describes a straight line that compare matching M produced in Ca and in Sr; the reciprocal of the [Ca] is the abscissa and the reciprocal of [Sr] that produces an equal M is the ordinate (253). The experi-

* The spare receptor assumption (252) as applied to y_{CA} may be stated as follows: If spare Ca binding sites are present over a certain range of low [Ca], then, as the K_{CA} for an agonist is low (a generally observed phenomenon when the K_{ME} is calculated for the ligand as a full agonist), the product of [Ca] $K_{CA} \ll 1$. Under these conditions, [Ca] K_{CA} is insignificant in the denominator of eqn 1 when compared to 1. Eqn 1 thus reduces to

$$y_{CA} = [Ca]\, K_{CA} \qquad \text{eqn 11}$$

for the full agonist on the spare receptor assumption.

mental log [Me]-M curves when plotted in accordance with eqn 10c followed the predicted straight line (figure 6B). At $1/[Ca] = 0$, then K_{SR} may be determined as $1/[Sr] = -K_{SR}$. (As is shown in figure 6B, the K_{SR} may also be estimated by the ratio of the intercept to the slope.) The K_{SR} in this experiment was 0.25 mM^{-1} (the mean of all experiments was 0.26 mM^{-1}; see table 2). Another method for determining K_{SR} on the spare receptor assumption is to compare matching M in Ca and in Ca + Sr solutions (eqn 13; appendix A 2). At its limits, when $e_{SR} = 0$, eqn 13 reduces to the Schild equation. The mean K_{SR} calculated by this method was 0.24 mM^{-1} (table 2). The first three values for K_{SR} listed in table 2 are statistically indistinguishable and are thus independent of the method of calculation if equal M's are compared. These results provide additional evidence for the presence of spare Ca receptors, since methods which invoke the spare receptor assumption produce the same K_{SR} as those that do not require this assumption.

What is the value of K_{CA} as calculated from receptor theory? It may be somewhat surprising to the reader, but there is only one valid equation for calculating the affinity for the full agonist. It is derived by comparing *equal M* before and after irreversible blockade of a significant number of receptor sites (89, 266, 51, 253) and assuming that *equal M* reflects *equal S* (for details, see appendix A 3). As applied to irreversible block by La, this equation (eqn 14) is shown below and in simplified form in figure 6C. Thus

$$\frac{1}{[Ca]} = \frac{1}{1-z}\frac{1}{[Ca_{LA}]} + \frac{zK_{CA}}{1-z} \qquad \text{eqn 14}$$

where $[Ca_{LA}]$ is the concentration of calcium after irreversible blockade that produces matching M to [Ca] before irreversible blockade; z is the fraction of receptors irreversibly blocked by La. This equation describes a straight line. As figure 6C shows, z may be estimated from the slope and at $1/[Ca] = 0$, $1/[Ca]_{LA} = -zK_{CA}$. K_{CA} was found to range between 0.02 and 0.06 mM^{-1} (240). This value is 1.5 orders of magnitude lower than the affinity calculated by extrapolation methods and over 2 orders of magnitude lower than the K_{CA} as a competitive inhibitor. These discrepancies will be discussed below and in appendix A 3. For the present purposes, it appears that Ca has a very low affinity as a full agonist, a result consistent with the spare receptor assumption.

With regard to efficacy, the scale is set by the following convention: a partial agonist, which occupies all the receptors and produces a response half that produced by a full agonist, has an efficacy of one. Thus $S = 1$ at the [Ca] that produces a 50% maximal response ($[Ca_{50}]$) (252). Then by rearranging eqn 10 and on the spare receptor assumption:

$$e_{CA} = 1/(K_{CA}\,[Ca_{50}]) \qquad \text{eqn 15}$$

Thus e_{CA} may be determined from the measured $[Ca_{50}]$ and the calculated K_{CA}; e_{CA} values ranged from 9 to 20 (240).

To determine e_{SR}, note that the intercept of eqn 10c is equal to $e_{CA}K_{CA}/e_{SR}$. Rearranging eqn 15

$$[Ca_{50}] = 1/e_{CA}K_{CA} \qquad \text{eqn 15a}$$

Thus

$$e_{SR} = ([Ca_{50}] * \text{intercept of eqn 10c})^{-1} \qquad \text{eqn 16}$$

The e_{SR} values determined from equation 16 ranged from 0.2 to 0.5 (240).

Although these values for e_{SR} are in excellent agreement with those of Meiri and Rahamimoff (175), the concordance is fortuitous (see appendix A, 5).

iii. Constructing theoretical curves for ACh release in Ca and Sr solutions. Using these experimentally determined values of e_{ME} and K_{ME} and the assumption that complexities in the log [Me]-M curves lie beyond S, it should be possible to obtain a decoder curve to calibrate the complex relationship between S and M by *using the Ca-M curve on the spare receptor assumption* (252). This curve should serve to link stimulus and response for any agonist. Such a curve is shown in figure 6D; it was created by calculating S at each [Ca] in accordance with $S_{CA} = e_{CA}[Ca]K_{CA}$ (the equation for S using the spare receptor assumption—see eqn 11a, appendix A 2) and then by plotting the calculated S against the experimentally observed M (see figure 6 legend for further details). At each concentration of Ca, the curve of figure 6D was then used to obtain the theoretical log[Ca]-M curve shown in figure 2A (dashed line through circles). Note that the theoretical curve shown in figure 2A is in excellent agreement with the experimental results for Ca (circles). More significantly, however, as the [Sr] is varied and S calculated at each [Sr] by $S_{SR} = e_{SR}y_{SR}$ (eqn 10), the calibration curve of figure 6D accurately predicts the experimental results in Sr solutions (the dashed line in figure 2A is the predicted [Sr]-M relationship). These results provide strong support for the notion that the quantitative behavior of motor nerve ending resembles that of a pharmacological Ca receptor (240, 241). A mathematical description of the S-M curve (e.g. figure 8B) will be provided below.

iv. Physical correlates of affinity and efficacy. From the observation of spare Ca channels in mammalian brain and spare Ca receptors, X, at the motor nerve ending, it appears that the X site, and thus K_{ME} and y_{ME}, refers to the external surface of the Ca channel [see figure 7A (240, 241)]. The evidence that Me agonists and antagonists interact at a common extracellular site prior to coupling depolarization to secretion supports this contention (133, 178). (For further discussion see ref. 240 and section VI.) By this view, spare receptors are equivalent to spare Ca channels. With respect to efficacy, namely, the events beyond the external Me binding it

has been suggested that e_{ME} may reflect the mobility of the ion in the Ca channels (175, 237). An alternative perspective has emerged, however, as a result of experiments in my laboratory in which Ca, Sr, and Mg were delivered to the nerve terminal cytoplasm by using liposomes as a vehicle (133, 178). We have found that when Ca channels are bypassed, the selectivity pattern of Ca > Sr > Mg is preserved at an intracellular locus associated with *M*. This selectivity was not due to the differential binding of the Me species within the phosphatidylcholine liposomes (see ref. 178). As a result of these liposome studies, it was suggested that efficacy for *M* represented the *intraterminal* affinity of Me for a calcium binding protein (fig. 7A, bp) associated with synchronous ACh release (240, 241, 178); thus $e_{CA} > e_{SR} > e_{MG}$ reflects decreasing apparent affinity at an intracellular site necessary for *M*. A recent study on squid giant synapse has provided support for this suggestion; the selectivity sequence of Ca > Sr > Mg for *M* also occurs at an intracellular locus in this non-cholinergic synapse (8).

By the results described in this section, Ca, the full agonist produces maximal *M* using only a minor fraction of the total number of Ca channels (low y_{CA} at site *X*). This is possible because the high intracellular affinity at bp allows Ca to be concentrated at strategic intracellular regions at the active zone. The localized intracellular Ca can then catalyze the fusion of the synaptic vesicle with the nerve ending in temporal harmony with the action potential. Sr, the partial agonist of low efficacy has low affinity at the intracellular bp. Sr must thus use all the Ca channels to produce an order of magnitude smaller *M* because, by virtue of its low intracellular affinity, only moderate amounts of Sr can be concentrated at strategic releasing regions. It is of interest in this regard that Me selectivity is conferred on artificial secretory systems only when a Ca binding protein is incorporated into the

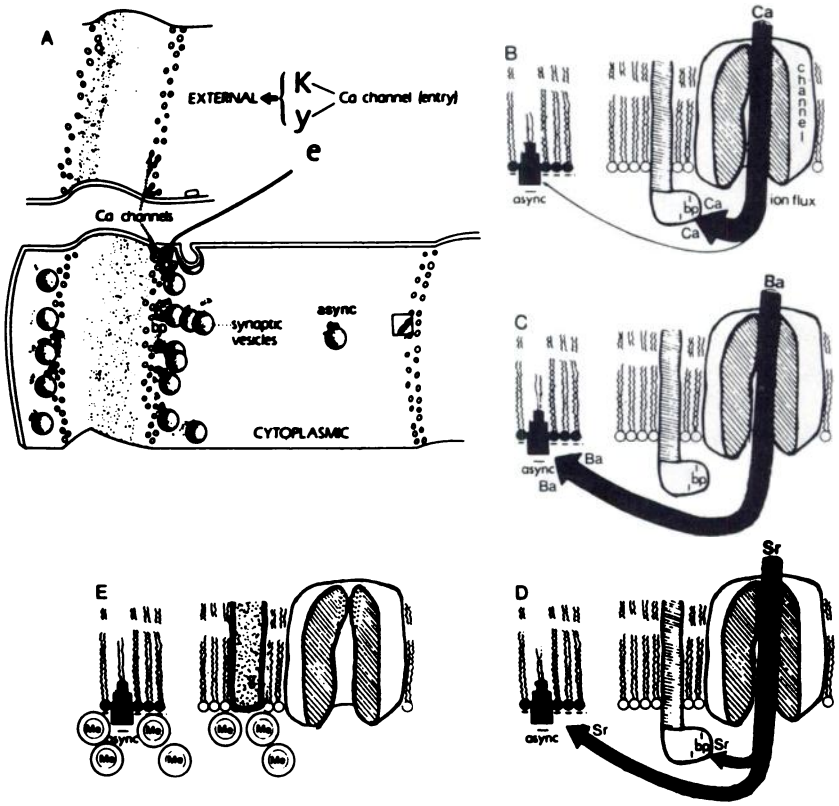

FIG. 7. Possible structural correlates of Me function in nerve endings. A shows the details of the morphology of an active zone (see e.g. figure 1B and ref. 41). At the external surface, paired rows of particles thought to represent Ca channels are shown. The internal openings of these channels, synaptic vesicles in different stages of membrane association, and the hypothetical Ca binding protein (bp) are shown at the cytoplasmic surface of the nerve ending. Asynchronous release (async) is illustrated outside the active zone (41, 248) although it also occurs at the active zone (41). Sketches B to E, which represent an enlarged view of a small part of the active zone, provide a possible explanation for the behavior of Me agonists in the processes of synchronous (*M*) and asynchronous release. In B to D, the nerve terminal is depolarized by an action potential and Ca, Ba, or Sr is shown entering the nerve ending cytoplasm through an open Ca channel. The magnitude of *M* is determined by the Me affinity for bp (shown in its active state), with the residuum of cation that is not bound to bp stimulating more distant asynchronous release sites. Nerve stimulation is not a prerequisite for asynchronous release to occur (41, as is illustrated in E). E shows an inactive bp, such as might occur in the absence of nerve stimulation or with prolonged depolarization (e.g. high K). Under these conditions, release occurs non-selectively in accordance with Me valency and is likely to occur by screening as the ions are not consumed by binding to active bp. Although bp is shown in association with the plasma membrane, Ca binding proteins associated with synaptic vesicles could also serve to buffer or "consume" Me. For further speculations, see ref 248.

equivalent of the nerve terminal membrane i.e., into the planar bilayer in liposome-planar bilayer fusion studies (see ref. 280 and section IV).

What fraction of the Ca channels is required to produce maximal M? With the value of $K_{CA} = 0.025$ mM^{-1} and the observation that in some experiments maximal M was obtained at a [Ca] as low as 3.6 mM (figure 5A, ref. 240), then by eqn 1, maximal M may be achieved by using only about 8% of the Ca channels, in turn leaving 92% spare.

What then is responsible for the complex relationship between S and M? This has been speculated to result from the complex relationship between intracellular Me in the vicinity of bp and calmodulin, or other Ca binding proteins, demonstrated on the synaptic vesicle (193, 231, 240, 241) and in other parts of the nerve terminal (70; see also section V B). It is of interest that calmodulin antagonists have been found recently to inhibit evoked but not spontaneous ACh release at cholinergic nerve endings (207, 256, 232).

v. Relationship of synchronous to asynchronous release. The discussion thus far concerns M, the synchronous release of ACh in response to a nerve impulse. Any model that professes to explain Me function must also provide a plausible explanation for Me-dependent asynchronous release as well. It has already been shown in section II B that the extracellular Me selectivity sequence for asynchronous release *by nerve impulses* is Ba > Sr > Ca, the opposite selectivity to M (248). When a asynchronous release is evoked, *not* by nerve impulses, but by liposomes (178), ionophore (134), or high K (177), all Me species appear equipotent. A model from my laboratory, based upon experiments made with A. M. Mellow and B. D. Perry is illustrated (178) in figure 7 B to E. As all forms of evoked release are mediated by the Ca channel, each record focuses on the internal surface of the Ca channel. In figure 7B, Ca enters the nerve terminal in response to an action potential and is adsorbed to a Ca binding protein (bp), which is assumed to be in an active state for M only transiently after the nerve impulse (55, 200, 208, 214, 248). The high affinity intraterminal Ca binding illustrated in figure 7B is reflected in the high e_{CA} and by the high potency of intracellular Ca (e.g. Ca liposomes) for M. Once bound to Cabp, Ca promotes synchronous release, and is then cleared from the nerve ending (30, 212). Thus, the high affinity binding to bp, in effect, "consumes" Ca that has entered the nerve ending and prevents Ca from further participation in the secretory process. By this view, Ba, which does not support M (235, 237), is not consumed by bp (figure 7C) and is free to move without restriction to more distant asynchronous release sites within the nerve ending (labeled asynch in figure 7 A to E). This behavior is reflected electrophysiologically in the outpouring of MEPPs produced by nerve stimulation in Ba solutions. Extracellular Sr is intermediate in effect between Ca and Ba for M and MEPPf. Thus some of the entering Sr is bound by bp (figure 7D) in proportion to e_{Sr} and supports M while the unencumbered fraction produces asynchronous release. When the bp is not active (figure 7E), (e.g. when asynchronous release is evoked by Me-containing liposomes or when prolonged depolarization is produced by high potassium), then the Me species are equipotent as these ions are not consumed by high affinity binding.

By this model, then, selectivity of extracellular Me species for MEPPf is only apparent and actually reflects Me concentration differences in the region of asynchronous release sites; these concentration differences are produced by selective binding of the translocated cation to sites associated with M (i.e. bp in figure 7). If this is true, then it is likely that increases in MEPPf are produced non-selectively by Me screening of intraterminal fixed negative charges. This will be discussed more fully in section IV.

Recent publications from other laboratories support this view (41, 255). Proteins that might confer Me selectivity are found in the active zone near the cytoplasmic openings of Ca channels, and exocytotic profiles associated with asynchronous release have been observed along the entire length of the nerve ending and not exclusively at the active zone (41). Finally, strong support for the notion that intracellular binding limits ion diffusion has been provided in a recent theoretical paper (255).

vi. Additional properties of the Ca receptor model. Why does Ca have a high affinity as an antagonist yet a low affinity as an agonist? It may be argued teleologically that, as Ca must be present at the external surface of the nerve ending prior to depolarization to support M (125), then the high affinity would tend to concentrate Ca strategically at X sites prior to the arrival of an action potential (figure 8A 1; see ref. 100 for justification). When the membrane is depolarized by an action potential (AP) (figure 8A 2) a low K_{CA} would be more profitable physiologically as high affinity could retard Ca entry (52) during the fleeting Ca conductance change that follows the action potential.* Figure 8A 2 illustrates the changes in the Ca channel and bp conformations upon depolarization (see figure 8 legend).

One of the deficiencies of the approach to secretion taken by this author is the vagueness of the term efficacy. The calculated values of efficacy may be put into a more

*One physical explanation for these different affinity states relates to the coordination chemistry of Ca and is presented in the concluding section of the review (VI B). Another explanation is that, in addition to the high affinity external Ca binding site detected by the Schild equation (eqn 2) using Ca as an antagonist, there is a subsequent high affinity site for Ca beyond the external surface of the Ca channel (see ref 240, page 426). This would make the affinity for Ca as an agonist an apparent Briggs-Haldane constant (240, 233) whereby a second stage of Ca binding in the channel is also included in the overall Ca affinity and lowers the measured affinity substantially. This interpretation is consistent with the results of Hess and Tsien (107a), who studied Ca currents in isolated heart cells. For other possibilities, see appendix A 3.

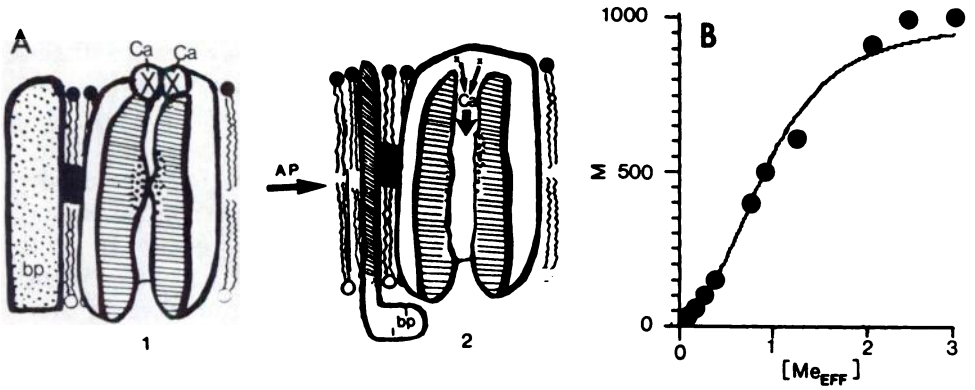

FIG. 8. Additional aspects of the Ca receptor model for synchronous ACh release. A shows site X that controls entry at the external surface of the Ca channel and the bp (a speculated linkage of bp to a gating site in the Ca channel is illustrated by the blackened strip). In A1, depolarization has not yet occurred and Ca is shown bound to X with high affinity; the Me channel is closed and bp is in an inactive state. In A2, the action potential (AP) opens the Ca channel and also activates bp. The speculated effect of the AP in activating bp is illustrated as a voltage dependent "squeeze" of the Ca binding "foot" of bp into the cytoplasm. Ca then enters the terminal, adsorbs with high affinity to the freshly activated bp, and promotes exocytosis. For further details and other alternatives, see footnote, sections III A3 and VI B, Appendix A3, and refs. 240, 241, 248. B shows a theoretical [Me_{EFF}]-M curve calculated from Adair-Pauling simple sequential model of cooperativity (for the units of [Me_{EFF}] and other details see appendix A 9). The curve in A was drawn to eqn 44a (appendix A 9) by an Apple IIe computer system. Points (●) are from the Stimulus-M decoder curve in figure 6D. Note that this model provides a reasonable description of synchronous ACh release.

useful quantitative framework if it is realized that e_{ME} values are of the same magnitudes as the relative effectiveness of an Me species for synchronous and asynchronous ACh release. If this is so, then it is possible to define an effective normalized intracellular Ca concentration, [Ca_{EFF}] at synchronous release sites as follows: $[Ca_{EFF}] = [([Ca]K_{CA})/(1 + [Ca]K_{CA})]$ (availability for bp/MEPPf) where the availability of Ca at bp/MEPPf = e_{CA}. In a general sense, the Me delivered to the cytoplasm as a result of y_{ME} is partitioned intracellularly in accordance with e_{ME} into synchronous and asynchronous release. The [Me_{EFF}] (i.e. Ca_{EFF} or Sr_{EFF}) is thus linearly related to extracellular Me occupancy and the complexity in the log [Me]-M relationship is introduced in the relationship between [Me_{EFF}] and binding proteins at the vesicular membrane or nerve terminal membranes. What is the nature of this relationship? It was suggested independently by two laboratories (240, 22) that a sequential binding model for multiple site enzymes (1, 204, 139, 233) might explain the shapes of the [Me]-evoked ACh secretion curves. The theoretical Me_{EFF}-M curve constructed on such a model by using four sites is shown in figure 8B. (The details are provided in appendix A 9.) Note the similarity between stimulus-M curve (figure 6D) and the theoretical [Ca_{EFF}]-M curve (figure 8B).

In conclusion, it appears that the concept of spare Ca channels when applied in conjunction with the mathematical theory of the drug-receptor interaction provides an accurate description of evoked ACh release at the frog neuromuscular junction.

C. THE KINETIC MODEL (HUBBARD AND COLLEAGUES). This model was proposed by Hubbard, Jones, and Landau in 1968 (116, 117) at approximately the same time as the fourth power model, but was based upon experiments in mammalian muscle. Hubbard et al. began with the same initial framework, namely eqn 1 (Michaelis-Menten kinetics) but elaborated upon the equations considerably. This expansion was necessary because spontaneous and evoked release were both affected by alterations in [Ca] and [Mg] in this mammalian preparation (rat phrenic-nerve hemidiaphragm). In the frog, similar effects of extracellular Me on spontaneous release were not observed unless the terminals were depolarized extrinsically.

The model used by Hubbard et al. is similar to that used by chemists to describe the ionization of phosphoric acid. Much as the phosphate moiety can be protonated in three successive steps, each with its own proton affinity constant, the X site can have its properties altered by sequential "calcification" into states with 1, 2, or 3 Ca bound and with effective affinity constants K_{CA1}, K_{CA2}, K_{CA3} as follows:

$$\begin{array}{ccccccc} & K_{CA1} & & K_{CA2} & & K_{CA3} & \\ & +\,Ca & & +Ca & & +Ca & \\ X & \rightleftarrows & CaX & \rightleftarrows & Ca_2X & \rightleftarrows & Ca_3X \\ \downarrow & & \downarrow & & \downarrow & & \downarrow \\ k_0 & & k_1 & & k_2 & & k_3 \end{array}$$

This is thus a four state model: a bare site X and singly, doubly, or triply occupied X sites (for mathematical details, see appendix A 6). The efficacy of each state in producing ACh release is represented by the magnitudes of the rate constants (k_0–k_3). The situation for spontaneous release is illustrated above, with the relative length of the arrows indicating the relative efficacy of that state. This scheme explains the predominant dependence of MEPPf on the first power of the Ca concentration in this preparation but also explains its dependence on other complexes (especially Ca_3X). The nerve impulse

is believed to produce an enormous rise in the value of k_3 (a millionfold increase restricted to a period of a millisecond). This would be responsible for the approximately third power relationship of evoked release on Ca (the limiting slope of the log M-log [Ca] plot was =2.7). This result contrasts with the fourth power (or possibly even a higher power, ref. 270) relationship seen at frog neuromuscular junctions. The model also proposes a fraction of spontaneous release that is not dependent upon Ca (unliganded site X with efficacy k_0). Mg is believed to compete with Ca at all the occupied sites but, as Mg could also weakly support increases in MEPPf in the absence of extracellular Ca, it may be described as a partial agonist in this system.

The basic equation for the fraction of binding sites occupied, eqn 21, is

$$y_{CA} = \text{the sum of the bound states}/X_T = \frac{[Ca]K_{CA1} + [Ca]^2K_{CA1}K_{CA2} + [Ca]^3K_{CA1}K_{CA2}K_{CA3}}{1 + [Ca]K_{CA1} + [Ca]^2K_{CA1}K_{CA2} + [Ca]^3K_{CA1}K_{CA2}K_{CA3}} \quad \text{eqn 21}$$

(For complete derivation, see appendix A 6.) Now, if Michaelis-Menten kinetics are assumed (233), whereby maximal ACh release is defined as = $k_N X_T$; then inserting the rate constants of the above "calcification" scheme into eqn 21 produces an expression for the release process:

$$y_{RELEASE} = \frac{k_0 + k_1[Ca]K_{CA1} + k_2[Ca]^2K_{CA1}K_{CA2} + K_3[Ca]^3K_{CA1}K_{CA2}K_{CA3}}{k_N(1 + [Ca]K_{CA1} + [Ca]^2K_{CA1}K_{CA2} + [Ca]^3K_{CA1}K_{CA2}K_{CA3})} \quad \text{eqn 22}$$

The values chosen for the rate and affinity constants were those that minimized the sum of the squared deviations.

Despite the drawback of suffering from a large number of rate and equilibrium constants required to fit the experimental results, the model had considerable thermodynamic justification (138) and provided a more versatile approach to ACh secretion than had been formulated previously. The physical picture presented by Hubbard et al. is one in which the various X species move through the membrane at different rates (k values). Indeed, if Ca carriers mediate ACh release, then in this reviewer's impression, this kinetic model should be the most favored model of ACh release. As experiments with the patch clamp (which allows the picoampere currents through individual ion channels to be recorded) suggest the presence of Ca channels in nerve (105), a model which considers both the extracellular events that initiate ion permeation through Ca channels and the subsequent intracellular behavior of the ion at the secretory apparatus needs to be considered more seriously at present (240, 241, 63). One such model developed for mammalian motor nerve, that of Quastel and his colleagues (53–56, 208, 209), will be considered in part C of this section. It is first necessary to discuss the statistician's approach to ACh release.

B. Statistical Models

The urge to relate the statistical parameters of the *average probability* of release (p) and the *immediately available store of ACh quanta* (n) to the emerging ultrastructural details of the nerve ending provided the impetus for extensive literature on the statistics of transmitter release. Although parts of this section are primarily of historical interest, the results are outlined here as a necessary prelude to subsequent sections of the review. The informed reader, or the reader who has perceived a lack of intrinsic appeal of the subject matter, might prefer to skip to part C with a fleeting glance at figure 9.

1. Evoked release. A. POISSON AND BINOMIAL STATISTICS. In their classic 1954 paper, Castillo and Katz (67) suggested "... suppose we have, at each nerve-muscle junction, a populations of 'n' units capable of responding to a nerve impulse. Suppose further that the average probability of responding is 'p' ... then the number of units responding to one nerve impulse is:

$$M = n \cdot p \ldots" \quad \text{eqn 23}$$

where, M as before, is the mean number of ACh quanta released synchronously. Initially, it was suggested that n represented the number of synaptic vesicles immediately available for release and p was related to Ca concentration. For example, if $p = 0.5$ then each synaptic vesicle would be, in effect tossing a coin, deciding whether to release or not release in response to a nerve impulse (e.g. if "heads" = release). By eqn 23, if there were $n = 200$ quanta immediately available for release and $p = 0.5$, then, on the average, there would be $M = n \cdot p = 100$ quanta released by a nerve impulse. Envisaging transmitter release as a quantal coin-tossing exercise in which the vesicle has two choices, release or not release, makes secretion a study in binomial statistics. Now imagine a very large number ($n > 1000$) of quanta are "tossed" and instead of coins, vesicles were 20-sided objects in which only side 1 produced release, i.e. $p = 1/20 = 0.05$. Under these conditions, as the probability of any one vesicle releasing its contents becomes very low, the binomial distribution changes its form. Specifically, if one uses low Ca/high Mg solution to block neuromuscular transmission, then "... under these conditions, when p is very small, the number of units x which make up the EPP in a large series of observations should be distributed in the characteristic manner described by *Poisson's law* ..." (67). Both binomial and Poisson distributions are discrete distributions in which the value of M for each trial is an integer (e.g. figure 1A(1) where 0, 1, 2, 3, 4, or 5 quanta are released by a nerve impulse) and is independent of other events. Poisson statistics, however, describe events that are very rare, i.e., random events in space or time. The Poisson distribution may be derived from the

binomial by taking the exponential limits as p approaches 0 and n gets very large.

According to Poisson's law, the probability of observing 0, 1, 2, 3, or x quanta released (p_x) is described (50, 122, 171) by:

$$p_x = \frac{\exp(-M)M^x}{x!} \qquad \text{eqn 24}$$

The M is determined as the ratio EPP/MEPP (figure 1A(1)) and is independent of the particular statistical distribution. With the experimentally determined value of M, eqn 24 may be used to predict the theoretical probability of observing 0, 1, 2, 3, or x quanta released. The predictions are then compared with the histogram of evoked responses to determine how accurately the observed synchronous release distribution obeys Poisson statistics. Poisson's law also predicts that M can be calculated from the number of stimuli that *fail* to produce ACh release (much as the mean number of red blood cells may be determined by counting the number of *empty* hemocytometer squares). Specifically, the probability of observing 0 quanta released (p_0) = the number of stimuli that fail to release (= failures)/the total number of stimuli delivered. Substituting $x = 0$ into eqn 24, then (50, 122, 171)

$$M = \ln \frac{\text{number of stimuli}}{\text{number of failures}} \qquad \text{eqn 24a}$$

Finally, for Poisson distributions (50, 122, 171)

$$M = \text{Variance} \qquad \text{eqn 25}$$

i.e., the mean is equal to the variance of the number of quanta released by each nerve impulse. At the vast number of synaptic junctions studied in low Ca/high Mg solution, M determined by eqn 24a and 25 agreed with M determined from measuring the ratio of EPP to MEPP, and the observed distributions were accurately described by Poisson statistics. In a practical sense, eqns 24a and 25 are frequently used to measure M at ganglionic synapses where measurements of MEPSPs are time-consuming due to their low rate of occurrence (e.g. 28, 246).

It appears from eqn 24 that Poisson's law describes only a single parameter, M, with n and p having no distinct meaning. To illustrate, if one looks at the random decay of radioactive nuclei, the mean number of disintegrations per second is finite (e.g. $m = 2$) because it is the product of an infinitely large number of nuclei ($n = 10^{20}$), each with an infinitely small average probability of decay ($p = 2{*}10^{-20}$). To obtain estimates of n and p at cholinergic nerve endings, it is necessary to change the experimental conditions.

"... What happens under more normal conditions when we raise the Ca and lower the Mg concentration? The value of M becomes large and the statistical analysis unsatisfactory .... Now suppose the size of the population n remains constant, then the increase in M would be due to an increased probability p. If the population is uniform, the distribution of responses would change from a Poisson to a binomial form ..." [Castillo and Katz (67)]. If quantal release is distributed binomially, then the probability of observing x quanta released is (50, 171)

$$p_x = \frac{n!}{x!(n-x)!} p^x(1-p)^{n-x} \qquad \text{eqn 26}$$

where p is again, *the average probability of release of a single quantum* (e.g. $p = 0.5$ if tossing heads on a quantal coin produces release) and n is the number of quanta immediately available for release. It is apparent that in this binomial distribution, which actually represents the number of ways of combining n quanta x at a time, both n and p are required to describe the distribution. If the experimental results follow a binomial distribution, then p may be determined independently as

$$p = (1 - \text{Variance})/M \qquad \text{eqn 27}$$

for binomial distributions (50, 95). Thus, with M and Variance of the individual evoked quantal responses measured from the experimental results, p can be determined from eqn 27. As $n = M/p$ (eqn 23) n may be estimated as well.

These convenient properties of binomial distributions (95) have served as the impetus for a number of studies on the statistics of transmitter release (21, 36, 186, 271, 282). Indeed, as M was raised, the experimental results at a variety of peripheral cholinergic synapses appeared to obey binomial statistics and to provide values for n and p and the nerve ending (21, 36, 186, 271; for review, see ref. 171). The calculate values of n and p did not agree with the number of synaptic vesicles at active zones, however, as a typical published value of $n = 124$, $p = 0.47$, and $M = 58$ (ref. 271, table 6) will illustrate. While this p value is consistent with the coin-tossing analogy, the value of $n = 124$ presents a problem as it is 2 orders of magnitude less than the number of synaptic vesicles at the active zone and 3 to 4 orders of magnitude less than the total number of synaptic vesicles in the nerve terminal (41, 95). Based on evidence that n correlates directly with the length of the nerve terminal, it was suggested that n represents the number of active zones of release which are occupied by synaptic vesicles (282, 271). This suggestion, based on the assumption that no more than one quantum is released per active zones, initially provided an intellectually agreeable view of the secretion process. Unfortunately, the experimental results did not coincide with this simple interpretation. For example, when Ca is raised, both n and p were found to increase (36, 21, 171). It is not difficult to envisage Ca increasing the probability of release, but an increase in the number of active zones is not consistent with the fixed morphology of the nerve terminal in these different Ca solutions. In addition, the decline in ACh release

during high frequency stimulation was associated with a reduction in both n and p while the increase in ACh release during repetitive stimulation in low Ca/high Mg solutions was related to a rise in both n and p (see ref. 171 for review). One could propose a more complicated scheme whereby n = release sites with filled vesicles and adequate Ca (171) and p represents a complex, compound probability, e.g., the probability that a release site will be occupied by a quantum *and* the probability that a nerve impulse will activate the occupied release site (98). The simplicity of the original proposal is lost in such statistical manipulations, however. Finally, under some conditions (e.g. stimulation in 4-aminopyridine, which increases the duration of nerve terminal depolarization), a single stimulus releases 1.5 to 2 orders of magnitude more quanta than the number of release sites (109). It is not easy to relate n to the number of active zones in this instance, although it is possible that under these conditions the action potential is sufficiently long that the active zone can recycle several times.

The main difficulty with the binomial approach to secretion was proffered as a caution in the 1954 Castillo and Katz paper (67): "The other factor which may be involved is that different members of the same population may *not* have the same chance of success and that for large values of M some individual units have a high probability and respond almost every time, while others have a low probability and contribute to the EPP only occasionally . . . ." In such a non-uniform population, it is impossible to obtain reliable estimates of n and p (39, 18). This is because the simple binomial approach requires that p is the same for all releasing structures and that both n and p are constant during the experiment (39). Suppose for example that instead of quantal coins (where p = 0.5) *or* quantal dice (in which, if only 1 = release, p = 1/6 or 0.128), the nerve ending contained *both* coins and dice. Under these conditions, there exists a non-uniform population of quanta in which some quanta (coins) have a much greater likelihood than other quanta (dice) of being released. Non-uniform populations can produce experimental histograms that are statistically indistiguishable from a binomial distribution; however, the values of n and p may be so much in error that the use of eqns 26 and 27 would be unjustified (39, 18). For example, it might be that quanta closer to the nerve terminal membrane have a higher probability of release than more distant quanta or that some release sites are more active than others. If this is true, then binomial estimates of p would be biased towards higher probability by the proximal quanta or the more active sites and n would thus appear smaller because it would be associated with quanta or sites of high p, which are much fewer in number than the total population. The problem becomes exacerbated when the effect of a particular experimental perturbation on n and p is examined. Even if that perturbation increased only p, a change in the uniformity of the distribution as might be produced by a depletion of quanta with high p would produce a falacious increase in n as well as p (39). Finally, even small variations in n over space or time will produce errors in estimation of n (39, 18, 171). As a number of studies suggest that p and/or n may vary spatially or temporally (18, 22, but see ref. 16), then the simple binomial distribution appears to be an unsatisfactory means of quantifying ACh release *in the absence of any estimate of the variance of p.* Because of the problems just outlined, binomial statistics will be discussed no further in this review. The precise methods, cautions, and references to the large literature on the subject may be found in excellent reviews by Martin (167), McLachlan (171), and Barrett and Magleby (15).

B. DISTRIBUTION OF LATENCIES. The individual EPCs recorded with the focal extracellular microelectrode at low M have a highly variable latency between the downward-going peak of the ntp and the beginning of the EPC (figure 9A). The latency represents a synaptic delay due almost exclusively to Ca entry and the subsequent reduction of an energy barrier by intracellular Ca (123, 14). The fluctuations in latency are thought to reflect the essentially probabilistic nature of the transmitter release process after a nerve impulse (122, 123, 17) and, when plotted as a histogram (figure 9B) provide a picture of the rise and fall of "phasic" quantal release probability over time. It is not known to what degree this probability reflects the parameters n and p of the binomial distribution (15) although the assumption that it reflects p has been made (see table 4). Studies on the temperature and ionic dependence of the phasic-release histogram suggest that phasic release (and thus M) is related to a chemical reaction associated with the binding of Ca and Sr inside the nerve ending (17, 64). It is of interest that reducing the extracellular Ca concentration (figure 9B, lower curve) or substituting Sr for Ca, while altering the magnitude of phasic secretion, did not affect the time course (64).

The complex curves such as shown in figure 9B may be described by a variety of mathematical functions whose names cover the gamut of the Greek alphabet (e.g. gamma functions, alpha functions, beta density distributions, etc.). With respect to the secretion of ACh, the general curve resembles an alpha function (119), which Edwards, Hirst, and Silinsky (81) used to describe synaptic currents produced by ACh release in mammalian ganglion cells. The form of the alpha function used at mammalian ganglia was a simple one in which the synaptic current was proportional to $t \exp(-\text{alpha } t)$ where alpha is the reciprocal of the time to peak. The results of Datyner and Gage (64) shown in figure 9B may be fitted by

$$P \propto t^4 \exp(-3.8t) \qquad \text{eqn 28}$$

where P represents the probability density (see next section). Figure 9C shows computer-drawn curves of eqn 28 with the upper curve being described by $P = 54.6t^4\exp(-3.8t)$ and the lower curve by $P =$

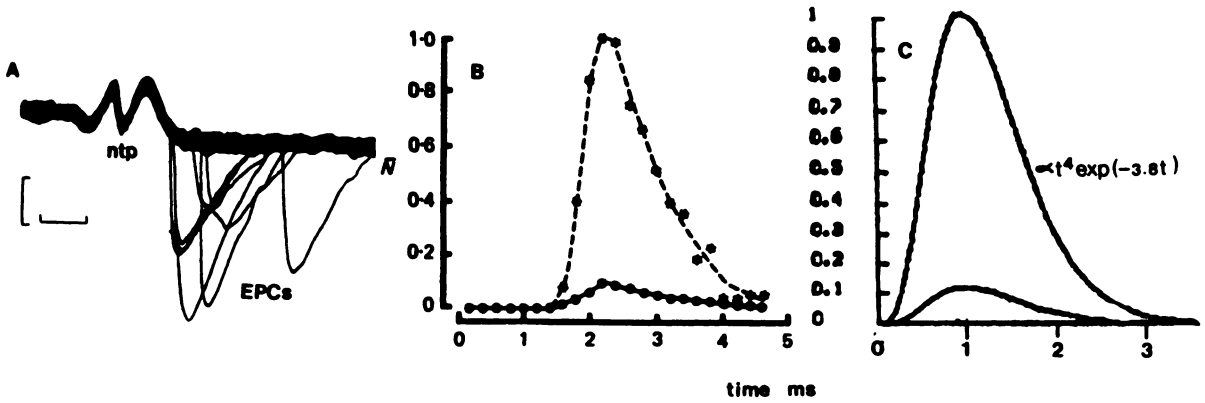

FIG. 9. Evoked ACh release as determined from latency fluctuations. A shows 35 consecutive traces of responses recorded with a focal electrode (see e.g. figure 1A), at the rat neuromuscular junction. Note the fluctuations in latency between the ntp and the individual EPCs. Calibrations: 100 μv, 1 msec. B shows two histograms made from experimental records such as those in A. The latency between the ntp and beginning of the EPC (msec) is plotted against the number of observations, $\bar{N}$ ($\bar{N}$, is actually the probability normalized to the maximal probability in 1 mM Ca). Such phasic secretion histograms vary in amplitude but not in time course when Ca is raised from 0.5 mM (B, lower curve) to 1 mM (upper curve) or substituted by Sr. [Mg] was 15 mM in for both curves in B. C, theoretical curves drawn to the alpha function. For the upper curve, $\bar{N} = 54.6\ t^4 \exp(-3.8\ t)$ and for the lower curve, $\bar{N} = 6.5\ t^4 \exp(-3.8\ t)$. Note the resemblance of the curves to the actual experimental results (B). It thus appears that the time course of phasic secretion in different [Ca] or [Sr] can be predicted theoretically by changing only the pre-exponential constant. Records in C were drawn by a Sharp model 1500 PC A "pocket" computer. Other investigators have used more complicated functions, e.g. a gamma function for the rise of phasic release and an exponential function for the decay (21) although the mathematician's definition of the gamma function is the integral of an equation similar to that shown in C (see also text, eqn 29 and refs. 16, 17, 21, 64 for more details). A and B were reproduced by permission from Datyner and Gage (64).

$6.5t^4\exp(-3.8t)$. Note the similarities in the rise and fall of experimental histograms made in high Ca (B, upper curve) and low Ca (B, lower curve) to the curves drawn to eqn 28 (C). As phasic release histograms in different Ca and Sr concentrations may be described by eqn 28 with only an alteration of the pre-exponential constant, it appears that differences in [Me]-M relationships for Ca and Sr are not due to differences in the kinetics of activation of the synchronous release mechanism. It may be speculated that the t^4 term could signify the sequential binding of Ca or Sr to four sites involved in controlling M (see figure 8B and appendix A 9). (For other functions that have been used to describe latency histograms, see refs. 16, 17, 21, 22, and table 4).

2. Spontaneous release. In section II A, the MEPP was introduced as a random, spontaneous event. Indeed, it was found that within any arbitrary interval of time (t), a histogram of the number of MEPPs that occurred in time t followed a Poisson distribution at the rat neuromuscular junction, suggesting that spontaneous quantal release occurs as a random process (92). Rather than studying the events themselves, the more usual test for randomness is to study the interval between consecutive events; if these intervals are distributed exponentially, then the process is considered random. Indeed, in their original study, Fatt and Katz (88) found that MEPPs at the frog neuromuscular junction could be fitted to an exponential distribution.

In subsequent studies on both mammalian muscle [Hubbard and Jones (115)] and frog muscle [Cohen et al. (48, 49)], significant deviations of spontaneous release from a simple Poisson process were observed. Both groups applied a series of statistical tests with bellicose titles to discover deviations from Poisson behaviour and concluded that release was more ordered than a Poisson process. Cohen et al. found that their experimental data fit a branching Poisson model, in which the initial release from a site behaves as a Poisson process but then increases the likelihood of subsequent release from that same site. Such a result, in which one quantal event "drags" up the probability of a subsequent event (the drag effect) had been postulated earlier by Martin and Pilar (168) at cholinergic synapses in chick ciliary ganglia (see also ref. 224). The results suggest, therefore that spontaneous release is not strictly a random process. It is possible, however, to retain the physical picture of randomness if one assumes that one active zone releases only one quantum and that MEPPs occur by the random phasing of a fixed number of active zones of release (115).

The discussion thus far has focused on the occurrence of MEPPs in time. What of the distribution of MEPP amplitudes? In the vast majority of studies, the MEPP amplitudes were normally distributed, as one would hope for the natural bell-shaped variation in the size of the quantum (67, 36, 88, 145, 186, 271). Some investigators, however, have found that a *gamma* distribution provides the best fit to the distribution of spontaneous potentials.*

* The gamma distribution may be viewed as the most generalized of all the distributions. Specifically, the probability density (P) of observing a MEPP of size x for a gamma distribution is (171):

$$P = \frac{(\overline{\text{MEPP}}/\text{variance})^K \exp(-\overline{\text{MEPP}}\ x/\text{variance})\ (x^{K-1})}{(K-1)!} \qquad \text{eqn 29}$$

where $\overline{\text{MEPP}}$ is the mean amplitude of the MEPP. (The term probability density is used for continuous functions such as the gamma, normal, exponential, and alpha distributions.) With large values of K,

At present, the difference between a normal and gamma distribution of MEPPS is a small matter compared to the more severe departure from the traditional view of MEPP amplitude distributions described by Kriebel and his colleagues (140). Specifically, it has been suggested that the quantum is in itself quantized, i.e. MEPPs are actually composed of smaller subunits (140, 132). Certainly such subunits have been observed in developing nerve terminals and after drug treatment but the prevalence of subunits in adult muscle is still a matter of controversy (140, 24, 132). Subunits are not part of the evoked release process at frog end-plates (24) and may represent the secretion of quanta that have not been allowed to ripen fully (171) or, speculatively, associated with release from immature nerve sprouts. If vesicles secrete ACh in an all-or-none fashion, then no morphological counterpart of the subunit has been observed at the neuromuscular junction (although there is no reason to exclude the notion that both normal and small MEPPs are produced from vesicles of the same size). If, however, synaptic vesicles have the option either to secrete into the extracellular fluid or deposit their contents into a larger vesicle before secretion—such compound exocytosis has been observed in some secretory systems (75)—then subunit electrophysiological behavior might be predicted. In view of our present state of ignorance, it seems best to admit that subunits are an experimental nuisance and to suggest that pharmacologists might avoid end-plates that reveal subunit behavior. Another deviation from the normal MEPPs are the giant MEPPs that appear in poisoned and regenerating nerve terminals (259); these spontaneous quantal events are resistant to changes in intracellular Ca and may provide a trophic function to the muscle during stages of stress or growth (259).

Finally, there is a form of spontaneous ACh release that is usually ignored by the electrophysiologist, namely non-quantal release (128, 265). Non-quantal release refers to the molecular leakage of ACh from a cytoplasmic pool into the extracellular fluid, possibly in exchange for extracellular choline via the choline carrier (128). Fortunately for the electrophysiologist, non-quantal ACh is not released by nerve impulses (128, 265).

C. A Model That Combines Binding and Statistical Aspects

This model of mammalian neuromuscular transmission by Cooke, Okakamoto and Quastel (53, 208, 54–55) represents a hybrid of several theories presented in earlier parts of section III. In the view of Cooke et al. (53), occupation by Ca of an *intracellular* site associated with release serves as an intermediary between the initiating *extracellular* events associated with Ca entry and the ultimate secretory response of the nerve ending. A simple rectangular hyperbola (eqn 1) is used to describe the intracellular binding and a modification of eqn 1 to describe the delivery of Ca to the intracellular binding site. The distribution of intracellular bound Ca is assumed to be Poissonian (eqn 24); and the rate of secretion is thought to be related to the bound intracellular Ca *exponentially*, as if bound Ca reduces an activation energy barrier for exocytosis. By such an exponential relationship, the *natural logarithm* of the secretory rate (ln MEPPf) is linearly related to the concentration of bound Ca. The essential details of this model will now be presented. The apparent complexity of the equations is really only algebraic, as the derivation in appendix A 7 shows. The reader should be aware, however, that in the original account of this model the *intracellular* site is labeled X and the extracellular membrane sites that move Ca into the terminal (previously termed X in this review) are termed Y sites.

Specifically, the fraction of intracellular X sites occupied, y_{IN}, is by eqn 1,

$$y_{IN} = [CaX]/X_T = \frac{[Ca_{IN}]K_{CA\,IN}}{1 + [Ca_{IN}]K_{CA\,IN}} \qquad \text{eqn 1f}$$

whereby X_T is the total intracellular site concentration, $[Ca_{IN}]$ is the intracellular [Ca] in the region of X, and $K_{CA\,IN}$ is the affinity constant of Ca for this intracellular site (site X in this model is equivalent to bp in figure 7). Thus

$$[CaX] = X_T y_{IN} \qquad \text{eqn 1g}$$

$[CaX]$ is thus directly related to the total number of X sites, the affinity of Ca for the intracellular sites and the concentration of Ca in the vicinity of the intracellular sites $[Ca_{IN}]$. The $[Ca_{IN}]$ is related in turn to the *extracellular* Ca concentration ([Ca]) by

$$[Ca_{IN}] = k_v[Ca_2Y] \qquad \text{eqn 30}$$

where k_v is a constant related to voltage-sensitive Ca entry, and Ca_2Y is a membrane translocation site occupied by *two* Ca ions. Thus by this model, only the Y complex with two Ca ions bound participates in translocation to intracellular site X. (An alternative explanation would be that Ca bound simultaneously to two different parts of the Ca channel is required for permeation.) The equation for the fraction of total number of transport sites occupied, $y_{TRANSPORT}$, is presented in appendix A 7. It is roughly equivalent to that used in the model of Hubbard et al. (eqn 21) only with two sites rather than three. The equation for $[Ca_2Y]$ in the model of Quastel et al. is eqn 21e in appendix A 7; the two affinity constants for this translocation sites are K_{CA1} and K_{CA2}.

The mathematical description for the concentration of bound intracellular Ca ($[CaX]$ is this model) as a function of extracellular Ca concentration is eqn 32:

$$[CaX] = \frac{\text{beta}}{1 + \text{gamma}^2(1/[Ca]^2 + \text{epsilon}/[Ca])} \qquad \text{eqn 32}$$

where, in the terminology of Cooke et al. (53, 208): *epsilon*

the gamma distribution resembles the normal distribution with a slight positive skew. With $K = 1$, the gamma distribution (eqn 29) reduces to the exponential distribution used to describe the interval between MEPPs. At slightly higher K, the gamma function looks like an alpha function (e.g., eqn 28, figure 9C). Finally, as n gets very large, both the binomial and Poisson distributions (two discrete distributions) approach a continuous distribution; namely, the gamma function with the appropriately chosen value of K. [For examples of this, see Stein (251, p. 98).]

is the affinity for the first extracellular binding reaction, i.e. epsilon = K_{CA1}; *beta* is related to the total number of sites available for translocation and release, to the entry rate constant (k_v) and to the intracellular Ca affinity, thus beta = $(k_v X_T Y_T)/(k_v Y_T + 1/K_{CA\,IN})$; and *gamma* is a lumped dissociation constant = $1/K^{1/2}$, where K is an effective affinity constant: $K = K_{CA1}K_{CA2}(K_{CA\,IN}k_v Y_T + 1)$. Finally, K_{CA2} is the affinity for the extracellular binding of the second Ca ion to site Y. Unfortunately, the equation cannot be simplified further and the various constants are interrelated as well.

With this expression for [CaX] (eqn 32), how then is release related to [CaX]? Quastel and his colleagues believe that CaX reduces an activation energy barrier required for release. As such barriers are described by exponential functions, then MEPPf = constant $\exp(a_1[\mathrm{Ca}X])$ or

$$\ln \mathrm{MEPPf} = a_0 + a_1[\mathrm{Ca}X] \qquad \text{eqn 34}$$

where a_0 = ln constant and reflects a Ca-independent fraction of MEPPf (a_1 is also a constant). Eqn 34 represents a mathematical statement of what is often termed the log model (53).

Quastel and his colleagues were concerned with describing all forms of ACh release detectable electrophysiologically. In their studies of a variety of drugs, ions, and experimental conditions (high potassium, focal depolarization, low M, high osmotic pressure, etc.) it was generally observed that a particular agent multiplied the effect of another agent with different chemical properties on MEPPf [e.g. ethanol multiplied the effect of Ca (209)]. On a log scale, this multiplicative effect would appear additive so that eqn 34 may be expanded in a general fashion to include these additional activators (eqn 35)

$$\ln \mathrm{MEPPf} = a_0 + a_1[\mathrm{Ca}X] + a_2[\text{drug } x] + a_3[\text{drug } y] + \ldots \qquad \text{eqn 35}$$

where a_2 and a_3 are constants.

Cooke, Okamoto, and Quastel (53) envisage the release probability as being continuously *graded* in accordance with how much a particular activator reduces an energy barrier. Each particle of activator (e.g. CaX) is assumed to produce the same reduction in energy barrier *independently* of another particle. If this is true and particles are distributed randomly along the nerve terminal, then the number of activators in a defined region of the nerve ending would be Poisson distributed. Thus, rather than assuming that exocytosis occurred in a Poisson manner, it was assumed that the activators which induce exocytosis were distributed spatially in accordance with Poisson's law.

This model of a continuum of finite release probabilities differs from the models of Dodge and Rahamimoff (74) and Hubbard et al. (116, 117) who assumed that an activator caused a huge leap in the probability of release from an infinitesimally small value to a finite one. In addition the fourth power and kinetic models assumed that only one form of activator acts on any one quantum, implying that the effects of each activator would be additive on MEPPf; this linear relation is in contrast to the multiplication predicted by the log model. If, however, the model of Hubbard et al. is modified slightly so that depolarization changes the number of CaX complexes that activate release, then the models of Cooke et al. and Hubbard et al. are compatible. Indeed, Cooke et al. found that depolarization increases *beta* much more than their model predicts. One interpretation for this increase in *beta* would be an increase in X_T, which, by eqn 1f, would result in an increase in the number of CaX complexes, and make the log and linear models equivalent.

The main force of the model of Cooke et al. at the time of its appearance (1973) was in its physical insight into the nerve ending. To recapitulate, extracellular Ca is delivered by a translocation process (Y) to an intracellular site (X) and is bound to that site (CaX). The CaX complexes are distributed at each release site (or vesicle) in accordance with Poisson's law, and reduce an activation energy barrier for release; this effect is manifested electrophysiologically as a multiplication of the resting ACh release rate. Unfortunately, the surfeit of constants in this model makes it difficult to envisage the physicochemical or morphological correlates of the various terms in eqn 25. Furthermore, this model assumes that Mg is both an intracellular and extracellular antagonist of M; studies on both frog and mammalian cholinergic nerves have shown that intracellular Mg does not antagonize ACh release (133, 60).

What is the nature of the intracellular energy barrier to transmitter secretion and how does the vesicle overcome it and undergo fusion and exocytosis? This is considered in the next section.

IV. Intracellular Physical Forces That Control Secretion

A. Is Intracellular Ca Required for Secretion?

One common feature of the models of Hubbard et al. (116, 117) and Cooke et al. (53) is the postulation of a Ca-independent fraction of quantal release. It is certainly conceivable that Ca is not necessary for all forms of quantal secretion; in model secretory systems, exocytosis occurs in the absence of Ca (46, 47, 279) although the rate of occurrence of the individual fusion events is increased in the presence of Ca (280). Some evidence, however, would not be in accord with this suggestion; experiments on amphibia have shown that the presumed Ca independent fraction of MEPPf may be reduced under conditions that would be expected to drive Ca out of the nerve ending [e.g., nerve stimulation in Ca-free, EGTA solution whereby the normally inwardly directed electrochemical gradient for Ca is now reversed (223)]. It is doubtful that the issue will be resolved in the near future

as one is always left with the nettling argument that any perturbation that increases MEPPf in the absence of extracellular Ca does so by liberating Ca from storage sites (e.g. 29, 237, 212). It is possible to conclude from the studies with Me-containing liposomes, however, that MEPPf is less sensitive to intracellular calcium than is synchronous release (133, 178).

B. Early Views on Electrostatic Energy Barriers

A 1968 study by Blioch et al. (31) on the effects of cations of differing valency on ACh release and on the rate of apposition of artificial phospholipid bilayers provided the first evidence suggesting that ACh release was initiated when intracellular multivalent cations screen fixed negative charges on synaptic vesicle and nerve terminal membranes. Although no quantitative discussion of diffuse double-layer theory was presented, these workers implied that the only properties of importance for a cation to promote exocytosis were the valency and concentration of the ion. In 1973, Van der Kloot and Kita (262) provided a valuable discussion of the biophysical processes that might underly the behavior of intracellular cations in supporting ACh release. In addition to presenting a lucid critical review of earlier theories of vesicle-membrane interactions, this paper (262) was the first to apply diffuse double-layer theory quantitatively to cholinergic nerve terminals.

Prior to 1973, it was generally believed that vesicles were in continuous Brownian motion, and when a particular vesicle attained sufficient thermal energy, it could overcome an energy barrier at the internal face of the axon membrane and undergo exocytosis. This energy barrier was envisaged by Bass and Moore in 1966 (20) to consist of both hydration and electrokinetic repulsive components. The hydration barrier was thought to consist of a layer of water molecules around the charged vesicles; this hydration shell keeps vesicles from fusing and must be stripped away to allow exocytosis. The electokinetic component was thought to be produced by the repulsion of the positively charged cytoplasmic surfaces of the vesicular membrane and the nerve terminal membrane; the positivity of both membranes was assumed to be caused by ion diffusion potentials. The suggestion of hydration and electrical energy barriers is certainly reasonable, but vesicles have been shown to be negatively charged (85). Furthermore, the assumption that membrane potentials created by ion diffusion extend into the cytoplasm is unlikely (see figure 5D, section III A and ref. 173). Simple, direct evidence against the Bass and Moore theory is that ACh release should increase in Ca-free media in response to a single nerve impulse because the reversal of the resting potential sign would profoundly reduce the energy barrier; this clearly does not happen. An extension of the Bass and Moore hypothesis considered vesicular and nerve terminal membranes to be negatively charged, the vesicles because of fixed negative charges and the nerve terminal because of the negativity produced by the resting potential (218). Again, the voltage drop across the membrane, i.e., the membrane potential, cannot extend significantly into the intracellular compartment (figure 5D and ref. 173). It is more likely that both vesicular and nerve terminal membranes have fixed negative charges and these fixed moieties produce the electrostatic repulsion that impedes exocytosis (31, 262).

Van der Kloot and Kita (262) applied the diffuse double-layer theory semiquantitatively to the nerve-ending cytoplasm in an attempt to explain why hypertonic solutions increase MEPPf and how intracellular cations control ACh release. With respect to osmotic effects, it was suggested that an increase in extracellular tonicity causes water to move out of the terminal, with the concomitant shrinkage of the nerve leading to an increase in the intracellular cation concentration. This increased cation concentration will, by eqn 4, reduce the electrostatic energy barrier between vesicular and nerve terminal membranes and allow MEPPs to occur more frequently. These authors also suggested that intracellular cations might bind to fixed negative charges but did not specify whether binding related to any particular form of ACh release. In a later study on the effects of ionophore X537A, it was implied that ACh release evoked by intracellular Me was produced by Me screening of fixed internal surface charges (263).

From the above discussion and that in section III A, there does not seem to be any evidence to dispel the notion that increases in MEPPf are produced when intracellular cations screen fixed negative charges on the surfaces of internal membranes, thus reducing an electrostatic energy barrier (248, 178). Indeed, the intracellular fixed charged density is generally very high as compared to the outside of nerve (42), which would make screening likely intracellularly [see section III A 2]. To provide a quantitative example, if the Gouy-Chapman equation (eqn 4) is solved for concentration (C)-eqn 4c

$$C = [272\sigma/(\exp\{z\psi_0/50\} - \exp\{-z\psi_0/50\})]^2 \quad \text{eqn 4c}$$

and it is inquired as to what concentrations of univalent, divalent, and trivalent cationic species are necessary to produce a certain surface potential (e.g. $\psi_0 = -135$ mV) given a fixed charge density of $\sigma = 1/60$ Å^2, then it is found that approximately 93 mM univalent, 0.4 mM divalent, and only 2 μM trivalent cation would produce that surface potential. These results are roughly equivalent to the relative effectiveness of cations of different valency, either applied extracellularly or in liposomes, in influencing ACh release (133, 213). Although screening may be responsible for MEPPf increases, the liposome studies suggest that synchronous release is mediated by selective Me binding to a Ca binding protein associated with of the secretory apparatus (240, 241).

The discussion thus far has implied that a reduction in an electrostatic energy barrier, either by binding or screening, is equivalent to exocytosis. This is undoubt-

edly too simplistic a picture as the main energy barrier to secretion is likely to change as the vesicle moves progressively nearer to adhesion with the nerve ending.

C. The Current View

What are the forces that would tend to promote or impede fusion of a synaptic vesicle with the nerve ending plasma membrane and how do the magnitudes of these forces change as the vesicle approaches the nerve terminal? A vesicle about 50 Å away from the nerve terminal is likely to be stabilized in position by the interplay of two opposing types of "long-range" forces (31, 201, 215). The first is the coulombic force produced by the fixed negative charges, namely *electrostatic repulsion*, which would tend to keep the vesicle away from other structures. The other force, an attractive one, results from fluctuating charges and constitutes a *Van der Waals attraction* force. The reader may be puzzled over the introduction of Van der Waals forces (originally proposed as correction factors for deviations from ideal behavior of gases) as long range forces. Indeed, Van der Waals forces fall off very steeply with distance (inversely as the sixth power generally) when molecular interactions are considered in vacuums or vaporous media. However, as vesicles are large bodies (50 nM) floating in cytoplasm, they behave as colloidal particles; under these conditions the Van der Waals forces extend over considerable distances and may even fall off less rapidly with distance than the inverse square dissipation of electrostatic forces (215). Much as these attractive forces can stabilize colloids, it is possible to suggest that such long-range Van der Waals forces act to stabilize synaptic vesicles in the nerve terminal. Specifically, it is possible to view the equilibrium distance between the nerve ending and vesicles (or between vesicles themselves) as a free energy minimum; moving the vesicle further away from the terminal—Van der Waals attraction draws it back while pushing it towards the nerve ending—electrostatic repulsion forces it away again.

Vesicles at the active zones of cholinergic nerve endings appear to be docked at releasing sites (figure 10A) at a distance of around 50 Å (41, 131). It is likely then that Van der Waals attraction acts in concert with the docking mechanism to keep vesicles close to the nerve ending; the main force preventing approach at this distance is still electrostatic repulsion (figure 10A, ψ). When Ca enters the nerve ending and reduces this electrostatic energy barrier, the vesicle may now move close to the nerve ending (figure 10B) but at this distance (e.g. 20 Å) a much more powerful repulsive force takes hold. This force is a *hydration* force (201, 215). In order for membranes to be stable in an aqueous milieu, their surfaces are covered by polar molecules with high affinity for water; the layers of water on the synaptic vesicle and inner face of the nerve ending represent an enormous energy barrier to adhesion [the hydration energy barrier, as originally suggested by Bass and Moore (20)]. The work necessary to overcome such a barrier is the work required to remove water from the approaching hydrophyllic surfaces. Not much is known about the hydration barrier except that at distances where membranes are nearly apposing, it is so strong as to make electrostatic forces insignificant. Evidently, some major structural rearrangement of the membrane components is required for the membranes to enter into close apposition (figure 10C). The specific mechanism by which this occurs is unknown. It has been speculated that if part of the membrane is cleared of polar groups or if the polar groups are neutralized or displaced laterally away from the region of the contact, then the barrier to fusion would be removed (201). For example a very fast phospholipase near the region of contact could be activated by Ca and decapitate the polar heads. A number of Ca-dependent biochemical mechanisms have been suggested to expedite the membrane rearrangements illustrated in figure 10C, e.g., Ca dependent contractile proteins of the cytoskeletal (figure 10A, cs) forcing the vesicle-docking protein-cytoskeleton complex towards the plasma membrane, vesicular ATPases hydrolyzing membrane ATP, etc. The main disadvantage with any enzymatic process is that it is restricted to a time interval of about 100 μsec; the participating enzyme would thus require a turnover rate of over 10^4 to catalyze more than one secretory event (131). It is conceivable that if repositioning or neutralization is all that is required to reduce the presence of polar groups in the region of fusion, then Ca binding to Ca binding proteins in the vesicle and nerve terminal membranes could be responsible for reducing this energy barrier to fusion (240, 241). (For further details of these processes, see figure 10 legend and ref 245a).

Once the membranes oppose at the hydrophobic regions, what forces might then produce fusion and exocytosis? Two speculative mechanisms for these last two stages are illustrated in figure 10 D to F. Specifically, fusion could be driven by a soap-bubble like incorporation of the highly curved vesicle into nerve ending (see figure 10D and ref. 107) with the ultimate discharge of neurotransmitter being produced by an osmotic bursting of the vesicle (see figure 10E, F and ref. 46). With respect to the fusion, Hall and Simon (107) have suggested that the relief of strain that ensues when the steeply curved vesicle is allowed to flatten into the nerve ending constitutes a potential driving force for fusion. These authors provide theoretical evidence that if Ca binds to the outer leaflet of the vesicle, then the area of the outer leaflet is reduced and the membrane curvature becomes very steep. This is very unfavorable state, energetically and quoting from Hall and Simon, "this energy can be reduced only by flattening but the vesicle can flatten only by fusing with the presynaptic membrane!" This model has an additional advantage in that it accounts for the recycling of synaptic vesicles observed morphologically (41). Specifically, after Ca entry has ceased, the newly incorporated negative lipid will no longer have its charges

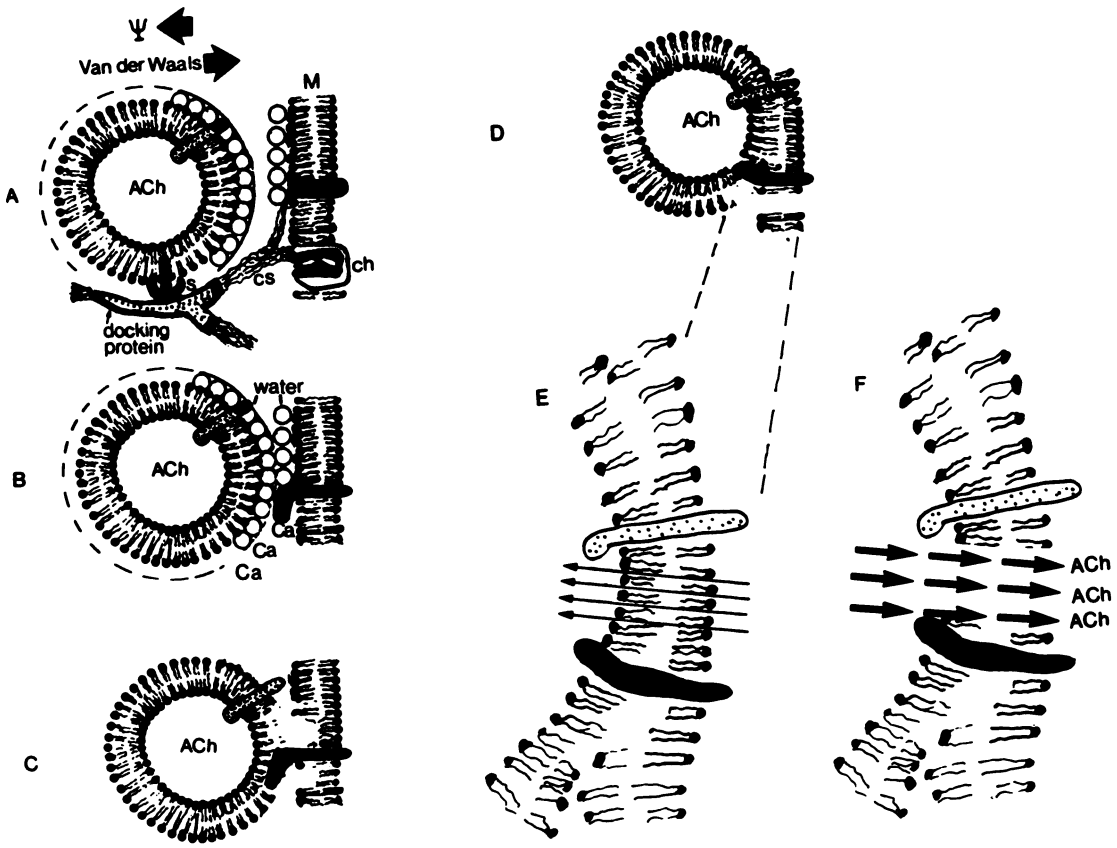

FIG. 10. Possible forces that control the exocytosis of ACh. A shows a cholinergic vesicle perched at a docking protein, 50 Å away from the nerve ending. In addition to the force that keeps the vesicle attached to the docking protein (a hypothetical anchor protein, *S*), electrostatic repulsion (ψ) may prevent the approach of the vesicle to the nerve terminal and Van der Waals attraction may favor the approach of the two membranes. In B, Ca has entered the cell, reducing ψ and allowing the vesicle to move closer to the nerve ending (20 Å). At this 20 Å distance, the major barrier to exocytosis is the hydration of vesicular and nerve terminal membranes. C shows membrane rearrangements in which polar groups are neutralized or eliminated from the membranes, reducing the hydration barrier and allowing the membranes to fuse into one continuous bilayer (D). Surface tension changes after Ca entry may favor fusion. It is also possible that cytoskeletal elements (cs) similar to those found in red blood cells might "contract" at this stage and allow close approach and fusion. In this regard the neuronal protein, fodrin, is thought to be analogous to spectrin in red blood cells and actin filaments are found in both red blood cells and attached to synaptic vesicles and cholinergic nerve endings (230, 189a). It should be stressed, however, that only a small (e.g. 7Å) movement is possible in the 100 μs allocated to such a contractile process. In E, water entry or some other destabilizing force locally breaks the septum in the newly fused bilayer (this process is frequently termed fission), causing ACh release to occur by exocytosis (F). For further details of the membrane phase transitions that have been suggested to occur in stages D to E, see ref. 131, and text. Hypothetical proteins originally present in the vesicle (stippled) and the nerve terminal membrane (blackened and possibly similar to bp in figures 7 and 8a) are shown as forming a canal to promote the osmotic bursting of the fused bilayer. Part A also shows a Ca channel (ch) connected by cytoskeletal elements (cs) to the docking protein and other membrane proteins associated with release (for justification and further details see refs. 230, 245 and 245a). One of the vesicle proteins shown may be similar to the calmodulin-associated vesicular protein, Synapsin I (previously termed protein I) (193, 217, 231, 245, 195a).

With respect to Me selectivity, it is possible that screening may be sufficient to facilitate the movement from 50 Å to within 20 Å as published micrographs suggest that Ca, Sr, and Mg are all capable of promoting movement of cholinergic vesicles to the nerve terminal (107b). In contrast, if a cytoskeletal transformation mediates the final stages of membrane fusion in the synchronous release process, then selectivity for Ca over Sr in *M* might be predicted based upon similar selectivity of these two cations in derepressing the troponin C-tropomyosin-actin complex in skeletal muscle (251). Cooperativity for Me's in ACh release is likely to be due to interactions of Me species with one or several of the indicated protein moieties. For details of the protein and lipid composition of the cholinergic synaptic vesicle, see refs. 189a and 271a).

After secretion, resynthesis of ACh occurs in the cytoplasm or at the external surface of the vesicle (33). The mechanism by which ACh is transported into vesicles is still somewhat uncertain. It is likely to be fueled indirectly by an ATP-dependent proton pump (217, 202a), i.e., a Ca,Mg-dependent ATPase similar to the F_1 ATPase of mitochondria and to the ATPase in chromaffin granules. The pumping of protons by the ATPase creates both a pH gradient (inside of vesicle with low pH) and an electrical potential (inside positive). The proton pump in the cholinergic vesicle requires bicarbonate ion to promote a high affinity, high velocity conformation capable of transporting protons (202a). This electrochemical gradient for protons may then drive an ACh/proton cotransport mechanism similar to the catecholamine-proton antiporter in the adrenal chromaffin granule.

screened or bound by Ca and the energy of the curved state will be favored over the flattened state. The vesicle membrane would thus be retrieved by endocytosis and recycling would occur. The model also makes some interesting predictions with respect to ACh release and vesicle recycling under different experimental conditions, predictions that are, as of yet, untested (see ref. 107, p. 616 for further details).

With respect to the bursting of the fused vesicle, Cohen and his colleagues (279, 47) studied the fusion of liposomes with planar lipid bilayers and found that, in their model system, an osmotic gradient was required for exocytosis of the liposomal contents (46). Specifically, the "cytoplasmic" compartment (the one with the liposomes) had to be hypertonic to the "extracellular" compartment for exocytosis to occur. They explain the process of exocytosis as follows. When the vesicle contacts the planar membrane, the two membranes behave as one. With the vesicle hyperosmotic to the extracellular compartment, water enters the vesicle, causes it to swell, and eventually to burst. Osmotic swelling in their view must precede exocytosis, but the swelling need not be produced in biological membranes by the above mechanism. For example, osmotic swelling could be produced by changes in the vesicle permeability to ions, increases in the active transport of ions into vesicles, or the recruitment of osmotically inert vesicular components (e.g. transmitter, ATP). Indeed, in some secretory systems, swelling has been observed to precede exocytosis (47). By whatever mechanism it occurs, it is the dilution of the vesicular contents by water movements that is the ultimate force for fracturing the enjoined membranes in the view of these authors. This is illustrated in figure 10E and F, in which a hypothetical canal formed from vesicular and nerve terminal proteins provides a waterway for osmotic bursting.

There is one drawback to this "osmotic" view. On the basis of this hypothesis, it might be predicted that ACh release is decreased when the extracellular fluid is made hypertonic; MEPPf frequency, however, increases greatly in hypertonic solutions. These authors argue reasonably that nerve terminals shrink in hypertonic solutions, with a subsequent rise in free cytoplasmic Ca causing the acceleration of MEPPf (cf, 262). Indeed, in the crayfish (195) and frog under certain conditions (135), a decrease in the transmitter release was produced by increasing extracellular osmolarity, a result consistent with the view of Cohen et al. The model of Hall and Simon (107) makes the same prediction as that of Cohen et al. concerning osmolarity. A more general criticism of the artificial membrane studies is that the fusion events occur at such a low rate that they are not relevant biologically (but see ref. 47).

With respect to nerve terminal membranes, the most relevant result of the artificial membrane studies is that incorporation of a Ca-binding protein (bp) into planar bilayers confers selectivity for Ca over Mg in increasing the frequency of liposome-bilayer fusion events (280). Specifically, in the absence of bp, concentrations of Ca, Ba, and Mg near 100 mM were needed to accelerate the fusion events. With bp, 10 μM Ca was now sufficient to enhance the frequency of these artificial secretory events but Mg was still required at its original high concentration for a similar accelerating effect to be observed.

In this section, I have attempted to provide the reader with a catalog of the physical and chemical forces that could promote and impede exocytosis as the vesicle approaches the nerve ending. The particular sequence of events summarized in figure 10 is speculative, and, for the most part, based on studies of artificial membrane systems (46, 47, 201, 215, 279, 280). Further speculations as to how these events might relate to the various models for Me selectivity are provided in the figure legend and in ref 245a. Whatever the mechanisms involved in the release process, however, once exocytosis occurs, the properties of the cholinergic nerve ending remain altered for a period of time after the secretory event.

V. Consequences of Ca-dependent ACh Release

It is apparent from the discussion thus far that an electrical stimulus delivered to the cholinergic nerve ending initiates a complex series of membrane and cellular events that ultimately leads to ACh secretion. The effect of nerve stimulation does not decay immediately. Depending upon the conditions, the nerve terminal is left in a state in which release to a subsequent nerve impulse may be depressed or increased.

A. Depression

A decrease in M during repetitive nerve stimulation is termed depression (D) (figure 11A) and is a consequence of nerve stimulation in normal Ca solutions, where several hundred quanta are released by a nerve impulse (for reviews see 95, 98, 166, 167). D is generally defined as a fractional change in M (eqn 36):

$$D = 1 - M\,(t)/M_{\text{CONTROL}} \qquad \text{eqn 36}$$

As the magnitude of depression was directly related to the amount of ACh release and not due to changes in the nerve terminal action potential (257, 260) it was suggested that depletion of ACh was responsible for neuromuscular depression (197). In early studies, the recovery

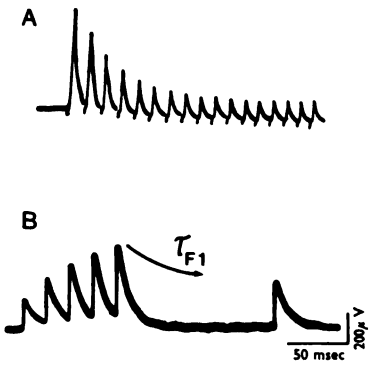

FIG. 11. Examples of calcium-dependent processes that outlast the nerve impulse. A, depression of ACh release from phrenic motor nerve endings in the rat. Bathing solution contained normal calcium and curare. Frequency of stimulation = 180 Hz; smallest EPPs at the end of stimulation are approximately 1mv. Reprinted with permission from Liley (145). B, facilitation recorded in solutions containing normal Ca with 17 mM Mg (to depress release presynaptically). The first five responses show the rise of F; τ_{F1} represents the approximate time constant of decay of the first phase of facilitation (F_1) after stimulation. The EPPs were recorded with an extracellular electrode at frog endplates. Reprinted with permission from Mallart and Martin (161).

of M after the depleting stimulus (the conditioning stimulus) was observed to be exponentially related to the time allowed for recovery between the conditioning and testing stimulus (166). If it is assumed that a *single* process, namely depletion of the immediately available store of ACh quanta (n), is responsible for depression (and thus p remains constant), then it is possible to obtain values for n and p by extrapolation of the electrophysiological data (specifically, a plot of log D against time extrapolates to p at zero time [for details, see Martin (166) and Ginsborg (95)]. Unfortunately, the majority of the experimental results are not consistent with this simple model. For example, it has been shown, that increasing $M_{CONTROL}$ (e.g. by raising Ca) produced less depression than would be predicted by this simple depletion model (25, 45, 167). A number of experiments have demonstrated that more than one process contributes to the depression of ACh release (25, 45); in the sense of the original quantal hypothesis, this would imply that *both* n and p are declining during depression of ACh release.

Depression of evoked release at 7 Hz stimulation is not associated with a measurable loss of the ACh content of the tissue (see ref. 114 for details and earlier references). One explanation for these observations is that a small but very active pool of vesicles near the nerve terminal is releasing and resynthesizing ACh and depletion of this small pool is responsible for D (281, 206). There is recent biochemical (271a, 281) and morphological (206) evidence for this small, "hot" pool which, if depleted, would represent the loss of an immeasurably small fraction of the total ACh in the terminal. Indeed, nerve stimulation increases ACh synthesis (see ref. 26 and appendix B 1), and newly synthesized ACh is preferentially released (33, 114), suggesting that the nerve terminal would attempt to maintain high release rates initially by replenishing the small active pool of vesicular ACh. At more stressful stimulation rates however (e.g., figure 11A), there is a much larger depression in ACh release, and this is associated with a reduction in the tissue concentration of ACh. At this stage it is likely that a somewhat larger pool of vesicles is depleted and contributes to the detectable loss of ACh stores in the nerve ending. Replenishment at this stage does not appear to require resynthesis [the Q_{10} is too low (166)], so it is possible that, with severe depletion, diffusion of filled vesicles to the active zones is required for restoring ACh release (114, 166).

It is also conceivable that a more subtle alteration in the properties of the active zones or synaptic vesicles contributes to depression of ACh release. One possibility is that a neuromodulatory substance is released together with ACh and acts by a negative feedback mechanism to depress ACh release (234). For example, ATP is packaged with ACh in synaptic vesicles (272, 232, 281) and released together with ACh (234, 247) from a vesicular pool (281, 232) and, under some conditions, from postsynaptic sources as well (180). In addition, ATP and its hydrolysis products ADP, AMP, and adenosine (as well as a variety of adenosine receptor analogues) inhibit ACh release at the skeletal neuromuscular junction (97, 220, 239, 243).*

It has been shown that adenosine derivatives reduce the apparent affinity of the secretory apparatus for Me agonists, thus reducing the ability of the release site or synaptic vesicle to respond optimally to Ca, Sr, or Ba (for further details, see refs. 240 and 243 to 245a). I have thus speculated (234) that negative feedback modulation by ATP and its hydrolysis products may be responsible for the inability to reconcile quantitative theories of neuromuscular depression with the simple vesicle hypothesis (see also ref. 219). If this is true, then a decrease in the intracellular Ca affinity could contribute to depression, prior to any depletion of ACh stores (243).

Evidently more studies are necessary to clarify this issue. Unfortunately, the situation is even more complicated than has been discussed thus far. For example, studies of depression even at moderate frequencies of stimulation could not be made at intervals between stimuli less than 200 μsec due to an accompanying facilitation of ACh release. In addition, although repetitive stimulation at very high frequencies produces a pronounced, long-lived depression, the process is not easily studied experimentally as it occurs at the same time as a powerful, long-lived enhancement of release known as potentiation (see below). The processes by which repetitive nerve stimulation increase ACh release are amenable to experimental analysis by a small alteration in the composition of the bathing fluid.

B. Facilitatory Processes

When the cholinergic nerve is bathed in a low Ca/high Mg solution, a nerve impulse releases only a small number of ACh quanta. In such solutions, depression is minimal and repetitive stimulation produces a progressive increase in M during stimulation (figure 11B) and a gradual decay of M back to control levels after stimulation. Analysis of the return of M to control levels at both motor nerve (159) and preganglionic nerve terminals (278) reveals four characteristic time constants [τ's (159)]; this has been generally interpreted as reflecting the exponential decay of four underlying cellular processes with different characteristics (e.g., different dependencies upon Ca, Sr, and Ba, see below). These four processes all depend on extracellular Ca in some fashion (162, 211) and at motor nerve endings have been termed: the first component of facilitation (F_1, $\tau = 50 - 60$ msec; refs. 161, 159), the second component of facilitation [F_2,

*ATP, but not adenosine, inhibits ACh release at sympathetic chain ganglia (246). At the skeletal neuromuscular junction (239) and cholinergic nerve terminals to smooth muscle (203), the effect of ATP may be due to the effects of its hydrolysis product, adenosine, on specific extracellular adenosine receptors (149, 242).

τ = 300 to 400 msec(161, 159)], augmentation [A, τ = 7 sec; (159)], and potentiation [P, τ ranged from seconds to minutes, depending upon the intensity of prior stimulation (159)]. Although the existence of facilitation and potentiation has been known since the 1940s (for references to these early papers see ref. 167), comprehensive studies of the properties of the four processes which increase ACh release are only quite recent (159, 277). Of the hypotheses advanced for the various phases of decay, the most widely accepted view is that the different time constants are due to differences in the rate of elimination of the activating Me species (or a subsidiary substance produced by Me dependent processes) from strategic region associated with secretion (159, 277). The reader who is not likely to become enraptured with the details of these processes may refer to table 3, which is provided as a summary of section V B, and then proceed to the concluding part of this review (section VI).

If the generalized parameter, I, is used to represent any one of the processes which *increase* ACh release, then I may be defined as the ratio of the increased EPP to the control EPP, i.e.

$$I = \mathrm{EPP}_I/\mathrm{EPP}_{\mathrm{CONTROL}} \qquad \text{eqn 37}$$

or as a fractional increase,

$$I = (\mathrm{EPP}_I - \mathrm{EPP}_{\mathrm{CONTROL}})/\mathrm{EPP}_{\mathrm{CONTROL}} \qquad \text{eqn 38}$$

The decay of I as a function of time after the cessation of nerve stimulation, $I(t)$, is described by an exponential equation of the sort:

$$I(t) = I_0\exp(-t/\tau_I) \qquad \text{eqn 39}$$

where I_0 is the maximum increased release and τ_I is the time constant of the decay of the particular process (for an alternative view see ref. 255). A specific quantitative treatment of the individual processes follows.

1. Facilitation. The pioneering observation that facilitation in truth reflects two different processes, F_1 and F_2, was made by Mallart and Martin in 1967 (161).

TABLE 3

Processes by which repetitive nerve stimulation increases ACh release

Name (abbreviation)	Equation* {time constant = τ} (selective agonist)	Comments and speculations(?)
Facilitation, first phase (F_1)	$F_1(t) = F_{1,0}\exp(-t/\tau_{F1})$ {τ_{F1} = 50–60 msec}	Maximal size ($F_{1,0}$) and τ_{F1} independent of previous history; F_1 may be produced by residual Ca at the nerve terminal plasma membrane (?)
Facilitation, second phase (F_2)	$F_2(t) = F_{2,0}\exp(-t/\tau_{F2})$ {τ_{F2} = 300–400 msec} (strontium ion)	Maximal size ($F_{2,0}$) and τ_{F2} independent of previous history; F_2 may be produced when a Ca or Sr residue is present at both vesicular and nerve terminal membranes(?)
Augmentation (A)	$A(t) = A_{0(\mathrm{STIM})}\exp(-t/\tau_A)$ {τ_A = 7 sec} (barium ion)	Termed an intermediate process in earlier papers because τ_A is intermediate between τ_{F2} and τ_P; may be the predominant facilitatory process under physiological conditions; amplitude ($A_{0(\mathrm{STIM})}$) depends on duration of stimulation (STIM) and on an *expression factor*, the expression factor decays slowly and thus produces greater A_0 during subsequent periods of stimulation; τ_A not dependent on previous history except for the early phase at high levels of release; A may be related to Me-dependent increases in the availability of releasable quanta at a docking protein (?)
Potentiation (P)	$P(t) = P_{0(\mathrm{STIM})}\exp(-t/\tau_{P(\mathrm{H})})$ {$\tau_{P(\mathrm{H})}$ is seconds to minutes} (lithium ion ?)	Equivalent to post-tetanic potentiation in the older literature; maximal size ($P_{0(\mathrm{STIM})}$) and $\tau_{P(\mathrm{H})}$ are both dependent upon previous history (H) and the stimulation parameters (STIM) but are controlled by different factors; P appears to be regulated by changes in the bulk [Ca] in the cytoplasm and possibly by subsequent phosphorylation of vesicular or plasma membrane proteins (?) (phosphorylation may be produced by a number of protein kinases; see text); increases in the number of available synaptic vesicles have been observed during P.

* The equations describe the decay of the four facilitatory processes from maximal levels. The development of the facilitatory processes is somewhat controversial (the linear summation and residual power models are described in the text). Speculations as to the mechanisms responsible for the decay of the facilitatory processes (e.g. clearance of the cations by synaptic vesicles, smooth endoplasmic reticulum or membrane Ca-ATPase, dephosphorylation, etc.) are provided in the text. The reader is referred to the most recent work of Magleby and Zengel (refs. 159 and 277) for precise quantitative details. Each of the four processes which produces an increase in M is also associated with an increase in MEPPf that follows a similar time course. F_1, F_2, A, and P are studied in low Ca/high Mg solution to minimize depression (D); D is described in section V A.

Defining facilitation (F) using eqn 38, i.e.

$$F = EPP_F - EPP_{CONTROL}/EPP_{CONTROL} \quad \text{eqn 38a}$$

it was suggested that the decay of F could be described by the sum of two exponential curves, suggesting that two separate facilitation processes, F_1 and F_2, might be involved. From studies on both the growth and decay of F_1 and F_2, the *linear model* of facilitation was suggested to describe each of these processes. For example, with respect to F_1, a single stimulus delivered at time $t = 0$ produced a certain amount of facilitation, (F_1), (as defined by eqn 38a) which decays towards control levels with time constant τ_{F1}. Another stimulus delivered at a brief time after the first is assumed to add an identical amount of facilitation, F_1, which *sums linearly* with the residue of F_1 that remained from the initial stimulus; F_1 from the second stimulus also decays with the same τ_{F1}. The decay of F_1 was described by an equation of the form of eqn 39 (39a):

$$F_1(t) = F_{1,0}\exp(-t/\tau_{F1}) \quad \text{eqn 39a}$$

where $F_{1,0}$ is the facilitation at zero time after nerve stimulation (i.e., maximal facilitation) and τ_{F1} was approximately 35 to 50 msec (e.g. figure 8B). The rise of facilitation could be described by eqn 40:

$$F_1 = \text{constant}\ (1 - \exp\{-t/\tau_{F1}\}) \quad \text{eqn 40}$$

where the constant is dependent on the maximum level of F_1($F_{1,0}$) and the frequency of nerve stimulation. A similar equation with τ_{F2} ranging from 250 to 300 msec could be used to describe the growth and decay of F_2; e.g. for the decay of F_2:

$$F_2(t) = F_{2,0}\exp(-t/\tau_{F2}) \quad \text{eqn 39b}$$

In confirmation of this work, Magelby in 1973 (152) found that overall decay of facilitation could be described as the sum of two exponential equations, $F = F_1 + F_2 = F_{1,0}\exp(-t/50) + F_{2,0}\exp(-t/300)$, and that F_1 and F_2 had properties consistent with the view of linear summation proposed by Mallart and Martin (but see below for later results).

At about the same time, Katz and Miledi (1968) attempted to put F into the framework of the Ca hypothesis (see section II B) by suggesting the *residual Ca hypothesis* (126). Specifically, they proposed that F may be due to a residue of active Ca, CaA, at strategic sites near the internal face of the nerve terminal membrane [this would correspond to a residue of active CaX in the terminology of Cooke et al. (53) and Cabp in this reviewer's usage (241); Katz and Miledi actually used a subscripted a to represent active Ca, however]. Although the local accumulation might be small in absolute terms, if a power relationship existed between CaA (an intracellular Ca residue) and release such that M was proportional to [CaA]^4, then small local Ca concentration changes inside the cell could produce large changes in ACh release.

To paraphrase their example, suppose that after a nerve impulse, [CaA] declines from its maximal level [Ca $A_{MAXIMUM}$] to some low level (e.g. 20% of maximum) over a rapid time course and then much more slowly thereafter. On a fourth power relationship, the ratio of M at this later time to the maximal M just after a nerve impulse would be: (0.2 [Ca$A_{MAXIMUM}$]/[Ca$A_{MAXIMUM}$]^4 or 0.0016, which would be an insignificant fraction of the maximal M. Now, if a second impulse produced the same [Ca$A_{MAXIMUM}$] immediately after the nerve impulse, then addition of the preceding residue (0.2 [Ca$A_{MAXIMUM}$] to the newly delivered [Ca$A_{MAXIMUM}$] produces on the fourth power relationship, $(1.2)^4$ = or 2.1-fold increase in M over the control.

By this view, both M and F are proportional to the fourth power of the same CaA complex at strategic releasing sites inside the cell. This paper was noteworthy for several reasons. It suggested that the fourth power relationship reflected an *intracellular* Ca residue and that Ca entry was linearly related to extracellular Ca concentration. It also postulated that residual Ca (i.e. CaA, or Cabp) was controlled by several factors, most notably, the effectiveness by which Ca is cleared from sites of release.

With respect to the dependency of F on extracellular Ca, Mallart and Martin (168) showed that increasing Mg increased F and Rahamimoff (211) found that increasing Ca decreased F.* These results would be expected from the residual Ca hypothesis as occupation of a larger fraction of the total number of Ca binding sites would occur in high Ca after the first stimulus and this would in turn decrease the number of sites available for binding the Ca that entered after the second stimulus. Rahamimoff (211) did not specify, however, whether he regarded the essential site of Ca action to be extracellular or intracellular.

Is the observation of linear summation of facilitation compatible with the residual fourth power model? Indeed it is not if the compartment which sums linearly is CaA; the linear model would predict that M is proportional to [CaA] while the residual Ca model predicts that M is proportional to [CaA]^4. Although several groups have found that linear summation describes F_1 after the first five or ten nerve impulses, the majority of workers have observed deviations from simple linear summation as the frequency or duration of nerve stimulation is increased (159, 277). Some but not all of these deviations may be due to the superposition of augmentation and potentiation on F (15).

In 1974, Younkin (274) found that the experimental results were compatible with the residual Ca hypothesis for both F_1 and F_2 yet need not be incompatible with the view of linear summation of F if some of the original constraints of the residual Ca model are removed. For example, say each impulse does not add a constant

* F in ref. 211 was described by eqn 37; by this equation increases in extracellular Ca decreased F. The *absolute difference* between the facilitated M and control M, however, was larger in high Ca solutions. See ref. 12 for an alternative result.

increment of CaA but impulses late in a period of nerve stimulation deliver progressively smaller and smaller increments of CaA (this might indeed be expected to occur as the occupancy of site A by Ca is increased early in the train of stimuli). Under these conditions, the two models can be made to accord.

As an illustration of this point using the earlier example from Katz and Miledi's work, the 2.1-fold facilitation (i.e. $\{1.2\}^4 = 2.1$) after the first impulse on the fourth power model assumes a residuum of 0.2[Ca$A_{MAXIMUM}$] at time t after the nerve impulse. The linear summation model would predict the same F using the same residuum by the equation F = constant (1.2) = 1.75 (1.2) = 2.1. Now, as the *new* maximum CaA, also decays to 20% it will be 0.24 maximum at time t after the nerve impulse. If the third nerve impulse now delivers the same increment in CaA, i.e. the maximum amount (= 1.0), then F is $(1 + 0.24)^4 = 2.4$ by the fourth power model and 1.75 (1.24) = 2.17 by the linear summation model. The predictions are thus different. If, however, the fourth power model is altered so that the third impulse only delivers 97.38% of the maximum CaA of the maximum CaA instead of 100%, then 0.9738 + 0.24 = 1.2138 and $(1.2138)^4 = 2.17$. The two models of facilitation are therefore compatible if the constant increment of CaA in the model of Martin and Mallart is changed to a progressively decreasing increment in the fourth power model.

Apart from considerations as to how F develops quantitatively, it is unlikely that changes in ntps or increases in Ca currents contribute to F_1 or F_2; neither ntps at cholinergic nerves (11; see also ref. 161) nor Ca entry at squid giant synapses (44) was altered during facilitation. By exclusion, one is left with the original view of Katz and Miledi (126), namely, that a residual effect of *intracellular* Ca contributes to the enhanced releasing capacity of the cholinergic nerve ending. The Ca hypothesis *as originally stated* will need to be expanded, however, in order to explain the high levels of F observed experimentally.

Specifically, in the experiments of Katz and Miledi (126) F (as defined by the ratio of EPPs in eqn 37) was two orders of magnitude larger than M. Even if [CaA] decayed so slowly after a nerve impulse that it remained at maximum for a long period of time, then a second nerve impulse would produce $([CaA_{MAXIMUM}] + [CaA_{MAXIMUM}])^4 = 2^4$, i.e., only a 16-fold multiplication of M if no other factor contributed to F. Furthermore, the kinetic expression suggested by Katz for the clearance of Ca, namely, $-dCaA/dt$ = constant $[Ca]^4$ does not predict the higher levels of F that were observed experimentally (see ref. 274). For the residual fourth power model to describe F under all conditions, then, additional factors must be postulated to account for the large increases in [CaA] after repetitive nerve stimulation.

The division of F into two phases on the basis of different time constants has been criticized (13). Strong evidence that F_1 and F_2 reflect different underlying processes is provided by the Me: pharmacology of F_2. Specifically, Sr selectively increases the magnitude and duration of F_2 without appreciable effects on F_1, augmentation or potentiation (275). Ba does not affect F_1 or F_2 (275).

From these results with Ca, Sr, and Ba, it may be speculated that an Me species must support M in order to activate either F_1 or F_2. If F_1 is produced by a residuum of active Ca, CaA, then Sr might not participate in F_1 because its low apparent intracellular affinity would prevent it from being bound to site A to any substantial degree at a short time after one nerve impulse. The decay of F_1 could reflect in turn the decay in the high affinity state of the synchronous Ca binding protein or a decrease in the number of activatable sites, i.e., an effective inactivation process (55, 14, 248, 200) as well as the return of the intracellular Ca concentration to resting levels. This last effect could be produced by any one of a number of organelles or membrane pumps, including the synaptic vesicle itself.*

Now, suppose that F_2 requires simultaneous Me occupation at both nerve terminal release sites and at the vesicle membrane (12). After longer periods of repetitive stimulation, enough Sr could accumulate at site A to overcome its low affinity and allow Sr to achieve sufficient occupancy at both A sites and vesicular binding sites to support F_2. The enhancement by Sr of the duration of F_2 might be due to poorer Sr clearance [e.g., nerve terminal mitochondria clear Sr less efficiently than Ca (216)]; this would leave a higher residual [Sr] in the vicinity of the vesicle.

To summarize, it appears that residual intracellular Ca may be responsible for the two processes of facilitation although F is related to residual Ca in a complex non-linear fashion. Sr is a selective agonist for one of these processes (F_2).

2. *Potentiation.* In his studies on facilitation, Magleby observed another process during repetitive stimulation that was much longer-lived and with more complex properties (152). This process, termed potentiation (P), develops after a single nerve impulse but is most apparent after high frequency stimulation. The decay of P occurs exponentially in accordance with eqn 39c:

$$P(t) = P_{0(STIM)}\exp(-t/\tau_{P(H)}) \qquad \text{eqn 39c}$$

where $\tau_{P(H)}$ is indicated as dependent on the previous history (H) of stimulation; $\tau_{P(H)}$ has been found to vary between 2 sec and 3 min depending upon the stimulation conditions (154). The maximum P (P_0) is dependent on the duration of stimulation (STIM) and is controlled by a different factor than $\tau_{P(H)}$. P may accumulate in a linear (155) or in non-linear manner (159) and may be selectively enhanced by Li (see appendix B).

Magleby (153) found that potentiation and the commonly studied post-tetanic potentiation (PTP) are the same process. This was a refreshing result in view of the befuddling array of disparate terminologies used previously. For example, the primary potentiation described by Hubbard in 1963 (113) in rat diaphragm is equivalent to the two phases of F described by Mallart and Martin in 1967 (161) and Magleby (152) while both secondary potentiation and post-tetanic potentiation of Hubbard (1963) are equivalent to P.

* Indeed, a unifying explanation for F_1 and for the relationship between synchronous and asynchronous ACh release (figure 7 B to D) would be that the vesicle discards Ca associated with bp to the extracellular fluid and reduces access of Ca to more distant sites.

In earlier studies, *P* was shown to require the presence of extracellular Ca during, but not before or after, tetanic stimulation (221, 268). Indeed, PTP may be observed in isotonic $CaCl_2$ with no extracellular Na (268). More recent studies, while confirming the suggestion that *P* requires Ca accumulation (84, 93), have cast doubt on the view that Ca entry is obligatory for the *development* of *P*; *P* has been observed when Ca is returned to the bathing solution *after* tetanic nerve stimulation in Ca-free solution (185). It has been suggested (27, 86) that *P* results from intracellular Ca that was acquired by the cell in exchange for the intracellular Na that had entered during high frequency nerve stimulation. Such Na/Ca exchange could occur across the surface membrane or by intracellular Na exchanging for the Ca sequestered in organelles such as mitochondria or smooth endoplasmic reticulum (29, 86). Na accumulation does not appear to be linked to PTP in a rigorous fashion; however, as in the mammal, metabolic inhibitors that cause a rise in intracellular Na (e.g. azide, ouabain) eliminate *P* rather than enhancing it (93). The situation is somewhat different in the frog (212, 86).

Despite these diverse impressions as to the sources of Ca for *P*, there appears to be general agreement with the suggestion by Hubbard (113) that *P* and *F* reflect different processes. Specifically, it has been observed that *P* is multiplicative with *F* (142, 153); if *P* and *F* reflect behavior of Ca at different links along a chain of sites that ultimately leads to secretion, then this multiplicative relationship would be expected. Additional support for Hubbard's original contention is provided by studies on the drug and cation selectivity of *P* and *F*. Azide and ouabain inhibited *P*, but had essentially no effect on *F* (93), while Sr selectively increased F_2 yet had no effect on *P*.

Regardless of the precise molecular nature of the determining event, *P* reflects a process of considerably more complexity, flexibility, and persistence than *F*. Although this process is dependent upon the previous history of the nerve terminal, it is not very fastidious about the source or the timing of the Ca translocation. It is thus possible that *P* is caused by a rise in the *bulk* cytoplasmic Ca concentration, irrespective of the mechanism (membrane channels, pumps, carriers, storage organelles, cytoskeletal binding proteins, etc.). This increased Ca could then produce some long-lasting alteration in the nerve terminal, such as phosphorylation of a structural component of the releasing apparatus and increase secretory activity at the active zone.

It is of interest in this regard that specific peptides on the vesicular protein, Synapsin I (formerly termed protein I), are phosphorylated by Ca/calmodulin-activated protein kinase (193, 231, 217) and increases in the number of synaptic vesicles near release sites have been observed in association with *P* at some cholinergic nerve endings (210). It is thus possible to suggest that phosphorylation could increase the concentration of available docked quanta (245). It is noteworthy that some of the *same* peptides on Synapsin I that are phosphorylated by Ca/calmodulin protein kinase are also phosphorylated by cAMP-dependent protein kinase [protein kinase A (231)] and exogenously applied cyclic AMP derivatives have been shown to produce a delayed but long-lasting potentiation of ACh release (245). It may thus be speculated that cyclic AMP could participate in potentiation in the same manner as Ca.* Finally, Synapsin I may also be a possible target protein for phosphorylation by protein kinase C, a kinase that is activated by Ca and phosphatidylinositol turnover (195a). If indeed phosphorylation is responsible for *P*, then it is possible that the decay of *P* is related to membrane dephosphorylation by nerve terminal phosphatases.

Regardless of the precise mechanism, it appears that if any one of the facilitatory processes is responsive to changes in the bulk [Ca] in the cytoplasm and is dependent upon phosphorylation, then *P* is likely to be that process.

3. Augmentation. Augmentation (*A*) is the last and most recently discovered of the processes by which repetitive nerve stimulation increases ACh release (156). It was initially termed an "intermediate process" (154, 15) because the decay time constant (τ_A = 7 sec) was intermediate between *F* and *P*. The newness of this process to the nomenclature of the nerve ending belies its importance; Magleby and Zengel (156) provide evidence that *A* may be the predominant physiological event during repetitive nerve stimulation at a variety of cholinergic nerve endings. In the early studies, it was found that τ_A was insensitive to changes in stimulus parameters while the magnitude of $A(A_0)$ was dependent on the duration of stimulation (156). Thus, the decay of *A* was described by

$$A(t) = A_{0(\mathrm{STIM})}\exp(1- t/\tau_A) \qquad \text{eqn 39d}$$

In later studies (157), it was found that at large levels of *A*, a rapid decay preceded the exponential (τ_A = 7 sec) process. The growth of *A* could be described by either a linear summation or a residual power model (277).

With respect to the factors responsible for maximal $A(A_0)$, it was observed that if *A* is allowed to develop and then decay to insignificant levels, then a second period of stimulation produced an increase in A_0 as compared to the preceding period, without an alteration in τ_A. A slowly, decaying *expression factor* was thus postulated to be required for "expression" of *A* (158). The magnitude of *A*, A_0, was directly related to this expression factor which appears to decay an order of magnitude more slowly than *A* itself. Zengel and Magleby have suggested that the expression factor could relate

* A possible contributor to increases in cyclic AMP in potentiation includes adenosine derivatives released by cholinergic activation (234, 245); a common after-effect of adenosine application is a prolonged enhancement of ACh release (239) (although inhibition of ACh release occurs *during* exposure to adenosine).

directly to the concentration of Ca at some strategic locus; the concentration profile in turn being inversely related to the buffering capacity of the nerve ending for Ca (277).

The mechanisms responsible for *A* are unknown. They are unlikely to include changes in the nerve terminal action potential as it would be expected that the concurrently developing *P* would be altered as well (86). The possibility that these events are related to membrane phosphorylation was also raised. Whatever the mechanism, *A* appears to be multiplicative with *F* and *P* (159).

With respect to the pharmacology of this process, *A* may be selectively highlighted by the use of Ba; in low concentrations, Ba increases the magnitude of *A* without affecting τ_A or the other facilitatory processes (275). This effect of Ba may provide a clue to the underlying mechanisms of *A*. As mentioned in Section II B, Ba is capable of supporting the discharge of enormous numbers of ACh quanta and over a prolonged time course (237). It is difficult to imagine an effect of this magnitude continuing for so long without extensive mobilization occurring from distant sources. It may be speculated that Ba directly interacts with a docking protein (figure 10A) and increases the availability of quanta during the critical phase of *A*. The expression factor might then be accounted for as follows. After an initial period of *A*, it is likely that some of the mobilized quanta might not have demobilized fully. Although a single stimulus would produce *M* at the original control level, repetitive stimulation would cause *A* to increase to larger levels than observed during the preceding stimulation period as the previously mobilized quanta could reoccupy the docking protein more readily not having fully redistributed themselves to the back of the nerve terminal. Indeed, the calculated time constant for the decay of the expression factor is consistent with this speculation (166). The τ_A might in turn reflect the clearance of Ba by the Ca-dependent ATPase (227) in the nerve terminal, which, in some systems has a higher affinity for Ba than other ions (32). A high affinity for Ba might be expected to produce progressive saturation of this buffering mechanism (see also ref. 198 and ref. 277, p. 608) as was postulated above by Magleby and Zengel. Ba would not be expected to affect F_1 or F_2 as Ba cannot support *M* nor to affect τ_{F1} or τ_{F2} as Ba is a poor substrate for uptake into smooth endoplasmic reticulum or mitochondria [likely clearance mechanisms for Ca and Sr (216, 30, 212)]. For further details about Ba, see Section VI and appendix B.

4. Relationship of Facilitatory Processes to Asynchronous Release. If increases in intracellular Ca are responsible for the persistent effects of repetitive nerve stimulation on *M*, then it might be expected that MEPPf would rise and fall over a similar time course to F_1, F_2, *A*, and *P*. Indeed, increases in MEPPf produced by nerve stimulation decay back to control levels with four time constants similar to those observed for *M* (276). With respect to ion selectivity, the Sr-dependent asynchronous release (e.g. figure 4) was associated with the time course of F_2 and evoked MEPPs supported by Ba were associated with the time course of *A* (276). Furthermore, when tetanic nerve stimulation is delivered in Ca free solution, an increase in MEPPf that decays with the time course of potentiation is observed (185); Mg has been shown to enhance this last process by which MEPPf is increased in response to prolonged, high-frequency nerve stimulation (118, 249). It is likely that some Mg enters the nerve ending during the prolonged tetanus (9) and blocks Ca extrusion or displaces Ca from storage sites; it has been shown that intracellular Mg enhances the effects of intracellular Ca on ACh release (133).

It thus appears that increases in MEPPf by repetitive nerve stimulation share some properties in common with facilitatory processes. In 1971 Miledi and Thies (183) suggested that all forms of ACh release may be described by the residual Ca hypothesis. In their experiments, Miledi and Thies were studying MEPPs associated with the process of potentiation and suggested that the EPP is equivalent to a certain MEPPf but over a brief period of time, for example $M = 1$ would be equivalent to a MEPPf of 1000/sec in a 1 msec period (assuming the transient increase in Ca at release sites lasts for only 1 msec). It has been shown, however, that MEPPf and *M* are differentially sensitive to many factors (14, 178) including intracellular Ca and Sr (178), rendering this assumption unlikely. Furthermore, Magleby and Zengel (159) have provided convincing arguments that the residual fourth power model cannot explain the effects of the various Me species on both EPP and MEPPf, except for F_1 studied at very low temperatures (see ref. 17).

In a theoretical sense, it is possible that a sequential interaction model (e.g. appendix A 9)—when corrected for the differences in Me selectivity for the various forms of ACh release and for the different potential Me clearance sites—might provide a reasonable description of all the facilitatory processes. The technical problems in further dissecting the overlapping facilitatory events are considerable, however. In the last of their series of publications, Magleby and Zengel (1982; ref. 159) outline the potential relationships between F_1, F_2, *A*, and *P* and the formidable barriers to further study. Whatever the nature of the underlying factors, the multiplicative relationship observed between *F*, *A*, and *P* and the selective ionic pharmacology for *M* and for MEPPf suggest that the two phases of facilitation, augmentation, and potentiation all reflect the intracellular actions of the alkaline earth metals on different processes occurring within the cholinergic nerve ending.

VI. Summary and Conclusions

A. The Sites of Me Action in the Nerve Ending

Table 4 summarizes the various models of secretion discussed in this review. All of the listed models postulate

TABLE 4
Review of various models of Ca-dependent ACh release

External initiation site		Subsequent events		Publication*
Term	Comments	Term	Comments	
X	CaX compound as inactive carrier; Mg blocks	X'	As active carrier liberated by depolarization	Castillo and Katz (66), Jenkinson (120).
X	Membrane Ca receptor; cooperative action of four Ca; Mg blocks	—		Dodge and Rahamimoff (74)
X	Ion channel for Ca and Sr; cooperativity	β	Intrinsic activity (~ efficacy); mobility in the ion channel	Meiri and Rahamimoff (175)
X	Receptor; cooperativity—one, two, or three bound Ca states; Mg blocks all states	k's	Michaelis-Menten "kinetic" rate constants of the various X states	Hubbard et al. (116, 117)
Y	Ca translocation site; cooperativity—requires two Ca ions bound; Mg blocks	X	Release site; bound CaX reduces activation energy barrier by Poisson's law; Mg blocks	Cooke et al. (53)
X	Receptor for Ca, Sr, and Ba near the external surface of the Ca channel; non-cooperative entry; Mg blocks; Ca entry linearly related to [Ca]	e_{ME}	Efficacy, intracellular affinity for Ca binding protein or synchronous release site; cooperativity between intracellular Ca and ACh release.	Silinsky (240, 241)
—	Ca entry linearly related to [Ca]	A (or Ca_A)	Cooperativity	Katz and Miledi (126)
—	Ca entry linearly related to [Ca]	X	Cooperativity	Crawford (58), Younkin (274), Dascal et al. (63), Andreu and Barrett (4), Barton et al. (19)
—	Ca entry linearly related to [Ca]	Y	Binomial parameter p, X Binomial parameter n (p is non-cooperative, n is third power)	Bennett et al. (21)
—	Ca entry linearly related to [Ca]	A, S	Cooperativity	Balnave and Gage (13)
—	Ca entry linearly related to [Ca]		Intracellular Ca buffers as possible determinants of cooperativity	Nachshen and Drapeau (192)

* All of the listed publications after 1973 assume that: (a) evoked ACh release is initiated by Me entry through Ca channels; (b) the magnitude of this entry is linearly related to extracellular [Ca]; and (c) cooperativity is produced by the relationship between intracellular Ca and ACh release. Those models that raise the possibility of an extracellular receptor that controls Ca entry, e.g. Silinsky (240, 241) and Bennett et al.'s (21) K'_{factor} must have an entry component as part of the cooperative number (even if $n = 1$ for entry) unless the occupancy of Ca as an agonist is so low that the rectangular hyperbola reduces to a straight line (e.g. ref. 240). In the models that do not postulate an Me binding site for Me entry, the entire cooperative relationship is determined intracellularly. The majority of the recent models assume that Mg blocks evoked ACh release near the external surface of Ca channels and that intracellular Mg may increase release.

an extracellular initiation site that regulates Ca translation (column 1) and a subsequent intracellular or membrane reaction that represents the efficacy of the Me species in provoking secretion (column 2). The majority of the recent models have considered the Ca channel as the vehicle for Ca translocation (in contrast to the older view of a membrane carrier) and have assumed that Ca entry is linearly related to extracellular Ca. By exclusion then, cooperativity in these models is a result of behavior at the cytoplasmic aspect of the nerve terminal.

To what do the various K_{ME} and e_{ME} values correspond functionally? It is likely the K_{ME}, as calculated by pharmacological null methods (i.e., by comparing matching levels of ACh release), reflects Me behavior near the external surface of the Ca channel (see section III, A 3 and ref. 240). Table 2 further supports this contention; the K_{CA}, K_{BA}, and K_{MG} values calculated from the Schild equation (eqn 2) are very similar to the K_{ME} for antagonism by Ca, Ba, and Mg of Ca entry into depolarized synaptosomes (table 2).* With respect to e_{ME}, it appears from the liposome studies (133, 178) that efficacy for M reflects the apparent affinity of the Me species for an intracellular binding site (Cabp, A, Y, or X). Although a component of Ca channel mobility in the e_{ME} cannot be excluded at cholinergic nerve endings, mobility does not appear to contribute to e_{ME} at squid giant synapses (8). Regardless of the correlates of K_{ME} and e_{ME}, the presence of spare Ca channels (240) suggests that an intracellular component of the secretory apparatus is the limiting substrate that determines the maximal level of secretion in Ca solutions (see also ref. 63).

As mentioned earlier, cooperatively is defined operationally by a departure from a simple rectangular hyperbolic relation between quantal ACh release and extracellular [Ca] or [Sr]. Positive cooperativity is described formally as $N > 1$ in equation of the form of 8a or 1[1] (for specific mathematical details, see appendix A 8 and A 9); it could reflect the need for simultaneous occupancy of several sites to produce a biological effect (74) or the sequential binding of Me to sites where the apparent K_{ME} increases progressively as each site is occupied (appendix A 9). Those models that raise the possibility of an extracellular Ca binding controlling Ca entry (see

* The situation for K_{SR} still remains to be resolved, however, see refs. 63, 191.

table 4) must include the extracellular binding site as a component of the cooperative number. For Ca as an *agonist* for *M*, however, the amount of Ca bound at the external receptor is so low (i.e., the rectangular hyperbola reduces to a straight line on the spare receptor assumption) that the measured cooperativity for Ca is likely to be entirely intracellular.

At the frog neuromuscular junction, the cooperative number N ranged between 2 and 3 at normal levels of release (120, 240, 104). In the frog at low *M*, (generally, $M < 10$), the fourth power relationship has been widely reproduced and interpreted as a requirement for the cooperative action of four Ca ions in the release of an ACh quantum (74). It has even been shown that the fourth power relationship extends down to very low levels of release ($M \lll 1$), where *M* is reflected as an occasional stimulus-locked MEPP (4; but see ref. 58). This is an unusual result because even in enzymes that are highly cooperative, cooperativity is eliminated at very low substrate concentrations (see e.g. ref. 233, p. 372). Why then is the cooperative number of 4 retained at such low *M*?. One possible explanation is that $N = 4$ in part reflects a process other than the direct activation of the release mechanism by Ca (e.g., secondary removal of Ca from sites of release). If cation clearance is of exaggerated importance as a determinant of the local intracellular [Ca] when preparations are bathed in low Ca/high Mg solutions [intracellular Mg may impair Ca clearance and increase *M* (133)], then cation clearance sites could theoretically make a substantial contribution to the value of the cooperative number (192).

At the frog cutaneous pectoris nerve-muscle junction, the [Ca]-*M* relationship is not so simple; most of the curves show slopes of 2 to 3 but also reveal a region of apparent negative cooperativity ($N < 1$) near normal (1.8 mM) Ca (240). Negative cooperativity, which occurs when the binding or effect of one ligand reduces the subsequent binding or effect of another ligand, is also observed in the range of normal Ca for the [Ca]-asynchronous release relationship (see figure 3, ref. 178).* If such asynchronous release occurs outside the active zone (see discussion in section III B), then negative cooperativity is more likely to be a property of vesicular proteins than membrane proteins at the active zone. As true negative cooperativity has been found at the level of the Ca + calmodulin interaction (136) and calmodulin binding proteins have been found in association with synaptic vesicles (193, 231), the complexities in the [Ca]-*M* relationship may reflect the complex relation between translocated Ca and calmodulin or a calmodulin-like Ca binding protein associated with the cholinergic vesicle. (See appendix A 9 and figure 8B for a mathematical treatment of this notion.)

* True negative cooperativity must be distinguished from an apparent negative cooperativity produced by the concomitant presence of low and high affinity binding sites for a particular ligand (see e.g. ref. 240 and Chapters 2 and 4 in ref. 52).

The actual situation, however, is probably still more complex. Even in artificial membranes, as two membranes progress closer and closer to the ultimate fusion event, the affinity of Ca for these membranes changes progressively during the course of the small pre-fusion movements (215); this would make cooperativity a function of the proximity of vesicular and nerve terminal membranes. Finally, despite the generality of the approach (199), the cooperative number as measured from the limiting slope of the log ACh release-log [Ca] relation (eqn 8‴, appendix A 8) may not be meaningful if there is a substantial Ca-independent fraction of ACh release (209, 19).

B. The Chemical Properties of the Me Species and ACh Release

Which aspects of the physiology of the cholinergic nerve ending may be attributed to the chemical properties of the Me species and to the microscopic environment of the ion in aqueous solution? As table 1, column 3 shows, an ionic potential of less than two is characteristic of an ion that is capable of supporting evoked ACh release, apart from any considerations of synchrony. In contrast, divalent cations with ionic potentials of greater than two are antagonists of evoked transmitter release. With respect to the primary hydration sphere (table 1, column 4), while hydration may explain the gross differences between Mg and the other Me species, it cannot account for the different efficiencies of Ca, Sr, and Ba in supporting *M*. Barium has the least negative free energy of hydration and the fastest rate constant of dehydration and thus loses its primary water shell with the greatest facility; Ba cannot support *M*, however. More insight into agonist behavior for the specific forms of ACh release may be found by examining the last column in table I, namely the coordination number (the number of coordinate bonds an ion can form with nearby moieties). The larger the ion, the more congenital its behavior with its neighbors and the larger the coordination number. Mg tends to coordinate with six and Ba with eight nearest neighbors. Ca, however, has a unique property: it can change its coordination number in a chameleon-like fashion from six to eight depending upon the state of the nearby ligand. It is thus possible that the ability of Ca to be such an efficient agonist is related to its coordination number of 8 prior to depolarization and a lower coordination number and reduced apparent affinity during depolarization. This would allow Ca to be optimally adsorbed at strategic channel regions prior to depolarization and then to enter the fiber without restraints during the action potential (see figure 8A). It might be speculated that divalent cations which have exclusively low coordination numbers (e.g. Mg, Co, Mn, Ni, and Cd) cannot be favorably positioned prior to depolarization and thus cannot readily enter nerve endings and activate Ca bp; this could explain the inability of Cd to support *M* despite its similarity to Ca in other respects (228, 57).

Further dissection of the biophysical pharmacology of secretion requires a discussion of the membrane binding sites. The equilibrium selectivity sequence for antagonism (Ca > Ba > Mg ≥ Sr) suggests the presence of a fairly strong negatively charged membrane site that controls Me entry. The selectivity sequence of K_{ME} values for Ba, Sr, and Ca using the value for Ca as anagonist (Ba > Sr > Ca) is that of a very weak site (sequence *I* as described in section III A 2). It is possible then, that during the fleeting conductance change provided by the action potential, the binding strength of site *X* weakens and allows Ca optimal access to intracellular sites associated with *M* (see figure 8 A 2). It might be speculated that the high affinity of Mg and the preference of Ba for sites of high coordination number (which may make Ba toxic, appendix B) excludes these ions from activating the intracellular binding proteins (e.g., bp in figures 7 and 8A) associated with *M*. With this exclusion, the active state of Cabp might be similar to the inactive *X* site as far as electrostatic site strength is concerned.

This is undoubtedly an oversimplified picture since interactions in the outer sphere of the aqueous environment of ions—the "less ordered" region in figure 5A—will almost certainly influence the biological behavior of the Me species. Relevant features include the specific magnitude of the dielectric constants (273, 262) and the strength and form of hydrogen bonds and are not trivial matters. The situation becomes even more complex when the wealth of potential effects of Ca on organic molecules is considered. Thus, while it might be tempting to postulate that Ca favors oxygen moieties and cooperative interactions between pairs of molecular "hands" on specific Ca binding proteins (94, 273, 61a), such generalities fail to do justice to the plethora of Me-dependent transport proteins, cyclases (adenylate and guanylate), kinases, decarboxylases, methyltransferases and phospholipids available for both short- and long-term regulation of nerve terminal processes (193, 217, 195a, 138a, 111a). For example, transmitter release that is independent of extracellular Ca could be mediated by an increased turnover of inositol phospholipids. Phosphatidylinositol turnover has been shown to induce Ca mobilization from cellular pools in a number of secretory systems (78a, 195a). On the other hand, persistent increases in ACh release might involve phosphorylation of presynaptic proteins by a variety of different protein kinases (see section V B). Despite all that has gone before, then, there are still many walls to crumble before we can understand how the cholinergic nerve ending maintains its graceful intricacy without sacrificing its functional integrity.

Acknowledgments. This work was supported by a Fogarty Senior International Fellowship and by a research grant from the U. S. Public Health Service. I wish to thank Dr. R. C. MacDonald for comments on sections II and III and Dr. P. H. Stern for discussions on the overall structure of the review. I am deeply grateful to Ms. S. J. Austin Silinsky (the Souzs) for comments on the introduction and for her patience during the course of my writing this manuscript.

APPENDICES

A. Derivations of the Equations Used to Study the Binding Constants and Efficacies of Me Antagonists and Agonists

1. The Schild Equation for Calculating K_{ME}'s of Competitive Inhibitors. The basic equilibrium expression for the fraction of Me receptors occupied, y_{ME} (eqn 1) has been derived in section III A 1 (small print). For Ca, eqn 1 is

$$Y_{CA} = \frac{K_{CA}[Ca]}{1 + K_{CA}[Ca]}$$

In this first section of appendix A, the relationship between eqn 1 (which describes y_{CA} alone) and the eqn 2e (which describes y_{CA} in the presence of a competitive inhibitor) will be illustrated on the path to deriving the Schild equation (eqn 2).

For the agonist, Ca, the release sequence may be illustrated as follows:

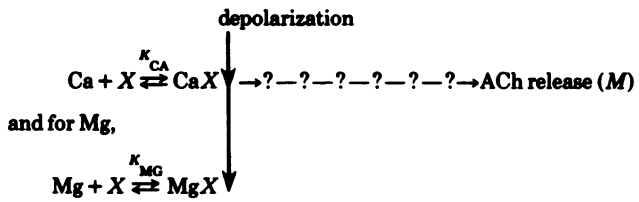

Both of these schemes are written for the Me species alone. Now, for Ca in the presence of Mg at equilibrium, where the rate of the forward reaction is equal to the rate of the backward reaction, the equilibrium expression for Ca is similar to eqn 1d (see text) only the fraction of free receptors, rather than being $1 - y_{CA}$, is 1 minus the fraction occupied by Ca minus the fraction occupied by Mg, i.e., $1 - y_{CA} - y_{MG}$. Thus

$$[Ca]K_{CA} = y_{CA}/(1 - y_{CA} - y_{MG}) \qquad \text{eqn 2a}$$

Now, the reduction in occupancy of Mg by Ca is described by

$$[Mg]K_{MG} = y_{MG}/(1 - y_{CA} - y_{MG}) \qquad \text{eqn 2b}$$

By eqns 2a and 2b, the ratio of the occupancy of Mg to that of Ca is:

$$\frac{y_{MG}}{y_{CA}} = \frac{[Mg]K_{MG}}{[Ca]K_{CA}} \qquad \text{eqn 2c}$$

Solving eqn 2c for y_{MG} and substituting into a rearranged 2a, $y_{CA} = [Ca]K_{CA}(1 - y_{CA} - y_{CA}[Mg]K_{MG}/[Ca]K_{CA})$. Simplifying

$$\frac{y_{CA}}{1 - y_{CA}} = \frac{[Ca]K_{CA}}{1 + [Mg]K_{MG}} \qquad \text{eqn 2d}$$

Solving eqn 2d for y_{CA} by adding the numerator to the denominator of each side,

$$y_{CA} = \frac{[Ca]K_{CA}}{1 + [Ca]K_{CA} + [Mg]K_{MG}} \qquad \text{eqn 2e}$$

Eqn 2e represents the typical equation for the fraction of sites occupied by the agonist in the presence of a competitive inhibitor (253) and has been used in physical chemistry to describe the competition of gases for adsorption onto e.g. charcoal (ref. 2, pp. 404–405).

If it is assumed that equal values of *M* produced by a low concentration of Ca, $[Ca_L]$ and by a higher concentration of Ca in the presence of Mg, $[Ca_H]$, are produced by equal levels of receptor occupancy, then by eqn 1 and 2e:

$$\frac{[Ca_L]K_{CA}}{1 + [Ca_L]K_{CA}} = \frac{[Ca_H]K_{CA}}{1 + [Ca_H]K_{CA} + [Mg]K_{MG}} \quad \text{eqn 2f}$$

Rearranging:

$$\frac{[Ca_H]}{[Ca_L]} - 1 = [Mg]K_{MG} \quad \text{eqn 2}$$

where the ratio of the two concentrations of agonist that produces matching responses, is, in Gaddum's (91) original terminology, called the DOSE RATIO. Thus

$$\text{DOSE RATIO} - 1 = [Mg]K_{MG} \quad \text{eqn 2}$$

Eqn 2 is generally known as the *Schild equation* (229, 6). It is independent of: the affinity constant for the agonist (K_{CA} cancelled in eqn 2f), the shape of the [Ca]-*M* curve, the particular *X* site agonist and the y_{CA}. The importance of this latter property of eqn 2, namely its independence on y_{CA} may be made more apparent if eqn 1a is reconsidered. Specifically, the assumption of equilibrium

$$k_{+1}[Me][X] = k_{-1}[MeX] \quad \text{eqn 1a}$$

may not apply to agonists which produce their effects rapidly after being bound; i.e., eqn 1a is only applicable to agonists when the binding reaction is rapid and thus essentially in equilibrium when compared to the much slower rates of the processes that ensue after binding. The rapid equilibrium assumption is characteristic of Michaelis-Menten kinetics and was used in the model of Dodge and Rahamimoff (eqn 8a) and Hubbard et al. (eqn 21 and 22).

Generally, the Schild equation describes the effect of any competitive inhibitor at *X* as follows:

$$\text{DOSE RATIO FOR AGONIST} - 1 = [Me]K_{ME} \quad \text{eqn 2}$$

where Me in eqn 2 is a competitive inhibitor at site *X*. When K_{ME} remains constant over a range of dose ratios, then it is highly probable that Me is a competitive inhibitor. The most stringent test for competitive inhibition, impracticable at motor nerve endings, is to examine dose ratios as high as 100 and to plot eqn 2 on a log-log plot (termed the Schild plot). If the slope of this plot is 1, then competitive inhibition is strongly suggested. In addition, Schild defined the pA_2, which = log K_{ME}. The pA_2 signifies that the negative log of the agonist concentration that produces a dose ratio = 2, equals the log K_{ME} on a Schild plot.

2. Determination of K_{SR}. The extrapolation method for determining K_{SR} from fourth root Lineweaver-Burk plots is described in the main text (section III A 3 eqn 9a and 9b). This present section focuses on the K_{SR} determined from the mathematical framework of receptor theory.

A. AS A COMPETITIVE INHIBITOR. To use the Schild equation to calculate K_{SR}, it is first necessary to reduce e_{SR} to 0. Such experiments are described in the text and shown in figure 6A.

B. AS A PARTIAL AGONIST ASSUMING SPARE Ca RECEPTORS. The parameter that Stephenson (252) termed the stimulus (*S*), is defined as a linear function of both *e* and *y*, thus for any Me species:

$$S_{ME} = e_{ME}y_{ME} \quad \text{eqn 10}$$

As part of this definition, it is assumed that non-linearities in the y_{ME}-*M* relationship are introduced beyond the sites of occupancy and efficacy.

There are several methods for calculating K_{SR} as a partial agonist on the spare receptor assumption. This assumption, translated into mathematical terms, is as follows. Ca is used in low concentrations and the K_{CA} as an agonist is generally low, therefore $[Ca]K_{CA} \ll 1$ and y_{CA} reduces to

$$y_{CA} = [Ca]K_{CA} \quad \text{eqn 11}$$

i.e., the concentration and affinity of Ca are negligible in the denominator of the adsorption isotherm (eqn 1).

i. Comparing equal M in Ca and in Sr. If a certain level of *M* produced in low Ca (M_{CA}) is matched by a higher concentration of Sr (M_{SR}), as $M_{CA} = M_{SR}$ then $S_{CA} = S_{SR}$. Thus by eqn 10, $e_{CA}y_{CA} = e_{SR}y_{SR}$, and by eqn 1

$$\frac{e_{CA}[Ca]K_{CA}}{1 + [Ca]K_{CA}} = \frac{e_{SR}[Sr]K_{SR}}{1 + [Sr]K_{SR}} \quad \text{eqn 10a}$$

On the spare receptor assumption (eqn 11), S_{CA} becomes

$$S_{CA} = e_{CA}[Ca]K_{CA} \quad \text{eqn 11a}$$

Thus eqn 10a simplifies to:

$$\frac{e_{CA}[Ca]K_{CA}}{1} = \frac{e_{SR}[Sr]K_{SR}}{1 + [Sr]K_{SR}} \quad \text{eqn 10b}$$

Taking reciprocals of both sides of eqn 10b and simplifying (253, 51),

$$\frac{1}{[Ca]} = \frac{e_{CA}K_{CA}}{e_{SR}K_{SR}[Sr]} + \frac{e_{CA}K_{CA}}{e_{SR}} \quad \text{eqn 10c}$$

As shown in figure 6B, eqn 10c is the equation of a straight line comparing matching levels of ACh secretion produced in a certain [Ca] (the reciprocal of this [Ca] is the abcissa) and in a certain [Sr] (the reciprocal of this [Sr] is the ordinate). The experimental results plotted in accordance with eqn 10c are shown in figure 6B. When $1/[Ca] = 0$, then $1/[Sr] = K_{SR}$. (As shown in figure 6B, K_{SR} may be estimated by the ratio of the intercept to the slope.)

ii. Comparing equal M in Ca and Ca + Sr. This treatment begins with an equation of the form of 2e, using Sr as a competitive inhibitor of Ca (eqn 2e′):

$$y_{CA(SR)} = \frac{[Ca_{SR}]K_{CA}}{1 + [Ca_{SR}]K_{CA} + [Sr]K_{SR}} \quad \text{eqn 2e′}$$

where $[Ca_{SR}]$ is the concentration of Ca in the presence of Sr that produces a matching *M* to calcium in the absence of Sr ([Ca]), and $y_{CA(SR)}$ is the occupancy of Ca in the presence of Sr. The stimulus for Ca in the presence of Sr is thus: $S_{CA(SR)} = e_{CA}y_{CA(SR)}$. Similarly, applying eqn 2e for Ca as a competitor for Sr binding sites

$$y_{SR} = \frac{[Sr]K_{SR}}{1 + [Sr]K_{SR} + [Ca_{SR}]K_{CA}} \quad \text{eqn 2e″}$$

Now, using Stephenson's assumption that stimuli are additive (252), as did Meiri and Rahamimoff (175), then $S_{CA+SR} = S_{CA(SR)} + S_{SR}$, substituting

$$S_{CA+SR} = \frac{e_{CA}[Ca_{SR}]K_{CA} + e_{SR}[Sr]K_{SR}}{1 + [Ca_{SR}]K_{CA} + [Sr]K_{SR}} \quad \text{eqn 12}$$

Eqn 12 is the equation used by Meiri and Rahamimoff only with $S_{CA+SR} = M$, $e_{CA} = 1$, and $e_{SR} = \beta$ (see eqn 12a, appendix A 5 and section III A 3). Eqn 12 is a commonly used expression but will not be employed further in this section. Instead, $S_{CA(SR)}$ will be simplified as follows. On the spare receptor assumption, the stimulus for Ca in the presence of Sr is $S_{CA(SR)} = e_{CA}[Ca_{SR}]K_{CA}(1 - y_{SR})$. Thus, as before, the denominator of y_{CA} is ignored, and, in addition, the occupancy for Ca is reduced from 1 by the fraction of sites occupied by Sr (i.e. the simplified y_{CA} is multiplied by $(1 - y_{SR})$ and by e_{CA} to produce the Stephensonian expression for the stimulus of Ca in the presence of Sr.

Now, equating stimuli for equal *M* in the presence and absence of Sr and assuming that equilibrium is reached and that stimuli are additive, $S_{CA} = S_{CA(SR)} + S_{SR}$. If spare receptors are present, then $e_{CA}[Ca]K_{CA} = e_{CA}[Ca_{SR}]K_{CA}(1 - y_{SR}) + e_{SR}y_{SR}$. Dividing both sides by y_{SR} and simplifying in accordance with $(1 - y_{SR})/y_{SR} = 1/[Sr]K_{SR}$ (eqn 1d), then

$$e_{CA}K_{CA}[Ca] = \frac{e_{CA}K_{CA}[Ca_{SR}] + e_{SR}y_{SR}}{1 + [Sr]K_{SR}}$$

or

$$[Ca] = \frac{[Ca_{SR}]}{(1 + [Sr]K_{SR})} + \text{INTERCEPT} \quad \text{eqn 13}$$

where the INTERCEPT = $e_{SR}K_{SR}[Sr]/\{e_{CA}K_{CA}(1 + [Sr]K_{SR})\}$ and is constant for a fixed [Sr]. Eqn 13 predicts a linear relationship between $[Ca_{SR}]$ and [Ca]; this indeed has been observed (see ref. 240). An inspection of eqn 13 reveals that $K_{SR} = \{(1/\text{slope}) - 1\}/[Sr]$; K_{SR} calculated by this method was 0.24 mM^{-1} (see table 2). Note that if $e_{SR} = 0$, eqn 13 reduces to the Schild eqn (eqn 2). It should be noted that in ref. 240, eqn 5a, K_{CA} should read K^1, where, $K^1 = K_{CA}e_{CA}K_{SR}^{-1}[1 + [Sr]K_{SR}]$.

3. Determination of K_{CA}. The extrapolation method for determining K_{CA} (eqn 8 to 8d) and its drawbacks are described in section III A 3. The following are the details of the calculation of K_{CA} by receptor theory (89, 266, 51, 253).

For this method, it is necessary to compare equal M in Ca before and after irreversible occlusion of a fraction (z) of the total number of X sites by La. $[Ca_{LA}]$ is the concentration of Ca after irreversible blockade that produces matching M in [Ca] before blockade.

Equating stimuli $S_{CA} = S_{CA\,LA}$ or

$$\frac{e_{CA}[Ca]K_{CA}}{1 + [Ca]K_{CA}} = \frac{e_{CA}[Ca_{LA}]K_{CA}(1 - z)}{1 + [Ca_{LA}]K_{CA}} \qquad \text{eqn 14a}$$

where $S_{CA\,LA}$ is the stimulus after irreversible block by La, and $1 - z$ is the fraction of receptors free. Thus to produce matching M, the [Ca] must be elevated to $[Ca_{LA}]$ because the maximal fraction of free receptors, has been reduced from 1 to $1 - z$. Linearization (eqn 14) does not require the spare receptor assumption, just a slight rearrangement:

$$\frac{1}{[Ca]} = \frac{1}{1 - z}\frac{1}{[Ca_{LA}]} + \frac{zK_{CA}}{1 - z} \qquad \text{eqn 14}$$

This equation describes a straight line relation between 1/[Ca] and $1/[Ca_{LA}]$. The value of z is determined from the slope ($=1/(1 - z)$) and K_{CA} from $1/[Ca]_{LA} = -zK_{CA}$ at $1/[Ca] = 0$. K_{CA} was found to range from 0.02 to 0.06 mM^{-1} (240).

The range of values estimated for K_{CA} as an agonist is 2 orders of magnitude less than the K_{CA} as an antagonist (eqn 2) for the external membrane site that controls Ca entry. One explanation for these differences has been presented in section III A 3 and figure 8A. An alternative explanation may be provided by examining a two-state model of the receptor (189, 121, 51, 52). In such models, the receptor is viewed as existing in two conformations when the membrane is depolarized, active (X^*) and inactive ($X-$). Ca, the full agonist, binds to the active state preferentially and dramatically shifts the $X- \leftrightarrow X^*$ equilibrium in favor of the active state. Antagonists (e.g. Mg) bind preferentially to the inactive state or with equal affinity to the active and inactive states. The ratio of inactive to active sites in the absence of Me is termed $L(= [X-]/[X^*])$; L thus represents an isomerization constant. This scheme is illustrated below.

$$\begin{array}{ccc} Ca + X^* \rightleftarrows CaX^* & \rightarrow & \text{ACh release} \\ \Updownarrow L & & \\ Ca + X- & & \end{array}$$

By the two-state model, the K_{CA} *when measured by eqn* 14 *for Ca as an agonist* is biased towards lower values by the isomerization constant, L (51). This is because part of the free energy of binding for full agonists is used in promoting the conformational change in the receptor. Thus if the ratio of resting to active sites is 320 and the K_{CA} as measured by eqn 14 is 0.025 mM^{-1}, then it can be shown (see ref. 51) that the microscopic affinity = $(LK_{CA}) = (320)\cdot(0.025)$ or 8 mM^{-1}; this was the K_{CA} measured as an antagonist. By this interpretation, the partial agonist, Sr, would be predicted to have the same affinity as an agonist and as an antagonist (e.g., table 2 and ref. 51).

The theoretical predictions of the two-state model are experimentally indistinguishable from the modified occupation theory of the receptor (51, 261). The modified occupation theory appears to provide a more appropriate physical picture of the nerve ending; however, as, by this theory, efficacy reflects the behavior of an Me species at a site beyond the extracellular Ca receptor. Indeed, it appears from the liposome studies that efficacy for M reflects the apparent affinity of the Me species for an intracellular binding site beyond the extracellular Ca receptor (see table 4). In contrast, the two-state model considers efficacy to represent the relative affinity of the Me species for $X-$ and X^* with no consideration of intracellular Me effects beyond the external receptor (51, 261).

4. Determination of e_{CA}. A. ASSUMING $e_{CA} = 1$. In the original work of Dodge and Rahamimoff (74), e_{ME} for the full agonist was assumed to equal 1; this is in accordance with the original Ariens approach to efficacy (intrinsic activity, ref. 5) that predated the observation of spare receptors. By this view, [Me] that produces a 50% maximum response $= 1/K_{ME}$. Ariens and colleagues have subsequently revised their views (264).

B. BY MODIFIED OCCUPATION THEORY. To determine e_{CA}, it is customary to define $S = 1$ at the [Ca] that produces a 50% maximum response ($[Ca_{50}]$) (252, 253). Then, by rearranging eqn 10 and using the spare receptor assumption:

$$e_{CA} = 1/(K_{CA}[Ca_{50}]) \qquad \text{eqn 15}$$

The e_{CA} may then be determined from the measured $[Ca_{50}]$ and the calculated K_{CA}; e_{CA} ranged from 9 to 20 (240).

5. Determination of e_{SR}. A. MEIRI AND RAHAMIMOFF'S METHOD. These authors (175) used the following variant of eqn 12 (see above).

$$M = \{[Ca]K_{CA} + \beta[Sr]K_{SR})/(1 + [Ca]K_{CA} + [Sr]K_{SR})\}^4 \qquad \text{eqn 12a}$$

β was determined indirectly by differentiating M in eqn 12a with respect to Sr and setting this value to zero. The resulting expression solved for β is

$$\beta = [Ca_{NULL}]K_{CA}/(1 + [Ca_{NULL}]K_{CA}) \qquad \text{eqn 17}$$

where $[Ca_{NULL}]$ refers to the Ca concentration at which changing the Sr concentration produces no effect on M (i.e. the Ca concentration at which dM/dSr = 0). Using their extrapolated K_{CA} value and the experimentally determined $[Ca_{NULL}]$, eqn 17 was used to calculate β. The β values ranged from 0.3 to 0.5—see next section, part b, for discussion.

B. BY MODIFIED OCCUPATION THEORY. The intercept in eqn 10 is equal to: $e_{CA}K_{CA}/e_{SR}$. Rearranging eqn 15

$$[Ca_{50}] = 1/e_{CA}K_{CA} \qquad \text{eqn (15a)}$$

Finally,

$$e_{SR} = ([Ca_{50}] * \text{intercept of eqn } 10)^{-1} \qquad \text{eqn 16}$$

The e_{SR} values determined from eqn 16 ranged from 0.2 to 0.5 (240). Although these values for e_{SR} are in excellent agreement with the β values of the preceding section, the similarities are more apparent than real.

Specifically, eqn 12a shows that β *is raised to the fourth power* so that β ranging from 0.3 to 0.5 means, that maximal M in Sr is $(0.3)^4$ to $(0.5)^4$ or 0.8% to 6.3% maximal M in Ca (recall β for Ca was assumed to = 1). To use the experiment shown in figure 2A as an example, with maximal M = 1000 quanta in Ca, then maximal M in Sr should be between 8 and 63 quanta. Such a relationship was never observed, suggesting that the fourth power model may not be applicable to partial agonists. Further experimental evidence not in accord with the fourth power model as a description of the entire [Me]-M relation is also illustrated by the experiment in figure 2A. Specifically, eqn 1a shows that when $y_{ME} = 0.5$, then the [Me] that produces this 50% maximal occupancy $= 1/K_{ME}$. By the fourth power model, if Sr and Ca have equal K_{ME}'s, then the individual [Ca]-M and [Sr]-M curves should be half maximal at the same [Me] regardless of the Me agonist. Again, this is not the case. It is likely that estimation of K_{CA} is inaccurate due to the presence of spare Ca receptors (253). Another source of error is the Lineweaver-Burk plot, which, even for analysis of first power concentration-response relationships has encountered considerable criticism (50); the inaccuracies are compounded by the fourth power relationship. As described above, the precise value of β is dependent on the K_{CA} calculated by Lineweaver-Burk extrapolation as well.

6. Equations for the Kinetic Model of Hubbard et al. This model (116) is outlined below. Note the three different effective affinity

constants for Ca, K_{CA1} to K_{CA3}, representing the sequential binding of Ca (three Ca per X site is the maximum possible in this model) and the rate constant (k's) for each of the states:

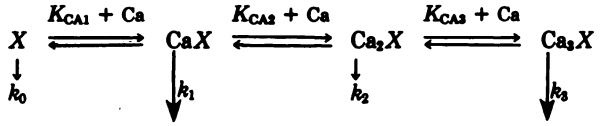

The effective affinity constants are defined in a fashion similar to the different liganded states of a polyprotic acid, thus:

$$K_{CA1} = [CaX]/[Ca][X] \qquad \text{eqn 18a}$$

$$K_{CA2} = [Ca_2X]/[Ca][CaX] \qquad \text{eqn 19a}$$

$$K_{CA3} = [Ca_3X]/[Ca][Ca_2X] \qquad \text{eqn 20a}$$

It should be stressed that these are only effective affinity constants; to obtain the intrinsic constants (microscopic constants), each of the three sites must be considered in isolation with respect to its interactions with the remaining sites, see A 9, below). By rearrangement of these equations, the concentrations of the different species are:

$$[CaX] = K_{CA1}[Ca][X] \qquad \text{eqn 18b}$$

$$[Ca_2X] = K_{CA2}[Ca][CaX] \qquad \text{eqn 19b}$$

$$[Ca_3X] = K_{CA3}[Ca][Ca_2X] \qquad \text{eqn 20b}$$

The occupancy, y_{CA} as before equals the sum of the bound states/X_T, thus

$$y_{CA} = \frac{[CaX] + [Ca_2X] + [Ca_3X]}{[X] + [CaX] + [Ca_2X] + [Ca_3X]} \qquad \text{eqn 21a}$$

Substituting the expressions for the various bound terms (eqns 18b to 20b) into eqn 21a produces

$$y_{CA} = \frac{[Ca]K_{CA1}[X] + [Ca]K_{CA2}[CaX] + [Ca]K_{CA3}[Ca_2X]}{X + [Ca]K_{CA1}[X] + [Ca]K_{CA2}[CaX] + [Ca]K_{CA3}[Ca_2X]}$$

Dividing numerator and denominator by $[X]$

$$y_{CA} = \frac{[Ca]K_{CA1} + [Ca]K_{CA2}([CaX]/[X]) + [Ca]K_{CA3}([Ca_2X])/[X]}{1 + [Ca]K_{CA1} + [Ca]K_{CA2}([CaX]/[X]) + [Ca]K_{CA3}([Ca_2X]/[X])} \qquad \text{eqn 21b}$$

Now as

$$[CaX]/[X] = K_{CA1}[Ca] \qquad \text{eqn 18c}$$

and

$$[Ca_2X]/[X] = K_{CA2}[Ca][CaX] \qquad \text{eqn 19c}$$

then substituting 18c into 19c

$$[Ca_2X]/[X] = K_{CA1}K_{CA2}[Ca]^2 \qquad \text{eqn 19d}$$

Finally, substituting 18c and 19d into 21b

$$y_{CA} = \frac{[Ca]K_{CA1} + [Ca]^2K_{CA1}K_{CA2} + [Ca]^3K_{CA1}K_{CA2}K_{CA3}}{1 + [Ca]K_{CA1} + [Ca]^2K_{CA1}K_{CA2} + [Ca]^3K_{CA1}K_{CA2}K_{CA3}} \qquad \text{eqn 21}$$

This is a description of the binding phenomenon. To describe ACh release, the kinetic constants (related to efficacy) are inserted so that for each particular liganded X, the fraction of the maximal ACh release contributed by that species is equal to the rate constant multiplied by the concentration of that species, e.g. ACh release from $CaX = k_1[CaX] = k_1[Ca]K_{CA1}$, etc. Much as the maximal reaction velocity in Michaelis-Menten kinetics is equal to the rate constant for product formation, multiplied by the total enzyme concentration, then maximal ACh release $= k_N X_T$.

This Michaelis-Menten "kinetic" model thus uses the rapid equilibrium assumption, i.e. the binding of Ca to X is assumed to be so rapid that it is in equilibrium compared to the subsequent steps (k's) that produce ACh release.

The final expression desired is

$y_{RELEASE}$ = (Ca-independent release + Ca-dependent release)/ maximal release eqn 22a

The denominator of $y_{RELEASE}$ is simply the denominator of eqn 21 multiplied by k_N. The numerator is the same as eqn 21 only each term is multiplied by the kinetic constant representing the "efficacy" of that species. In addition the constant k_0 is needed for the Ca-independent fraction of release. Thus the final expression is

$$y_{RELEASE} = \frac{k_0 + k_1[Ca]K_{CA1} + k_2[Ca]^2K_{CA1}K_{CA2} + k_3[Ca]^3K_{CA1}K_{CA2}K_{CA3}}{k_N(1 + [Ca]K_{CA1} + [Ca]^2K_{CA1}K_{CA2} + [Ca]^3K_{CA1}K_{CA3}K_{CA3})} \qquad \text{eqn 22}$$

7. The Equations of the Log Model of Cooke et al. This model (53, 208) is a hybrid of the adsorption isotherm for multiple sites (similar to that of Hubbard et al.) and the Poisson distribution. It should be noted that the X site here is an intracellular release site and the Y site is a cation translocation site.

Beginning with the release site, X, the behavior of this site is assumed to follow that of a simple rectangular hyperbola (eqn 1)

$$y_{IN} = [CaX]/X_T = \frac{[Ca_{IN}]K_{CA\,IN}}{1 + [Ca_{IN}]K_{CA\,IN}} \qquad \text{eqn 1f}$$

or

$$[CaX] = \frac{X_T[Ca_{IN}]K_{CA\,IN}}{1 + [Ca_{IN}]K_{CA\,IN}} \qquad \text{eqn 1g'}$$

(See, e.g., eqn 1g in section III C) Eqn 1g' serves as a link between intracellular Ca and the Poisson process that relates $[CaX]$ to ACh release. With respect to extracellular Ca, the process of ion translocation (Y is the site that transports Ca) is assumed to be activated when two and only two bound Ca (Ca_2Y) participate in Ca entry as follows:

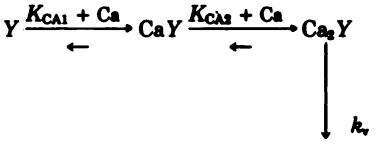

The constant k_v is related to Ca entry with the subscripted v indicating that it is voltage sensitive. The intracellular Ca concentration in the vicinity of X is related to this scheme by:

$$[Ca_{IN}] = k_v[Ca_2Y] \qquad \text{eqn 30}$$

The constant k_v is related to Ca entry with the subscripted v indicating that it is voltage sensitive. The intracellular Ca concentration in the vicinity of X is related to this scheme by:

$$y_{CA} = \frac{[Ca]K_{CA1} + [Ca]^2K_{CA1}K_{CA2}}{1 + [Ca]K_{CA1} + [Ca]^2K_{CA1}K_{CA2}} \qquad \text{eqn 21b}$$

Only Ca_2Y participates in transport, however, so the fraction of the occupied sites that produces Ca entry, $y_{TRANSPORT}$ is

$$y_{TRANSPORT} = [Ca_2Y]/Y_T = \frac{[Ca]^2K_{CA1}K_{CA2}}{1 + [Ca]K_{CA1} + [Ca]^2K_{CA1}K_{CA2}} \qquad \text{eqn 21c}$$

Solving for $[Ca_2Y] = y_{TRANSPORT}(Y_T)$ eqn 21d

$$[Ca_2Y] = \frac{Y_T[Ca]^2K_{CA1}K_{CA2}}{1 + [Ca]K_{CA1} + [Ca]^2K_{CA1}K_{CA2}} \qquad \text{eqn 21e}$$

What is desired, however, is an expression for $[CaX]$ (an intracellular bound Ca concentration) as a function of extracellular Ca ([Ca]).

Combining eqns 1g′ and 30:

$$[\mathrm{Ca}X] = \frac{X_T k_v [\mathrm{Ca}_2 Y] K_{\mathrm{CA\,IN}}}{1 + k_v [\mathrm{Ca}_2 Y] K_{\mathrm{CA\,IN}}}$$

Substituting for $[\mathrm{Ca}_2 Y]$ in accordance with eqn 21d and rearranging:

$$[\mathrm{Ca}X] = \frac{X_T k_v Y_T}{(1/y_{\mathrm{TRANSPORT}} K_{\mathrm{CA\,IN}}) + k_v Y_T} \qquad \text{eqn 31}$$

Substituting the expression for $y_{\mathrm{TRANSPORT}}$ (eqn 21c) into the denominator of eqn 31, and focusing on the DENOMINATOR only:

DENOMINATOR

$$= \frac{\{(1/[\mathrm{Ca}]^2) + (K_{\mathrm{CA1}}/[\mathrm{Ca}]) + K_{\mathrm{CA1}} K_{\mathrm{CA2}} + K_{\mathrm{CA1}} K_{\mathrm{CA2}} K_{\mathrm{CA\,IN}} k_v Y_T\}}{K_{\mathrm{CA1}} K_{\mathrm{CA2}} K_{\mathrm{CA\,IN}}},$$

which upon rearrangement produces DENOMINATOR

$$= \frac{K_{\mathrm{CA1}} K_{\mathrm{CA2}} (K_{\mathrm{CA\,IN}} k_v Y_T + 1) + (1/[\mathrm{Ca}]^2) + K_{\mathrm{CA1}}/[\mathrm{Ca}]}{K_{\mathrm{CA1}} K_{\mathrm{CA2}} K_{\mathrm{CA\,IN}}}$$

Defining the term an *effective affinity constant* K, as $K = K_{\mathrm{CA1}} K_{\mathrm{CA2}} (K_{\mathrm{CA\,IN}} k_v Y_T + 1)$, the denominator becomes:

$$\mathrm{DENOMINATOR} = \frac{K + (1/[\mathrm{Ca}]^2) + K_{\mathrm{CA1}}/[\mathrm{Ca}]}{K_{\mathrm{CA1}} K_{\mathrm{CA2}} K_{\mathrm{CA\,IN}}}$$

$$= \frac{1 + (1/K)\{(1/[\mathrm{Ca}]^2) + K_{\mathrm{CA1}}/[\mathrm{Ca}]\}}{K_{\mathrm{CA1}} K_{\mathrm{CA2}} K_{\mathrm{CA\,IN}}/K}$$

Using the definition of K whereby $K_{\mathrm{CA1}} K_{\mathrm{CA2}} K_{\mathrm{CA\,IN}}/K = K_{\mathrm{CA1}} K_{\mathrm{CA2}} K_{\mathrm{CA\,IN}}/K_{\mathrm{CA1}} K_{\mathrm{CA2}} (K_{\mathrm{CA\,IN}} k_v Y_T + 1) = 1/(k_v Y_T + 1/K_{\mathrm{CA\,IN}})$ and substituting into the denominator: DENOMINATOR $= (k_v Y_T + 1/K_{\mathrm{CA\,IN}})[1 + 1/K\{(1/[\mathrm{Ca}]^2) + K_{\mathrm{CA1}}/[\mathrm{Ca}]\}]$. Putting the denominator back into $[\mathrm{Ca}X] = k_v X_T Y_T/\mathrm{DENOMINATOR}$ (eqn 31a) produces

$$[\mathrm{Ca}X] = \frac{k_v X_T Y_T}{(k_v Y_T + 1/K_{\mathrm{CA\,IN}})[1 + (1/K)\{(1/[\mathrm{Ca}]^2) + [K_{\mathrm{CA1}}/[\mathrm{Ca}]\}]} \qquad \text{eqn 31b}$$

Now, using the terminology of Cooke et al., if *beta* is defined as $= (k_v X_T Y_T)/(k_v Y_T + 1/K_{\mathrm{CA\,IN}})$ where beta is thus related to the total number of sites available for translocation and release, to the entry rate constant (k_v) and to the intracellular Ca affinity, *epsilon* is defined as $= K_{\mathrm{CA1}}$, i.e., as the affinity for the first extracellular binding reaction, and *gamma* is a lumped dissociation constant $= 1/K^{1/2}$, then, at long last!!!!! we arrive at eqn 25 of Cooke et al. (see section III C; see also eqn 4.3, ref. 53).

$$[\mathrm{Ca}X] = \frac{\mathrm{beta}}{1 + \mathrm{gamma}^2\{1/[\mathrm{Ca}]^2 + \mathrm{epsilon}/[\mathrm{Ca}]\}} \qquad \text{eqn 32}$$

This equation describes the relationship between extracellular Ca and the amount of Ca bound at intracellular releasing sites. The terminology is that of Cooke et al. It should be realized that the constants are dependent on each other in an algebraically displeasing way. The only exception appears to be the independence of epsilon and beta.

The following mathematical treatment describes the relationship between $[\mathrm{Ca}X]$ and ACh release. Say R is the resting ACh release probability and r is a particle of an activating substance. The presence of one particle r increases the release probability to rR ($r > 1$). If another particle of activator r is present, then the release probability will be r^2R. For N particles then, the probability of release will be r^NR. If it is assumed that each particle causes the same reduction in energy barrier independently of any other particle, and the spatial distribution of particles is *random*, then these N particles will be Poisson distributed. Specifically, given a certain mean number of particles per area of release (termed λ where λ could be e.g. a certain $[\mathrm{Ca}X]$ at a release site), then the probability of finding a particular number (e.g., 0, 1, 2, 3, . . . , N) of these particles at a release site is described by Poisson's law:

$$p_N = \lambda^N \exp(-\lambda)/N! \qquad \text{eqn 24}$$

where

$$p_N = \frac{\text{number of sites with } N \text{ particles}}{\text{total number of sites}} = \frac{\mathrm{sites}_N}{c}$$

(The term "sites" need not refer to active zones but could be applied to vesicles as well.) Thus the *number* of sites: with 0 particles $= \mathrm{sites}_0 = cp_0 = c \exp(-\lambda)$; with 1 particle $= \mathrm{sites}_1 = cp_1 = c\lambda \exp(-\lambda)$; with 2 particles $= \mathrm{sites}_2 = cp_2 = c\lambda^2 \exp(-\lambda)/2$; and with N particles $= \mathrm{sites}_N = cp_N = c\lambda^N \exp(-\lambda)/N!$. Now, as the MEPPf is determined by all N sites, it is necessary to sum the contributions of all the individual sites. Assuming that r refers to molecules of $\mathrm{Ca}X$ and beginning with the first term, which is the Ca-independent fraction of MEPPf, then MEPPf $= \mathrm{sites}_0 R$, i.e. the number of sites with no $\mathrm{Ca}X$ multiplied by the probability of release in the absence of activator. The MEPPf in the presence of activator is thus the sum of the Ca-independent MEPPf and the contribution from all the other sites:

$$\mathrm{MEPPf} = \mathrm{sites}_0 R + \mathrm{sites}_1 Rr + \mathrm{sites}_2 Rr^2 + \mathrm{sites}_3 Rr^3 + \cdots + \mathrm{sites}_N Rr^N \qquad \text{eqn 33}$$

where each additional term is the resting probability (R) multiplied by the number of sites with N particles and the probability increment factor r^N. The term r is really an energy barrier *reduction* factor so that $r = \exp(-\Delta E_{\mathrm{ACT}}/\mathrm{RT})$ where RT = 34 at room temperature. Thus, the more activator particles (r) present, the greater the reduction in the activation energy barrier ($-\Delta E_{\mathrm{ACT}}$) and the greater the fraction of total number of quanta or release sites that can be involved in secretion.

Now, the Poissonian expression for the number of sites with N activators (sites_N) is:

$$\mathrm{MEPPf} = c \sum_{N=0}^{N=\infty} Rr^N \lambda^N \exp(-\lambda)/N! \qquad \text{eqn 33a}$$

which is the first equation of the log model (ref. 53, p. 462). Adding the individual terms of the Poisson distribution and then factoring

$$\mathrm{MEPPf} = cR \exp(-\lambda)\{1 + r\lambda + (r^2\lambda^2/2!) + (r^3\lambda^3/3!) + \cdots\} \qquad \text{eqn 33b}$$

If it is remembered that $\exp \lambda = 1 + \lambda + (\lambda^2/2!) + (\lambda^3/3!) + \cdots$ and $\exp(r\lambda) = 1 + r\lambda + (r^2\lambda^2/2!) + (r^3\lambda^3/3!) + \cdots$, then the term in { } of eqn 33b reduces to $\exp(r\lambda)$. Thus MEPPf $= cR \exp(-\lambda)\exp(r\lambda)$ or MEPPf $= cR \exp\{\lambda(r-1)\}$ (see ref. 53, p. 462). Finally, taking natural logs of both sides $\ln \mathrm{MEPPf} = \ln cR + \lambda(r-1)$ (see ref. 53, p. 462). Defining $a_0 = \ln cR$ and $[\mathrm{Ca}X]$ as proportional to λ (with the proportionality constant $= a_1$, then (see eqn 2.2, p. 463, ref. 53)

$$\ln \mathrm{MEPPf} = a_0 + a_1[\mathrm{Ca}X] \qquad \text{eqn 34}$$

where $[\mathrm{Ca}X]$ is described by eqn 32. *This represents the mathematical statement of the log model of Quastel and his colleagues.* As described in the main text, it can be extended to other activators as follows (see eqn. 2.1, ref. 53):

$$\ln \mathrm{MEPPf} = a_0 + a_1[\mathrm{Ca}X] + a_2[\text{drug } x] + a_3[\text{drug } y] + \cdots \qquad \text{eqn 35}$$

where a_2 and a_3 are constants. (Each constant a is akin to the "efficacy" of the particular activator.) For further details, see section III C and the original publications (53–56).

8. Equations used to Determine the Cooperative Number (N) for Ca in the Process of ACh Release. Regardless of the specific site(s) of cooperativity in the relationship between M and [Me] (i.e., binding or at loci beyond the binding site), departure of the [Me]-ACh release relationship from a simple rectangular hyperbola (eqn 1) suggests Me species cooperate in the process of secretion (51, 52, 233). Under some, but not all, conditions, the cooperative number N, reflects the number of agonist molecules that cooperate to produce the biological effect (see

ref. 51, 52, and 233 for details). Cooperativity may be described mathematically by eqns 8‴ or 1‴ presented in sections A and B below.

A. DODGE AND RAHAMIMOFF'S (74) METHOD. By eqn 8a, $y_{RELEASE} = \{e_{ME}y_{ME}\}^N$. If Me = Ca, and e_{CA} is assumed to be 1, then substituting for y_{CA} in accordance with eqn 1,

$$y_{RELEASE} = \{[Ca]K_{CA}]/(1 + [Ca]K_{CA})^N \qquad \text{eqn 8a'}$$

Now at low [Ca], $[Ca]K_{CA} \ll 1$ and the denominator of eqn 8a' reduces to 1. Thus, at low [Ca],

$$y_{RELEASE} = \{[Ca]K_{CA}\}^N \qquad \text{eqn 8a''}$$

Taking $\log_{10}$ of both sides of eqn 8a'' and assuming $y_{RELEASE}$ is proportional to EPP amplitude, then

$$\log_{10}EPP(C) = N \log_{10}K_{CA}[Ca] \qquad \text{eqn 8'''}$$

where both C and K_{CA} are constants.

Thus, a log-log plot of EPP against [Ca] would produce a slope of N at low concentrations of Ca. Dodge and Rahamimoff found a value of $N = 4$ using eqn 8‴, an observation that knighted the fourth power model. Additional details and some criticisms of this approach may be found in 270, 208, 19, and 199. The most salient criticism is that this equation does not hold if a substantial Ca-independent fraction of release exists (19). It may be noted that, in the model of Quastel and colleagues, the value of N as estimated by eqn 8‴, is skewed by the constant *beta* and does not represent the number of Ca ions that cooperate in release (208, but see 199).

B. THE COOPERATIVE NUMBER N AS A HILL COEFFICIENT. Application of eqn 1 to cooperativity in accordance with the framework of A. V. Hill's study on hemoglobin (233) produces eqn 1':

$$y_{RELEASE} = M/M_{MAXIMUM} = ([Ca]^N K_{CA'})/(1 + [Ca]^N K_{CA'}) \qquad \text{eqn 1'}$$

Rearranging, and for simplicity changing $K_{CA'}$ into $1/K_{d'}$, then

$$[Ca]^N\{(M_{MAXIMUM} - M)/M\} = K_{d'} \qquad \text{eqn 1''}$$

Taking logs of both sides of eqn 1'' and defining $M/(M_{MAXIMUM} - M)$ as logit M, then

$$\text{logit } M = N \log_{10}[Ca] - \log_{10}K_{d'} \qquad \text{eqn 1'''}$$

This is known as the Hill equation; a plot of log [Ca] against logit M (the Hill plot) produces a slope of N, which is the Hill coefficient. A value of $N > 1$ in the Hill equation is the operational definition of positive cooperativity and $N < 1$ defines negative cooperativity. Regardless of the mechanism of cooperativity (see section VI), it can be measured empirically as the Hill coefficient. For additional details, see 51, 52, 233. The $K_{d'}$ is "primed" because it is only an apparent dissociation constant that encompasses various interaction factors (see next section).

9. Equations for the Adair (1)-Pauling (204) Simple Sequential Model of Activation of Synchronous Release by Intracellular Me (Me_{EFF}). Initially, the reaction scheme appears similar to that described in A 7 except for the presence of four liganded sites here. The equations presented below, however, are intended to describe the relationship between intracellular Me (Me_{EFF}; see section III A 3) and ACh release. The intracellular Me binding protein will be characterized by the noncommital term Pr, and for convenience, the equations will be derived using Ca as the agonist, where $[Ca_{EFF}]$ represents the intracellular Ca concentration in the vicinity of synchronous release sites at the active zone. This model is outlined below.

Note the four different *effective* equilibrium affinity constants for Ca, K_1 to K_4, representing the sequential binding of four Ca to Pr and the rate constant (k's) for each of the states. The equations for the relationship between the effective affinity constants (K_1 to K_4) and the intrinsic equilibrium affinity constant $K_{CA\text{-}IN}$ will be presented for noncooperative binding first. The resulting expression (eqn 44) will then be altered by a series of interaction factors to explain cooperativity (eqn 44a). The binding phenomenon is described by eqn 41, which is the equivalent of equation 21 for four sites: y_{CA} = sum of the bound states/Pr_T, where Pr_T = total concentration of Ca binding protein Pr. Thus,

$$y_{CA} = \frac{[Ca_{EFF}]K_1 + [Ca_{EFF}]^2K_1K_2 + [Ca_{EFF}]^3K_1K_2K_3 + [Ca_{EFF}]^4K_1K_2K_3K_4}{1 + [Ca_{EFF}]K_1 + [Ca_{EFF}]^2K_1K_2 + [Ca_{EFF}]^3K_1K_2K_3 + [Ca_{EFF}]^4K_1K_2K_3K_4} \qquad \text{eqn 41}$$

and release at any particular $[Ca_{EFF}]$ as a fraction of maximum release, $y_{RELEASE}$ = ACh release at $[Ca_{EFF}]$/maximum ACh release, where maximal ACh release = $k_N Pr_T$. Thus

$$y_{RELEASE} = \frac{k_1[Ca_{EFF}]K_1 + k_2[Ca_{EFF}]^2K_1K_2 + k_3[Ca_{EFF}]^3K_1K_2K_3 + k_4[Ca_{EFF}]^4K_1K_2K_3K_4}{k_N(1 + [Ca_{EFF}]K_1 + [Ca_{EFF}]^2K_1K_2 + [Ca_{EFF}]^3K_1K_2K_3 + [Ca_{EFF}]^4K_1K_2K_3K_4)} \qquad \text{eqn 42}$$

(cf eqn 22).

Now the effective affinity constants (K_1 to K_4) describe the relation between free Ca_{EFF}, available protein Pr, and Ca_{EFF} bound to Pr. The intrinsic or microscopic Ca affinity constant ($K_{CA\text{-}IN}$), however, describes the relationship between free Ca_{EFF}, free Pr sites and the Ca_{EFF} + site complex. For example, if there were four identical sites on Pr, as has been suggested for calmodulin and related proteins (136), the concentration of free sites would be four times the concentration of Pr and $K_1 = 4K_{CA\text{-}IN}$. Thus, in eqn 42, the first term in the numerator would become $k_1 4[Ca_{EFF}]K_{CA\text{-}IN}$ and the second term in brackets in the denominator would equal $4[Ca_{EFF}]K_{CA\text{-}IN}$. This relationship between the intrinsic and effective binding constants reflects the number of ways of combining Ca with the four vacant sites on Pr (4) divided by the number of ways of dissociating Ca (1) from singly occupied Pr sites $\frac{4}{1} = 4$. For the next step in the reaction sequence (singly occupied to doubly occupied protein), as the number of ways of making $Ca_{EFF_2}Pr$ from $Ca_{EFF}Pr$ divided by the number of ways of dissociating the doubly occupied complex is $\frac{3}{2}$, then the effective affinity constant for this step $K_2 = \frac{3}{2}K_{CA\text{-}IN}$. Now, as $K_1K_2 = 6K_{CA\text{-}IN}^2$, then the second term in the numerator is $k_2 6\{[Ca_{EFF}]K_{CA\text{-}IN}\}^2$ and the second term in brackets in the denominator = $k_2 6\{[Ca_{EFF}]K_{CA\text{-}IN}\}^2$. Continuing in this manner, as $K_3 = \frac{2}{3}K_{CA\text{-}IN}$ and $K_4 = K_{CA\text{-}IN}/4$, for all four sites

$$y_{RELEASE} = \frac{k_1 4[Ca_{EFF}]K_{CA\text{-}IN} + k_2 6\{[Ca_{EFF}]K_{CA\text{-}IN}\}^2 + k_3 4\{[Ca_{EFF}]K_{CA\text{-}IN}\}^3 + k_4\{[Ca_{EFF}]K_{CA\text{-}IN}\}^4}{k_N(1 + 4[Ca_{EFF}]K_{CA\text{-}IN} + 6\{[Ca_{EFF}]K_{CA\text{-}IN}\}^2 + 4\{[Ca_{EFF}]K_{CA\text{-}IN}\}^3 + \{[Ca_{EFF}]K_{CA\text{-}IN}\}^4)} \qquad \text{eqn 43}$$

If k_1 is termed k_{ACH}, then on the assumption that the sites are independent, ACh release produced by $Ca_{EFF_2}Pr$ = twice that of $Ca_{EFF}Pr$ = $2k_{ACH}$, by $Ca_{EFF_3}Pr = 3k_{ACH}$, and by $Ca_{EFF_4}Pr = 4k_{ACH}$, then as $k_N = 4k_{ACH}$, substituting these values into eqn 43 produces

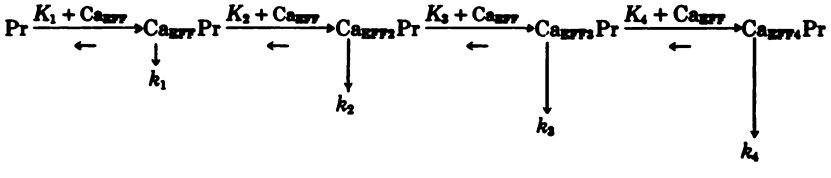

$$y_{RELEASE} = \frac{[Ca_{EFF}]K_{CA\text{-}IN} + 3\{[Ca_{EFF}]K_{CA\text{-}IN}\}^2 + 3\{[Ca_{EFF}]K_{CA\text{-}IN}\}^3 + \{[Ca_{EFF}]K_{CA\text{-}IN}\}^4}{1 + 4[Ca_{EFF}]K_{CA\text{-}IN} + 6\{[Ca_{EFF}]K_{CA\text{-}IN}\}^2 + 4\{[Ca_{EFF}]K_{CA\text{-}IN}\}^3 + \{[Ca_{EFF}]K_{CA\text{-}IN}\}^4} \quad \text{eqn 44}$$

Eqn 44 is the equation of ACh release with four *independent* sites on Pr using the microscopic affinity constant $K_{CA\text{-}IN}$ for the individual sites. The final equation requires the introduction of interaction factors to describe the effect of a particular bound Me species in altering the equilibrium affinity constant for the subsequent binding of Me to the remaining free sites.

Again, considering the relationship between effective and intrinsic binding constants, the binding of Ca when all four sites are unoccupied, is, as before, $K_1 = 4K_{CA\text{-}IN}$. In the second binding, however, $K_2 = i¾K_{CA\text{-}IN}$ where i is the first *interaction factor*, i.e. the factor by which the affinity of Ca for the remaining sites is changed when one site is occupied. If i is >1, then positive cooperativity occurs after the first binding site is occupied, while $i < 1$ indicates negative cooperativity. Now, for the transition from doubly occupied to triply occupied sites $K_3 = ij¼K_{CA\text{-}IN}$, where j is the new interaction factor introduced for this binding. For the last binding step, $K_4 = ijkK_{CA\text{-}IN}/4$, where k is the interaction factor for the last reaction in the binding to sites on Pr. Note that the interactions are cumulative, i.e. the interaction factor after the first binding is preserved and included in the next step, etc. Substituting these new values for K_2 to K_4 into eqn 43 (K_1 remains unchanged) and with k_{ACH} as defined above, then

$$y_{RELEASE} = \frac{[Ca_{EFF}]K_{CA\text{-}IN} + 3i\{[Ca_{EFF}]K_{CA\text{-}IN}\}^2 + 3i^2j\{[Ca_{EFF}]K_{CA\text{-}IN}\}^3 + i^3j^2k\{[Ca_{EFF}]K_{CA\text{-}IN}\}^4}{1 + 4[Ca_{EFF}]K_{CA\text{-}IN} + 6i\{[Ca_{EFF}]K_{CA\text{-}IN}\}^2 + 4i^2j\{[Ca_{EFF}]K_{CA\text{-}IN}\}^3 + i^3j^2k\{[Ca_{EFF}]K_{CA\text{-}IN}\}^4} \quad \text{eqn 44a}$$

Eqn 44a is thus a more generalized version of eqn 44 which allows for both positive and negative cooperative interactions in Me binding. If $i = j = k = 1$, then eqn 44a reduced to eqn 44. At the other extreme, if i, j, and k are very large, then all terms other than four bound Ca may be ignored, eqn 44a becomes eqn 44b,

$$y_{RELEASE} = [Ca_{EFF}]^4K_{CA'}/(1 + [Ca_{EFF}]^4K_{CA'}) \quad \text{eqn 44b}$$

where $K_{CA'} = i^3j^2kK_{CA\text{-}IN}^4$. This may be recognized as the Hill equation (eqn 1′, section A 8 B).

To describe ACh release at the motor end-plate (figure 8B) it is necessary to use values of $K_{CA\text{-}IN} = 0.3$, $i = 2.2$, $j = 0.035$, and $k = 20{,}000$ in eqn 44a. Specific units for $K_{CA\text{-}IN}$ are relative to the non-normalized units of $[Me_{EFF}]$. For example if $[Me_{EFF}]$ is in μM, then $K_{CA\text{-}IN}$ is in μM^{-1}.

These values suggest, that at cholinergic nerves in frog cutaneous pectoris muscle (which may differ from other nerve endings; ref. 104), the initial $K_{CA\text{-}IN}$ is increased after the first Ca binding and again when the last Ca is bound. For the transition from doubly to triply occupied Pr, however, negative cooperativity is observed; the $j < 1$ term is used to describe this negative cooperativity. Additional details and other alternatives will be provided in a future publication.

B. The Effects of Other Cations on ACh Release

Metal ions other than those discussed in the text exert significant stimulatory and inhibitory effects on cholinergic nerve endings. The most prominent effects of these additional cations are considered below.

1. Monovalent Cations. A. SODIUM. Sodium ions influence a number of different stages in the depolarization-release sequence. The first effect of Na is on the depolarization itself; decreases in extracellular [Na] and/or increases in intracellular [Na] reduce the Na currents associated with the action potential. Secondly, Na competes with Ca in a fashion similar to Mg for the sites that control Ca entry (129, 130). Thirdly, intracellular Na, delivered in liposomes (213) or by ionophore (174) is an extremely effective means of displacing Ca from storage sites and increasing ACh release (27, 86, 29, 213, 174). Finally, the high affinity uptake system for choline is dependent on Na for its activity (27, 86). As choline recapture is important for replacing the immediately available store of ACh, Na is important for ACh synthesis (33, 26). Indeed, nerve stimulation accelerates choline uptake and this helps to keep ACh stores constant during high levels of release. It has been speculated that intracellular Na that accumulates during high frequency nerve stimulation provokes the increased choline uptake (26, 86).

B. POTASSIUM. Potassium is used frequently by biochemists on the assumption that an increase in extracellular K concentration depolarizes the nerve terminal in a manner equivalent to electrical stimulation; this assumption is not strictly true, however. When a steady depolarization is provided by focal electrical stimulation of nerve endings, increases in [Ca] towards 10 mM continue to increase MEPPf (55). When nerve terminals are depolarized in 11 mM K, however, increasing the [Ca] from very low levels to 1 mM increases MEPPf but higher [Ca] produce a progressive decline in MEPPf (56, 169, 151, 177, 263). Furthermore, focal depolarization of the nerve ending, while increasing MEPPf, decreases M (117a); a matching increment in MEPPf frequency produced by raised K is associated with an increase in M (202).

The cause of this anomalous behavior of K is unknown. It has been argued that K decreases the Ca conductance of the nerve terminal (56) but the predominant view is that the decline in MEPPf as [Ca] is increased is produced by an effect of Ca on membrane surface charges (169, 151, 177, 263). The effect could occur if Ca screened fixed negative surface charges near Ca channels, hyperpolarizing the membrane locally and thereby closing voltage-sensitive Ca channels, but the inhibitory effect of Ca was not observed with focal electrical depolarization; it is thus more likely to reflect a specific interaction between K and Ca. It has been suggested that Ca screens fixed negative charges near K channels, reducing the surface potential and, by eqn 4, the K concentration near the K channels (151). As depolarization of the nerve would be expected to behave in a roughly Nernstian fashion with respect to the local extracellular [K] at the membrane, elevated Ca would be predicted to reduce the level of depolarization produced by a given K concentration. Evidence in support of cation screening near K channels has been obtained with various monovalent and divalent cations (151, 177, 263), e.g., Sr and Ca are equipotent in both their agonist and inhibitory effects on MEPPf in 11 mM K (177) [although selectivity may occur at higher levels of K depolarization (83)]. The inhibitory effects of some cations (e.g. Co) on K-evoked MEPPs, however, occur at concentrations far too low for substantial screening to occur (Mellow and Silinsky, unpublished). Thus, while surface charge effects still remain a viable explanation for the interaction of K with other cations, it is likely that binding participates in the process by which cations reduce the local [K].

The effect of K to increase M remains unexplained although it has been speculated that K increases the availability of ACh quanta for release (202).

C. HYDROGEN. Protons have been shown to be competitive inhibitors of extracellular Ca and thus antagonize M (141). Either a Michaelis-Menten kinetic approach or the binding of H to surface charges can quantitatively account for the experimental results with H as an inhibitor of ACh release. The pK_a ($-\log K_d$ for protons) varies depending upon the model, however, such that by the kinetic method the membrane group responsible for controlling Me entry is a weak acid ($pK_a = 5.7$; possibly an imidazole residue) while in the surface charge approach, the pK_a (3.6) suggests a carboxylic persuasion of the moiety. Protons have also been shown to produce increases in MEPPf (116, 141).

D. LITHIUM. The initial effect upon substituting Li for Na is a decrease in evoked ACh release (196, 130); this is presumably due to a reduction in the amplitude of the nerve terminal action potential. Li subsequently causes a slowly developing increase in the MEPPf, an effect similar to K-free solutions or ouabain (10). It was suggested that MEPPf under these circumstances is increased by changes in intracellular monovalent cation concentrations, secondarily to blockade of the Na-K ATPase (10). A variety of other time-dependent effects of Li

have also been described (59); most notably, Li may be a selective agonist for post-tetanic potentiation (59). It would be of interest to determine if any of these effects of Li are related to the accumulation of inositol 1-phosphate that is frequently observed after Li treatment (78a).

E. CESIUM. Cesium has been shown to produce an increase in M without altering MEPPf (96). This effect is likely to be produced by Cs entering the nerve terminal in exchange for K and increasing the duration of the prejunctional action potential (96); a well known action of intracellular Cs is to block K channels and thus delay the repolarization of the membrane potential.

2. *Divalent Cations.* A. BARIUM. Although barium was discussed in various sections of the main text, its effects are so complex that further discussion is required here. As a forewarning to readers contemplating studies with this ion, Ba is an extremely unpleasant Me species for the experimentalist (see ref. 237, pp. 159–160). The first effect that is often observed after substitution of Ba for Ca is a short-lived increase in MEPPf (144); this is presumed to be due to the transient displacement of membrane Ca by Ba. Next, an enormous fall in muscle membrane potential occurs due to inhibition by Ba of the K conductance of the muscle membrane (237). On occasion, this membrane effect may be reflected presynaptically as a change in the nerve terminal action potential (ntp), but alterations in ntps are *not* responsible for the failure of Ba to support M (see figure 1 in ref. 235). Finally some of the effects of Ba are irreversible, e.g., an irreversible avalanche of quantal secretion similar to the effect of the trivalent La (see section 3 in this appendix) may be observed on occasion in Ba solutions. Given these caveats, sections i and ii below describe certain additional effects of Ba on the synchronous release process.

i, Enhancement by an antagonist. Ba cannot support M (see also ii below) but in the presence of relatively impermeant divalent cation antagonists (e.g. Mg, Co) Ba may actually enhance M in response to a single stimulus under conditons when augmentation has not had the opportunity to develop. The results were found to be in quantitative agreement with a non-equilibrium model (99, 238) in which Ba entry through Ca channels makes Ba a rapidly dissociating competitive antagonist as compared to Mg or Co (99, 238). By this model, Ca cannot compete as effectively with Mg as it can with Ba because Ba dissociates rapidly from the external binding site by entering the Ca channel; this leaves the entry site free for reoccupation by Ca during the period of nerve terminal depolarization. Ba, added to a solution of high Mg, would thus occupy some of the sites previously held by Mg; Ca could then compete more favorably with Ba than with Mg for the sites that Ba had wrested from Mg. This model would explain why M is increased in Ca + Mg + Ba solutions over M in Ca + Mg alone (238). The possibility that some of these interactions occur at an intracellular site has also been raised (see ref. 238 for further details).

ii. Does $e_{BA} = 0$ for synchronous ACh release? In this review and in the papers from my laboratory, great care was taken to define M as the synchronous impulsive release of ACh in response to *individual nerve impulses*, i.e. M is a multiquantal EPP that does not require repetitive nerve stimulation to develop (e.g., ref. 178). Indeed, three independent groups have shown that Ba does not support EPPs (235, 170, 275; see also 237). On occasion, however, it is possible to observe a very small computer-averaged response in Ba that appears to be phase-locked to the nerve impulse during repetitive stimulation. It might be argued that, under these conditions, e_{BA} is greater than zero. This effect, rather than being produced by a direct effect of Ba on M, *could be due to the liberation of Ca from storage sites by Ba.* (The effect of Ba on MEPPf could also be due to a displacement of Ca from storage sites, although arguments to the contrary have been published; see refs. 134, 237.) For the purposes of illustration, however, suppose that in 4 mM Ba, the direct action of Ba on release is to produce one MEPP, phased-locked to the nerve impulse every 10 stimuli, i.e. M in Ba = 0.1. To produce equal M in Ca solution would require only very small [Ca], say e.g. 0.01 mM. Now using the values determined experimentally for K_{CA} (0.025 mM^{-1}), K_{BA} (1.1 mM^{-1}) and e_{CA} (10), then it should be possible to calculate a value for e_{BA} assuming equal stimuli (S) produce equal M (252). Specifically, if M in Ca = M in Ba and $S_{CA} = S_{BA}$, then $e_{CA}y_{CA} = e_{BA}y_{BA}$. Substituting $10 * 0.01 * 0.025/(1 + 0.01 * 0.025) = e_{BA} * 4 * 1.1/(1 + 4 * 1.1)$, then $e_{BA} = 0.003$. This value is 2 orders of magnitude less than e_{SR} (240). It thus appears that even if one chooses to ignore the possibility of an indirect effect of Ba during repetitive nerve stimulation, the e_{BA} is so low that "aw [w]ell call it zero" (A. J. Austin, personal communication).

A final effect of Ba: On occasion one stimulus in Ba + Ca solutions produces a train of EPPs much like repetitive nerve stimulation. Although this could be due to repetitive firing of nerve terminal action potentials, it could also occur if Ba inhibited the inactivation of an intracellular release site (e.g. bp) after it is activated by Ca and nerve stimulation.

B. MN AND OTHER DIVALENT CATION ANTAGONISTS. Mn behaves as a competitive inhibitor of M (176), much as has been described in the text for Co and with about the same affinity (267). At higher concentrations (>1 mM), Mn and Co increase MEPPf. A variety of other cations produce similar effects; these include Be (31), Ni (23), Zn (23), Pb (163), and Cd (228, 57). Ni and Zn have been also shown to increase the duration of ntps (23). Other likely antagonists of M are cupric and cerium ions, as these divalent cations cannot substitute for Ca in producing ACh release (181).

C. MERCURY. The effects of mercuric ions are complex and generally discussed in conjunction with the known effects of mercury on sulfhydril groups. At the motor nerve ending, it has been suggested that regulation of SH groups, possibly through intracellular glutathione, may be important for ACh secretion and that the formation of Ca-dithiolate salts is an important step in ACh release (40). Indeed, Hg forms dithiolate salts and Hg (1 μM) increases ACh release shortly after application (164). Miyamoto (188) has shown that Hg increases ACh release initially, but during continued exposure this ion causes an irreversible depolarization of the nerve terminal and subsequent irreversible block of ACh release. Hg produces all of these effects intracellularly by entering the nerve terminal through Na channels or Ca channels. It has been speculated that Hg toxicity may be due to the extremely tight association between Hg and SH groups inside the nerve ending (188).

3. *Trivalent Ions.* A. LANTHANUM AND OTHERS. Because it possesses certain physical properties in common with Ca (e.g. similar ionic radius lanthanum has been used as a common tool for studying Ca-dependent processes (269). When 0.1 mM to 1 mM La solutions are applied to the neuromuscular junction, an immeasurable, irreversible increase in MEPPf rapidly ensues until, after many hours, all of the vesicles at the active zone are depleted (108). At lower concentrations, two different effects of La may be discerned. At the external surface of the nerve ending, concentrations of La as low as 1 μM block Ca or Sr dependent M in an irreversible fashion, as described in section III (65, 240); this effect is presumably due to a blockade of Me entry by La (182). At an intracellular site, La causes an increase in the frequency of MEPPfs. The mechanism of this intracellular effect of La in increasing MEPPf is unknown. It has been speculated that La and related lanthanides (e.g. praseodymium) displace Ca from storage organelles (3) or exert a direct action at the active zone (108, 269, 133). These different La effects have been dissociated by using La-containing liposomes; at some time after these liposomes had produced substantial increases in MEPPf, addition of La to the extracellular fluid produced the characteristic decrease in M (133). The irreversibility of La-mediated effects is reminiscent of some of the noxious effects of Ba; perhaps toxicity is due to the high coordination number of both species (see Gillard, ref. 94).

Other trivalents with similar effects include yttrium (35) and praseodymium (3).

4. *Tetravalent Ions.* A. THALLIUM. Thallium has been reported to increase MEPPf, but solubility problems have prevented a comprehensive study of the effects of this ion (31).

REFERENCES

1. ADAIR, G. S.: The hemoglobin system. VI. The oxygen dissociation curve of hemoglobin. J. Biol. Chem. **63**: 529–545, 1925.

2. ADAMSON, A. W.: Physical Chemistry of Surfaces, pp. 697, Wiley, New York, 1976.
3. ALNAES, E., AND RAHAMIMOFF, R.: Dual action of praseodymium (Pr^{3+}) on transmitter release at the frog neuromuscular synapse. Nature (Lond.) **247:** 478–479, 1974.
4. ANDREU, R., AND BARRETT, E. F.: Calcium dependence of evoked transmitter release at very low quantal contents at the frog neuromuscular junction. J. Physiol. (Lond.) **308:** 79–97, 1980.
5. ARIENS, E. J., AND DEGROOT, W. M.: Affinity and intrinsic activity in the theory of competitive inhibition. III. Homologous decamethonium-derivatives and succinyl-choline esters. Arch. Int. Pharmacodyn. Ther. **99:** 193–295, 1954.
6. ARUNLAKSHANA, O., AND SCHILD, H. O.: Some quantitative use of drug antagonists. Br. J. Pharmacol. **14:** 48–58, 1959.
7. ASIMOV, I.: Asimov's Biographical Encyclopedia of Science and Technology, Doubleday and Co. Inc., Garden City, NY, 1964.
8. AUGUSTINE, G. J., AND ECKERT, R.: Divalent cations differentially support transmitter release at the squid giant synapse. J. Physiol. (Lond.) **346:** 257–271, 1984.
9. BAKER, P. F., AND CRAWFORD, A. C.: Mobility and transport of magnesium in squid giant axons. J. Physiol. (Lond.) **227:** 855–874, 1972.
10. BAKER, P. F., AND CRAWFORD, A. C.: A note on the mechanism by which inhibitors of the sodium pump accelerate spontaneous release of transmitter from motor nerve terminals. J. Physiol. (Lond.) **247:** 209–226, 1975.
11. BALDO, G. J., COHEN, I. S., AND VAN DER KLOOT, W.: Facilitation and the conduction of the nerve action potential at the frog neuromuscular junction. Pflüger Arch. Eur. J. Physiol. **399:** 161–165, 1983.
12. BALNAVE, R. J., AND GAGE, P. W.: On facilitation of transmitter release at the toad neuromuscular junction. J. Physiol. (Lond.) **239:** 657–675, 1974.
13. BALNAVE, R. J., AND GAGE, P. W.: Facilitation of transmitter secretion from toad motor nerve terminals during brief trains of action potentials. J. Physiol. (Lond.) **266:** 435–451, 1977.
14. BARRETT, E. F., BARRETT, J. N., BOTZ, D., CHANG, D. B., AND MAHAFFEY, D.: Temperature sensitive aspects of evoked and spontaneous transmitter release at the frog neuromuscular junction. J. Physiol. (Lond.) **279:** 253–273, 1978.
15. BARRETT, E. F., AND MAGLEBY, K. L.: Physiology of cholinergic transmission. *In* Biology of Cholinergic Function, ed. by A. M. GOLDBERG AND I. HANIN, pp. 29–100, Raven Press, New York, 1976.
16. BARRETT, E. F., AND STEVENS, C. F.: Quantal independence and uniformity of presynaptic release kinetics at the frog neuromuscular junction. J. Physiol. (Lond.) **227:** 665–689, 1972.
17. BARRETT, E. F., AND STEVENS, C. F.: The kinetics of transmitter release at the frog neuromuscular junction. J. Physiol. (Lond.) **227:** 691–708, 1972.
18. BARTON, S. B., COHEN, I. S.: Are transmitter release statistics meaningful? Nature (Lond.) **268:** 267–268, 1977.
19. BARTON, S. B., COHEN, I., AND VAN DER KLOOT, W.: The calcium dependence of spontaneous and evoked quantal release at the frog neuromuscular junction. J. Physiol. (Lond.) **337:** 735–751, 1983.
20. BASS, L., AND MOORE, W. J.: Electrokinetic mechanism of miniature postsynaptic potentials. Proc. Natl. Acad. Sci. **55:** 1214–1217, 1966.
21. BENNETT, M. R., FISHER, C., FLORIN, T., QUINE, M., AND ROBINSON, J.: The effect of calcium ions and temperature on the binomial parameters that control acetylcholine release by a nerve impulse at amphibian neuromuscular synapses. J. Physiol. (Lond.) **271:** 641–672, 1977.
22. BENNETT, M. R., AND LAVIDIS, N. A.: The effect of calcium ions on the secretion of quanta evoked by an impulse at nerve terminal release sites. J. Gen. Physiol. **74:** 426–456, 1979.
23. BENOIT, P. R., AND MAMBRINI, J.: Modification of transmitter release by ions which prolong the presynaptic action potential. J. Physiol. (Lond.) **210:** 681–695, 1970.
24. BEVAN, S.: Sub-miniature end-plate potentials at untreated frog neuromuscular junctions. J. Physiol. (Lond.) **258:** 145–155, 1976.
25. BETZ, W. J.: Depression of transmitter release at the neuromuscular junction of the frog. J. Physiol. (Lond.) **206:** 629–644, 1970.
26. BIRKS, R. I.: Activation of feline acetylcholine synthesis in the absence of release: dependence on sodium, calcium and the sodium pump. J. Physiol. (Lond.) **344:** 347–357, 1983.
27. BIRKS, R. I., AND COHEN, M. W.: The influence of internal sodium on the behavior of motor nerve endings. Proc. R. Soc. Lond. B Biol. Sci. **170:** 401–421, 1968.
28. BLACKMAN, J. G., GINSBORG, B. L., AND RAY, C.: On the quantal release of the transmitter at a sympathetic synapse. J. Physiol. (Lond.) **167:** 402–415, 1963.
29. BLAUSTEIN, M. P.: The interrelationship between sodium and calcium fluxes across cell membranes. Rev. Physiol. Biochem. Pharmacol. **70:** 33–82, 1974.
30. BLAUSTEIN, M. P., RATZLAFF, R. W., AND KENDRICK, N. K.: The regulation of intracellular calcium in presynaptic nerve terminals. Ann N.Y. Acad. Sci. **307:** 195–212, 1978.
31. BLIOCH, Z. L., GLAGOLEVA, I. M., LIBERMAN, E. A., AND NENASHEV, V. A.: A study of the mechanism of quantal transmitter release at a chemical synapse. J. Physiol. (Lond.) **199:** 11–35, 1968.
32. BLUMENTHAL, R., AND SHAMOO, A. E.: Incorporation of transport molecules into black lipid membranes. *In* The Receptors, A Comprehensive Treatise, ed. by R. D. O'Brien, vol. 1, pp. 215–245, Plenum Press, New York, 1979.
33. BLUSZTAJN, J. K., AND WURTMAN, R. J.: Choline and cholinergic neurons. Science **221:** 614–620, 1983.
34. BOCKRIS, J. O'M., AND REDDY, A. K. N.: Modern Electrochemistry, 1432 pp., Plenum Press, New York, 1977.
35. BOWEN, J. M.: Effects of rare earths and yttrium on striated muscle and the neuromuscular junction. Can. J. Physiol. Pharmacol. **50:** 603–611, 1972.
36. BRANISTEANU, D. D., MIYAMOTO, M. D., AND VOLLE, R. L.: Effects of physiologic alterations on binomial transmitter release at magnesium-depressed neuromuscular junctions. J. Physiol. (Lond.) **254:** 19–37, 1976.
37. BRIGANT, J. L., AND MALLART, A.: Presynaptic currents in mouse motor nerve endings. J. Physiol. (Lond.) **333:** 619–636, 1982.
38. BROWN, A. N., AKAIKE, N., AND LEE, K. S.: The calcium conductance of neurons. Ann. N.Y. Acad. Sci. **75:** 330–344, 1978.
39. BROWN, T. H., PERKEL, D. H., AND FELDMAN, M. W.: Evoked neurotransmitter release: Statistical effects of nonuniformity and nonstationatity. Proc. Natl. Acad. Sci. **73:** 2913–2917, 1976.
40. CARLEN, P. L., KOSOWER, E. M., AND WERMAN, R.: The thiol-oxidizing agent diamide increases transmitter release by decreasing calcium requirements for neuromuscular transmission in the frog. Brain Res. **117:** 257–276, 1976.
41. CECCARELLI, B., AND HURLBUT, W. P.: Vesicle hypothesis of the release of quanta of acetylcholine. Physiol. Rev. **69:** 396–441, 1980.
42. CHANDLER, W. K., HODGKIN, A. L., AND MEVES, H.: The effect of changing the internal solution on sodium inactivation and related phenomena in giant axons. J. Physiol. (Lond.) **180:** 821–836, 1965.
43. CHAPMAN, D. L.: A contribution to the theory of electrocapillarity. Phil. Mag. **25:** 475–481, 1913.
44. CHARLTON, M. P., SMITH, S. J., AND ZUCKER, R. S.: Role of presynaptic Ca ions and channels in synaptic facilitation and depression at the squid giant synapse. J. Physiol. (Lond.) **323:** 173–193, 1982.
45. CHRISTENSEN, B. N., AND MARTIN, A. R.: Estimates of probability of transmitter release at the mammalian neuromuscular junction. J. Physiol. (Lond.) **210:** 933–945, 1970.
46. COHEN, F. S., AKABAS, M. H., AND FINKELSTEIN, A.: Osmotic swelling of phospholipid vesicles causes them to fuse with a planar phospholipid bilayer membrane. Science **217:** 458–460, 1982.
47. COHEN, F. S., ZIMMERBERG, J., AND FINKELSTEIN, A.: Fusion of phospholipid vesicles with planar phospholipid bilayer membranes. II. Incorporation of a vesicular membrane marker into the planar membrane. J. Gen. Physiol. **75:** 251–270, 1980.
48. COHEN, I., KITA, H., AND VAN DER KLOOT, W.: The intervals between miniature end-plate potentials in the frog are unlikely to be independently or exponentially distributed. J. Physiol. (Lond.) **236:** 327–339, 1974a.
49. COHEN, I., KITA, H., AND VAN DER KLOOT, W.: The stochastic properties of spontaneous quantal release of transmitter at the frog neuromuscular junction. J. Physiol. (Lond.) **236:** 341–361, 1974b.
50. COLQUHOUN, D.: Lectures in Biostatistics, 425 pp., Clarendon Press, Oxford, 1971.
51. COLQUHOUN, D.: The relation between classical and cooperative models for drug action. *In* Drug Receptors, ed. by H. P. RANG, pp. 149–182, Macmillan, New York, 1973.
52. COLQUHOUN, D.: The link between drug binding and response: Theories and observations. *In* The Receptors, A Comprehensive Treatise, ed. by R. D. O'BRIEN, vol. 1, pp. 93–142, Plenum Press, New York, 1979.
53. COOKE, J. D., OKAMATO, K., AND QUASTEL, D. M. J.: The role of calcium in depolarization-secretion coupling at the motor nerve terminal. J. Physiol. (Lond.) **228:** 459–497, 1973.
54. COOKE, J. D., AND QUASTEL, D. M. J.: Transmitter release by mammalian motor nerve terminals in response to focal polarization. J. Physiol. (Lond.) **228:** 377–405, 1973.
55. COOKE, J. D., AND QUASTEL, D. M. J.: Cumulative and persistent effects of nerve terminal depolarization on transmitter release. J. Physiol. (Lond.) **228:** 407–434, 1973.
56. COOKE, J. D., AND QUASTEL, D. M. J.: The specific effect of potassium on transmitter release by motor nerve terminals and its inhibition by calcium. J. Physiol. (Lond.) **228:** 435–458, 1973.
57. COOPER, G. P., AND MANALIS, R. S.: Cadmium: effects on transmitter release at the frog neuromuscular junction. Eur. J. Pharmacol. **99:** 251–256, 1984.
58. CRAWFORD, A. C.: The dependence of evoked transmitter release on external calcium ions at very low mean quantal contents. J. Physiol. (Lond.) **240:** 255–278, 1974.
59. CRAWFORD, A. C.: Lithium ions and the release of transmitter at the frog neuromuscular junction. J. Physiol. (Lond.) **246:** 109–142, 1975.
60. CROSLAND, R. D., MARTIN, J. W., AND MCCLURE, W. O.: Effect of liposomes containing various divalent cations on the release of acetylcholine from synaptosomes. J. Neurochem. **40:** 681–687, 1983.
61. DALE, H. H., FELDBERG, W., AND VOGT, M.: Release of acetylcholine at voluntary motor nerve endings. J. Physiol. (Lond.) **86:** 353–380, 1936.

61a. DALGARNO, D., KLEVIT, R. E., LEVINE, B. A., AND WILLIAMS, R. J. P.: The calcium receptor and trigger. Trends Pharmacol. Sci. **5:** 266–271, 1984.

62. D'ARRIGO, J. S.: Screening of membrane surface charges by divalent cations: An atomic representation. Am. J. Physiol. **235:** C109–C117, 1978.

63. DASCAL, N., LANDAU, E. M., AND LASS, Y.: Divalent cations and transmitter release at low concentrations of tetrodotoxin. Biophys. J. **35:** 573–586, 1981.
64. DATYNER, N. B., AND GAGE, P. W.: Phasic secretion of acetylcholine at a mammalian neuromuscular junction. J. Physiol. (Lond.) **303:** 299–314, 1980.
65. DE BASSIO, W. A., SCHNITZLER, R. M., AND PARSONS, R. L.: Influence of lanthanum on transmitter release at the neuromuscular junction. J. Neurobiol. **2:** 263–278, 1971.
66. DEL CASTILLO, J., AND KATZ, B.: The effect of magnesium on the activity of motor nerve endings. J. Physiol. (Lond.) **124:** 553–559, 1954.
67. DEL CASTILLO, J., AND KATZ, B.: Quantal components of the end-plate potential. J. Physiol. (Lond.) **124:** 560–573, 1954.
68. DEL CASTILLO, J., AND KATZ, B.: Changes in end-plate activity produced by presynaptic polarization. J. Physiol. (Lond.) **124:** 586–604, 1954.
69. DEL CASTILLO, J., AND KATZ, B.: La base "quantale" de la transmission neuro-musculaire. In Microphysiologie comparée des éléments excitables. Coll. Int. C.N.R.S. Paris, **67:** 245–258, 1957.
70. DE LORENZO, R. J.: Calmodulin in neurotransmitter release and synaptic function. Fed. Proc. **41:** 2265–2282, 1982.
71. DIAMOND, J. M., AND WRIGHT, E. M.: Biological membranes: The physical basis of ion and non-electrolyte selectivity. Annu. Rev. Physiol. **31:** 581–646, 1969.
72. DIEBLER, H., EIGEN, M., ILGENFRITZ, G., MAAB, G., AND WINKLER, W.: Kinetics and mechanism of reactions of main group metal ions with biological carriers. Pure Applied Chem. **20:** 94–115, 1969.
73. DODGE, F. A. JR., MILEDI, R., AND RAHAMIMOFF, R.: Strontium and quantal release of transmitter at the neuromuscular junction. J. Physiol. (Lond.) **100:** 267–283, 1969.
74. DODGE, F. A. JR., AND RAHAMIMOFF, R.: Co-operative action of Ca ions in transmitter release at the neuromuscular junction. J. Physiol. (Lond.) **138:** 434–444, 1967.
75. DOUGLAS, W. W.: Involvement of calcium in exocytosis and the exocytosis-vesiculation sequence. Biochem. Soc. Symp. **39:** 1–28, 1974.
76. DOUGLAS, W. W., LYWOOD, D. W., AND STRAUB, R. W.: The stimulant effect of barium on the release of acetylcholine from superior cervical ganglion. J. Physiol. (Lond.) **156:** 515–522, 1961.
77. DOUGLAS, W. W., AND POISNER, A. M.: Stimulus-secretion coupling in a neurosecretory organ: the role of calcium in the release of vasopressin from the neurohypophysis. J. Physiol. (Lond.) **172:** 1–18, 1964.
78. DOUGLAS, W. W., AND POISNER, A. M.: Calcium movements in the neurohypophysis of the rat and its relation to the release of vasopressin. J. Physiol. (Lond.) **172:** 19–39, 1964.
78a. DOWNES, C. P.: Inositol phospholipids and neurotransmitter-receptor signalling mechanisms. Trends Neurosci. **6:** 313–316, 1983.
79. DRAPEAU, P., AND BLAUSTEIN, M. P.: Initial release of [^{3}H]dopamine from rat striatal synaptosomes:correlation with calcium entry. J. Neurosci. **3:** 703–713, 1983.
80. ECCLES, J. C.: Understanding the Brain. McGraw-Hill, New York, 1973.
81. EDWARDS, F. R., HIRST, G. D. S., AND SILINSKY, E. M.: Interaction between inhibitory and excitatory synaptic potentials at a peripheral neuron. J. Physiol. (Lond.) **259:** 647–663, 1976.
82. EISENMANN, G.: Cation selective glass electrodes and their mode of operation. Biophys. J. **2:** 259–323, 1962.
83. ELMQVIST, D., AND FELDMAN, D. S.: Calcium dependence of spontaneous acetylcholine release at mammalian motor nerve terminals. J. Physiol. (Lond.) **181:** 487–497, 1965.
84. ELMQVIST, D., AND QUASTEL, D. M. J.: A quantitative study of end-plate potentials in isolated human muscle. J. Physiol. (Lond.) **178:** 505–529, 1965.
85. ELUL, R.: Fixed charges in the cell membrane. J. Physiol. (Lond.) **189:** 351–366, 1967.
86. ERULKAR, S. D.: The modulation of neurotransmitter release at synaptic junctions. Rev. Physiol. Biochem. Pharmacol. **98:** 64–175, 1983.
87. FATT, P., AND KATZ, B.: An analysis of the end-plate potential recorded with an intracellular electrode. J. Physiol. (Lond.) **115:** 320–370, 1951.
88. FATT, P., AND KATZ, B.: Spontaneous subthreshold activity at motor nerve endings. J. Physiol. (Lond.) **117:** 109–128, 1952.
89. FURCHGOTT, R. F.: The use of beta-haloalkylamines in the differentiation of receptors and in the determinations of dissociation constants of receptor-agonist complexes. Adv. Drug Res. **3:** 21–55, 1975.
90. FURCHGOTT, R. F., AND BURSZTYN, P.: Comparison of dissociation constants and of relative efficacies of selected agonists acting on parasympathetic receptors. Ann. N.Y. Acad. Sci. **144:** 882–898, 1968.
91. GADDUM, J. H.: The action of adrenalin and ergotamine on the uterus of the rabbit. J. Physiol. (Lond.) **61:** 141–150, 1926.
92. GAGE, P. W., AND HUBBARD, J. I.: Evidence for a Poisson distribution of miniature end-plate potentials and some implications. Nature (Lond.) **208:** 395–396, 1965.
93. GAGE, P. W., AND HUBBARD, J. I.: An investigation of the post-tetanic potentiation of the end-plate potentials at a mammalian neuromuscular junction. J. Physiol. (Lond.) **184:** 353–375, 1966.
94. GILLARD, R. D.: The simple chemistry of calcium and its relevance to biological systems. *In* Calcium and Cellular Function, ed. by A. W. CUTHBERT, pp. 3–9, Macmillan, London, 1970.
95. GINSBORG, B. L.: The vesicle hypothesis for the release of acetylcholine. *In* Excitatory Synaptic Mechanisms. Proceedings of the Fifth International Meeting of Neurobiologists, pp. 77–82, University of Oslo Press, Oslo, 1970.
96. GINSBORG, B. L., AND HAMILTON, J. T.: The effect of caesium ions on neuromuscular transmission in the frog. Quart. J. Exp. Physiol. **53:** 162–169, 1968.
97. GINSBORG, B. L., AND HIRST, G. D. S.: The effect of adenosine on the release of the transmitter from the phrenic nerve of the rat. J. Physiol. (Lond.) **224:** 629–645, 1972.
98. GINSBORG, B. L., AND JENKINSON, D. H.: Transmission of impulses from nerve to muscle. *In* Neuromuscular Junction, Handbook of Experimental Pharmacology, ed. by E. Zaimis, pp. 229–364, Springer Verlag, New York, 1976.
99. GINSBORG, B. L., AND STEPHENSON, R. P.: On the simultaneous action of two competitive antagonists. Br. J. Pharmacol. **51:** 287–300, 1974.
100. GINSBURG, S., AND RAHAMIMOFF, R.: Is extracellular calcium buffering involved in the regulation of transmitter release at the neuromuscular junction? Nature (Lond.) **306:** 62–64, 1983.
101. GLAGOLEVA, I. M., LIBERMAN, E. A., AND KHASHAEV, Z. KH-M.: Effect of uncouplers of oxidative phosphorylation on output of acetylcholine from nerve endings. Biofizika **15:** 76–83, 1970.
102. GOUY, M.: Sur la constitution de la charge électrique à la surface d'un électrolyte. Compt. Rend. **149:** 654–657, 1909.
103. GRAHAME, D. S.: The electrical double layer and the theory of electrocapillarity. Chem. Rev. **41:** 441–501, 1947.
104. GRINNELL, A. D., AND HERRERA, A. A.: Physiological regulation of synaptic effectiveness at frog neuromuscular junctions. J. Physiol. (Lond.) **307:** 301–317, 1980.
105. HAGIWARA, S., AND BYERLY, L.: The calcium channel. Trends Neurosci. **6:** 189–193, 1983.
106. HAGIWARA, S., FUKUDA, J., AND EATON, D. C.: Membrane currents carried by Ca, Sr and Ba in barnacle muscle fibre during voltage clamp. J. Gen. Physiol. **63:** 564–578, 1974.
107. HALL, J. E., AND SIMON, S. A.: A simple model for calcium-induced exocytosis. Biochim. Biophys. Acta **436:** 613–616, 1976.
107a. HESS, P., AND TSIEN, R. W.: Mechanism of ion permeation through calcium channels. Nature (Lond.) **309:** 453–456, 1984.
107b. HEUSER, J. E.: Synaptic vesicle exocytosis revealed in quick-frozen frog neuromuscular junctions treated with 4-aminopyridine and given a single electrical shock. *In* Approaches to the Cell Biology of Neurons, ed. by W. M. COWAN, and J. A. FERRENDELLI, pp. 215–239, Society for Neuroscience Symposium 2, 1977.
108. HEUSER, J. E., AND MILEDI, R.: Effect of lanthanum on function and structure of frog neuromuscular junctions. Proc. R. Soc. Lond. B Biol. Sci. **179:** 247–260, 1971.
109. HEUSER, J. E., REESE, T. S., JAN, Y., JAN, L., AND EVANS, L.: Synaptic vesicle exocytosis captured by quick freezing and correlated with quantal transmitter release. J. Cell. Biol. **81:** 275–300, 1979.
110. HILL, A. V.: The mode of action of nicotine and curari, determined by the form of the contraction curve and the method of temperature coefficients. J. Physiol. (Lond.) **39:** 361–373, 1909.
111. HILLE, B., WOODHULL, A. M., AND SHAPIRO, B.: Negative surface charge near sodium channels of nerve: Divalent ions, monovalent ions, and pH. Phil. Trans. R. Soc. B **270:** 301–318, 1975.
111a. HIRATA, F., AND AXELROD, J.: Phospholipid methylation and biological signal transduction. Science (Wash. DC). **209:** 1082–1090, 1980.
112. HOUSE, C. R.: Water Transport in Cells and Tissues, 562 pp., Williams & Wilkins, Baltimore, 1974.
113. HUBBARD, J. I.: Repetitive stimulation at the neuromuscular junction and the mobilization of transmitter. J. Physiol. (Lond.) **169:** 145–165, 1963.
114. HUBBARD, J. I.: Microphysiology of vertebrate neuromuscular transmission. Physiol. Rev. **53:** 674–723, 1973.
115. HUBBARD, J. I., AND JONES, S. F.: Spontaneous quantal transmitter release: A statistical analysis and some implications. J. Physiol. (Lond.) **232:** 1–21, 1973.
116. HUBBARD, J. I., JONES. S. F., AND LANDAU, E. M.: On the mechanism by which calcium and magnesium affect the spontaneous release of transmitter from mammalian motor nerve terminals. J. Physiol. (Lond.) **194:** 355–380, 1968.
117. HUBBARD, J. I., JONES, S. F., AND LANDAU, E. M.: On the mechanism by which calcium and magnesium affect the release of transmitter by nerve impulses. J. Physiol. (Lond.) **196:** 75–86, 1968.
117a. HUBBARD, J. I., AND WILLIS, W. D.: The effects of depolarization of motor nerve terminals upon the release of transmitter by nerve impulses. J. Physiol. (Lond.) **194:** 381–405, 1968.
118. HURLBUT, W. P., LONGNECKER, H. B., AND MAURO, A.: Effects of calcium and magnesium on the frequency of miniature end-plate potentials during prolonged tetanization. J. Physiol. (Lond.) **219:** 17–38, 1971.
119. JACK, J. J. B., NOBLE, D., AND TSIEN, R. W.: Electric Current Flow in Excitable Cells, pp. 502, Clarendon Press, Oxford, 1975.
120. JENKINSON, D. G.: The nature of the antagonism between calcium and magnesium ions at the neuromuscular junction. J. Physiol. (Lond.) **138:** 434–444, 1957.
121. KARLIN, A.: On the application of a plausible model of allosteric proteins to the receptor for acetylcholine. J. Theor. Biol. **16:** 306–320, 1976.
122. KATZ, B.: The Release of Neural Transmitter Substances. The Sherrington

Lectures X. Liverpool University Press, Liverpool, U.K. 1969.
123. KATZ, B., AND MILEDI, R.: The measurement of synaptic delay, and the time course of acetylcholine release at the neuromuscular junction. Proc. R. Soc. Lond. B Biol. Sci. **161:** 483–495, 1965.
124. KATZ, B., AND MILEDI, R.: The effects of calcium on acetylcholine release from motor nerve terminals. Proc. R. Soc. Lond. B Biol. Sci. **161:** 496–503, 1965.
125. KATZ, B., AND MILDEI, R.: The timing of calcium action during neuromuscular transmission. J. Physiol. (Lond.) **189:** 535–544, 1967.
126. KATZ, B., AND MILEDI, R.: The role of calcium in neuromuscular facilitation. J. Physiol. (Lond.) **195:** 481–492, 1968.
127. KATZ, B., AND MILEDI, R.: Spontaneous and evoked activity of motor nerve endings in calcium Ringer. J. Physiol. (Lond.) **203:** 689–706, 1969.
128. KATZ, B., AND MILEDI, R.: Does the motor nerve impulse evoke "nonquantal" transmitter release? Proc. R. Soc. Lond. B Biol. Sci. **212:** 131–137, 1981.
129. KELLY, J. S.: Antagonism between Na^+ and Ca^{2+} at the neuromuscular junction. Nature (Lond.) **205:** 296–297, 1965.
130. KELLY, J. S.: The antagonism of Ca^{2+} and Na^+ and other monovalent ions at the frog neuromuscular junction. Quart. J. Exp. Physiol. **53:** 239–249, 1968.
131. KELLY, R. B., DEUTSCH, J. W, CARLSON, S. S., AND WAGNER, J. A.: Biochemistry of neurotransmitter release. Annu. Rev. Neuroci. **2:** 399–446, 1979.
132. KELLY, S. S., AND ROBBINS, N.: Bimodal miniature and evoked end-plate potentials in adult mouse neuromuscular junctions. J. Physiol. (Lond.) **346:** 353–363, 1984.
133. KHARASCH, E. D., MELLOW, A. M., AND SILINSKY, E. M.: Intracellular magnesium does not antagonize calcium-dependent acetylcholine secretion. J. Physiol. (Lond.) **314:** 255–263, 1981.
134. KITA, H., AND VAN DER KLOOT, W.: Effects of the ionophore X-537A on acetylcholine release at the frog neuromuscular junction. J. Physiol. (Lond.) **259:** 177–198, 1976.
135. KITA, H., AND VAN DER KLOOT, W.: Time course and magnitude effects of changes in tonicity on acetylcholine release at frog neuromuscular junction. J. Neurophysiol. **40:** 212–224, 1977.
136. KLEE, C. B., CROUCH, T. H., AND RICHMAN, P. G.: Calmodulin. Annu. Rev. Biochem. **49:** 489–515, 1980.
137. KLOTZ, I. M.: Water: its fitness as a molecular environment. *In* Membranes and Ion Transport, ed. by E. E. BITTAR, vol 1, pp. 93–122, Wiley-Interscience, New York, 1970.
138. KLOTZ, I. M.: Ligand-receptor interactions: What we can and cannot learn from binding measurements. Trends. Pharmcol. Sci. **4:** 253–255, 1983.
138a. KOENIG H., GOLDSTONE, A., AND LU, C. Y.: Polyamines regulate calcium fluxes in a rapid plasma membrane response. Nature (Lond.) **305:** 530–534, 1983.
139. KOSHLAND, D. E. JR., NEMETHY, G., AND FILMER, D.: Comparison of experimental binding data and theoretical models in proteins containing subunits. Biochemistry **5:** 365–385, 1966.
140. KRIEBEL, M. E., LLADOS, F., AND MATTESON, D. R.: Histograms of the unitary evoked potential of the mouse diaphragm show multiple peaks. J. Physiol. (Lond.) **322:** 211–222, 1982.
141. LANDAU, E. M., AND NACHSHEN, D. A.: The interaction of pH and divalent cations at the neuromuscular junction. J. Physiol. (Lond.) **251:** 775–790, 1975.
142. LANDAU, E. M., SMOLINSKY, A., AND LASS, Y.: Post-tetanic potentiation and facilitation do not share a common calcium-dependent mechanism. Nature, New Biol. **244:** 155–157.
142a. LANG, B., NEWSOM-DAVIS, J., PRIOR, C., AND WRAY, D.: Effect of passively transferred Lambert-Eaton myasthenic syndrome antibodies on the calcium sensitivity of transmitter release in the mouse. J. Physiol. (Lond.) **357:** 28P, 1984.
143. LANGMUIR, I.: The absorption of gases on plane surfaces of glass, mica and platinum. J. Am. Chem. Soc. **40:** 1361–1403, 1918.
144. LASKOWSKI, M. B., AND THIES, R.: Interactions between calcium and barium on the spontaneous release of transmitter from mammalian motor nerve terminals. Int. J. Neuroci. **4:** 11–16, 1972.
145. LILEY, A. W.: The quantal components of the mammalian end-plate potential. J. Physiol. (Lond.) **133:** 571–587, 1956.
146. LINEWEAVER, H., AND BURK, D.: The determination of enzyme dissociation constants. J. Am. Chem. Soc. **56:** 658–666, 1934.
147. LLINAS, R. R.: Calcium in synaptic transmission. Sci. Am. **247:** 56–65, 1982.
148. LLINAS, R. R., STEINBERG, I. Z., AND WALTON, K.: Relationship between presynaptic calcium current and postsynaptic potential in squid giant synapse. Biophys. J. **33:** 323–351, 1981.
149. LONDOS, C., AND WOLFF, J.: Two distinct adenosine-sensitive sites on adenylate cyclase. Proc. Natl. Acad. Sci. **74:** 5282–5284, 1977.
150. LONGNECKER, H. E. JR., HURLBUT, W. P., MAURO, A., AND CLARK, A. W.: Effects of black widow spider venom on the frog neuromuscular junction. Nature (Lond.) **225:** 701–703, 1970.
151. MADDEN, K. S., AND VAN DER KLOOT, W.: Surface charges and the effects of calcium on the frequency of miniature end-plate potentials at the frog neuromuscular junction. J. Physiol. (Lond.) **276:** 227–232, 1978.
152. MAGLEBY, K. L.: The effect of repetitive stimulation on facilitation of transmitter release at the frog neuromuscular junction. J. Physiol. (Lond.) **234:** 327–352, 1973.
153. MAGLEBY, K. L.: The effect of tetanic and post-tetanic potentiation on facilitation of transmitter release at the frog neuromuscular junction. J. Physiol. (Lond.) **234:** 352–371, 1973.
154. MAGLEBY, K. L., AND ZENGEL, J. E.: A dual effect of repetitive stimulation on post-tetanic potentiation of transmitter release at the frog neuromuscular junction. J. Physiol. (Lond.) **245:** 163–182, 1975.
155. MAGLEBY, K. L., AND ZENGEL, J. E.: A quantitative description of tetanic and post-tetanic potentiation of transmitter release at the frog neuromuscular junction. J. Physiol. (Lond.) **245:** 183–208, 1975.
156. MAGLEBY, K. L., AND ZENGEL, J. E.: Augmentation: a process that acts to increase transmitter release at the frog neuromuscular junction. J. Physiol. (Lond.) **257:** 449–470, 1976.
157. MAGLEBY, K. L., AND ZENGEL, J. E.: Long term changes in augmentation, potentiation, and depression of transmitter release as a function of repeated synaptic activity at the frog neuromuscular junction. J. Physiol. (Lond.) **257:** 471–494, 1976.
158. MAGLEBY, K. L., AND ZENGEL, J. E.: Stimulation-induced factors which affect augmentation and potentiation of transmitter release at the neuromuscular junction. J. Physiol. (Lond.) **260:** 687–717, 1976.
159. MAGLEBY, K. L., AND ZENGEL, J. E.: A quantitative description of stimulation-induced changes in transmitter release at the frog neuromuscular junction. J. Gen. Physiol. **80:** 613–638, 1982.
160. MALLART, A.: Presynaptic currents in frog motor endings. Pflügers Arch. Eur. J. Physiol. **400:** 8–13, 1984.
161. MALLART, A., AND MARTIN, A. R.: An analysis of facilitation of transmitter release at the neuromuscular junction of the frog. J. Physiol. (Lond.) **193:** 679–694, 1967.
162. MALLART, A., AND MARTIN, A. R.: The relation between quantum content and facilitation at the neuromuscular junction of the frog. J. Physiol. (Lond.) **196:** 593–604, 1968.
163. MANALIS, R. S., AND COOPER, G. P.: Presynaptic and postsynaptic effects of lead at the frog neuromuscular junction. Nature (Lond.) **243:** 354–355, 1973.
164. MANALIS, R. S., AND COOPER, G. P.: Evoked transmitter release is increased by inorganic mercury at the frog neuromuscular junction. Nature (Lond.) **257:** 690–691, 1975.
165. MARTIN, A. R.: A further study of the statistical composition of the end-plate potential. J. Physiol. (Lond.) **130:** 114–122, 1955.
166. MARTIN, A. R.: Quantal nature of synaptic transmission. Physiol. Rev. **46:** 51–66, 1966.
167. MARTIN, A. R.: Junctional transmission. II. Presynaptic mechanisms. *In* Handbook of Physiology, vol. 1, Section 1, The Nervous System, ed. by E. R. KANDEL, pp. 329–355, American Physiological Society, Bethesda, MD, 1977.
168. MARTIN, A. R., AND PILAR, G.: Quantal components of the synaptic potential in the ciliary ganglion of the chick. J. Physiol. (Lond.) **175:** 1–16, 1964.
169. MATTHEWS, G., AND WICKELGREN, W. O.: On the effect of calcium on the frequency of miniature end-plate potentials at the frog neuromuscular junction. J. Physiol. (Lond.) **266:** 91–101, 1977.
170. MCLACHLAN, E. M.: The effects of strontium and barium ions at synapses in sympathetic ganglia. J. Physiol. (Lond.) **267:** 497–518, 1977.
171. MCLACHLAN, E. M.: The statistics of transmitter release at chemical synapses. Int. Rev. Physiol. **17:** 49–117, 1978.
172. MCLACHLAN, E. M., AND MARTIN, A. R.: Non-linear summation of end-plate potentials in the frog and mouse. J. Physiol. (Lond.) **311:** 307–324, 1981.
173. MCLAUGHLIN, S., AND EISENBERG, M.: Antibiotics and membrane biology. Annu. Rev. Biophys. Bioeng. **4:** 335–366, 1975.
174. MEIRI, H., ERULKAR, S. D., LERMAN, T., AND RAHAMIMOFF, R.: The action of the sodium ionophore, monensin, on transmitter release at the frog neuromuscular junction. Brain Res. **204:** 204–208, 1981.
175. MEIRI, U., AND RAHAMIMOFF, R.: Activation of transmitter release by strontium and calcium ions at the neuromuscular junction. J. Physiol. (Lond.) **215:** 709–726, 1971.
176. MEIRI, U., AND RAHAMIMOFF, R.: Neuromuscular transmission: Inhibition by manganese ions. Science **176:** 308–309, 1972.
177. MELLOW, A. M.: Equivalence of Ca^{2+} and Sr^{2+} in transmitter release in K^+-depolarised nerve terminals. Nature (Lond.) **282:** 84–85, 1979.
178. MELLOW, A. M., PERRY, B. D., AND SILINSKY, E. M.: Effects of calcium and strontium in the process of acetylcholine release from motor nerve endings. J. Physiol. (Lond.) **328:** 547–562, 1982.
179. MELLOW, A. M., PHILLIPS, T. E., AND SILINSKY, E. M.: On the conductance pathway traversed by strontium in mediating the asynchronous release of acetylcholine by motor nerve impulses. Br. J. Pharmacol. **63:** 229–232, 1978.
180. MEUNIER, F. M., ISRAEL, M., AND LESBATS, B.: Release of ATP from stimulated nerve-electroplaque junctions. Nature (Lond.) **257:** 407–408, 1975.
181. MILEDI, R.: Strontium as a substitute for calcium in the process of transmitter release at the neuromuscular junction. Nature (Lond.) **212:** 1233–1234, 1966.
182. MILEDI, R.: Lanthanum abolishes the "calcium response" of nerve terminals. Nature (Lond.) **229:** 410–411, 1971.
183. MILEDI, R., AND THIES, R.: Tetanic and post-tetanic rise in frequency of miniature end-plate potentials in low calcium solutions. J. Physiol. (Lond.) **212:** 245–257, 1971.

184. MISLER, S., AND HURLBUT, W. P.: Tests of an electrostatic screening hypothesis of the inhibition of neurotransmitter release by cations at the frog neuromuscular junction. Biophys. J. **31:** 9–30, 1980.
185. MISLER, S., AND HURLBUT, W. P.: Post-tetanic potentiation of acetylcholine release at the frog neuromuscular junction develops after stimulation in Ca^{2+}-free solutions. Proc. Natl. Acad. Sci. **80:** 315–319, 1983.
186. MIYAMOTO, M. D.: Binomial analysis of quantal transmitter release at glycerol treated frog neuromuscular junctions. J. Physiol. (Lond.) **250:** 121–142, 1975.
187. MIYAMOTO, M. D.: Estimates on magnitude of non-linear summation of evoked potentials at motor end plate. J. Neurophysiol. **41:** 589–599, 1978.
188. MIYAMOTO, M. D.: Hg^{2+} causes neurotoxicity at an intracellular site following entry through Na and Ca channels. Brain Res. **267:** 375–379, 1983.
189. MONOD, J., WYMAN, J., AND CHANGEUX, J. P.: On the nature of allosteric transitions: a plausible model. J. Mol. Biol. **12:** 88–118, 1965.
189a. MORRIS, S. J.: The structure and stoichiometry of electric ray synaptic vesicles. Neuroscience **5:** 1509–1516, 1980.
190. MULLER, R. V., AND FINKELSTEIN, A.: The electrostatic basis of Mg^{2+} inhibition of transmitter release. Proc. Natl. Acad. Sci. **71:** 923–926, 1974.
191. NACHSHEN, D. A., AND BLAUSTEIN, M. P.: Some properties of potassium-stimulated calcium influx in presynaptic nerve endings. J. Gen. Physiol. **76:** 709–728, 1980.
192. NACHSHEN, D. A., AND DRAPEAU, P.: A buffering model for calcium-dependent neurotransmitter release. Biophys. J. **38:** 205–208, 1982.
193. NESTLER, E. J., AND GREENGARD, P.: Protein phosphorylation in the brain. Nature (Lond.) **305:** 583–588, 1983.
194. NICKERSON, M.: Receptor occupancy and tissue response. Nature (Lond.) **178:** 697–698, 1956.
195. NILES, W. D., AND SMITH, D. O.: Effects of hypertonic solutions on quantal transmitter release at the crayfish neuromuscular junction. J. Physiol. (Lond.) **329:** 185–202, 1982.
195a. NISHIZUKA, Y.: Turnover of inositol phospholipids and signal transduction. Science **225:** 1365–1370, 1984.
196. ONODERA, K., AND YAMAKAWA, K.: The effects of lithium on the neuromuscular junction of the frog. Jpn. J. Physiol. **16:** 541–550, 1966.
197. OTSUKA, M., ENDO, M., AND NONAMURA, Y.: Presynaptic nature of neuromuscular depression. Jpn. J. Physiol. **12:** 573–584, 1962.
198. PARNAS, H., AND SEGEL, L. A.: A theoretical explanation for some effects of calcium on the facilitation of neurotransmitter release. J. Theor. Biol. **84:** 3–29, 1980.
199. PARNAS, H., AND SEGEL, L. A.: A theoretical study of calcium entry in nerve terminals, with application to neurotransmitter release. J. Theor. Biol. **91:** 125–169, 1981.
200. PARNAS, H., AND SEGEL, L. A.: Exhaustion of calcium does not terminate evoked neurotransmitter release. J. Theor. Biol. **107:** 345–365, 1984.
201. PARSEGIAN, V. A.: Considerations in determining the mode of influence of calcium on vesicle-membrane interactions. *In* Approaches to the Cell Biology of Neurons, ed. by W. M. COWAN, and J. A. FERRENDELLI, pp. 161–171, Society for Neurosciences Symposium 2, 1977.
202. PARSONS, R. L., HOFMAN, W. W., AND FEIGEN, G. A.: Presynaptic effects of potassium ion on the mammalian neuromuscular junction. Nature (Lond.) **208:** 590–591, 1965.
202a. PARSONS, S. M., CARPENTER, R. S., KOENIGSBERGER, R., AND ROTHLEIN, J. E.: Transport in the cholinergic vesicle. Fed. Proc. **41:** 2765–2768, 1982.
203. PATON, D. M.: Evidence for A_1 receptors for adenosine in heart and in adrenergic and cholinergic nerves. *In* Physiology and Pharmacology of Adenosine Derivatives, pp. 113–118, ed. by J. W. DALY, Y. KURODA, P. H. SHIMIZU, and M. UI. Raven Press, New York, 1982.
204. PAULING, L.: The oxygen equilibrium of hemoglobin and its structural interpretation. Proc. Natl. Acad. Sci. **21:** 186–191, 1935.
205. PEPER, K., BRADLEY, R. J., AND DREYER, F.: The acetylcholine receptor at the neuromuscular junction. Physiol. Rev. **62:** 1271–1340, 1982.
206. PHILLIPS, T. E., AND BOYNE, A. F.: Liquid nitrogen-based quick freezing: Experiences with bounce-free delivery of cholinergic nerve terminals to a metal surface. J. Elec. Mic. Tech. **1:** 9–29, 1984.
207. PUBLICOVER, S. J.: Inhibitory effect of the "calmodulin inhibitor" trifluoperazine on stimulated transmitter release at the frog neuromuscular junction. J. Physiol. (Lond.) **338:** 3P–4P, 1983.
208. QUASTEL, D. M. J.: Excitation-secretion coupling at the mammalian neuromuscular junction. *In* Synaptic Transmission and Neuronal Interaction, ed. by M. V. L. BENNETT, pp. 23–43, Raven Press, New York, 1974.
209. QUASTEL, D. M. J., HACKETT, J. T., AND COOKE, J. D.: Calcium: Is it required for transmitter secretion? Science **172:** 1034–1036, 1971.
210. QUILLIAM, J. P., AND TAMARIND, D. L.: Some effects of preganglionic nerve stimulation on synaptic vesicle populations in rat superior cervical ganglion. J. Physiol. (Lond.) **235:** 317–331, 1973.
211. RAHAMIMOFF, R.: A dual effect of calcium ions on neuromuscular facilitation. J. Physiol. (Lond.) **195:** 471–480, 1968.
212. RAHAMIMOFF, R., LEV-TOV, A., AND MEIRI, H.: Primary and secondary regulation of quantal transmitter release: Calcium and sodium. J. Exp. Biol. **89:** 5–18, 1980.
213. RAHAMIMOFF, R., MEIRI, H., ERULKAR, S. D., AND BARENHOLZ, Y.: Changes in transmitter release induced by ion-containing liposomes. Proc. Natl. Acad. Sci. **75:** 5214–5216, 1978.
214. RAHAMIMOFF, R., AND YAARI, Y.: Delayed release of transmitter at the frog neuromuscular junction. J. Physiol. (Lond.) **228:** 241–257, 1973.
215. RAND, R. P.: Interacting phospholipid bilayers: measured forces and induced structural changes. Annu. Rev. Biophys. Bioeng. **10:** 277–314, 1981.
216. RASGADO-FLORES, H., NACHSHEN, D. A., AND BLAUSTEIN, M. P.: ATP-dependent uptake of Ca, Sr, Ba and Mn by intracellular organelles in synaptosomes. Proc. Soc. Neurosci. Abstr. **8:** 833, 1982.
217. REICHARDT, L. F., AND KELLY, R. B.: A molecular description of nerve terminal function. Annu. Rev. Biochem. **52:** 871–926, 1983.
218. REMLER, M. P.: A semiquantitative theory of synaptic vesicle movements. Biophys. J. **13:** 104–117, 1973.
219. RIBEIRO, J. A.: Purinergic modulation of transmitter release. J. Theor. Biol. **80:** 259–270, 1979.
220. RIBEIRO, J. A., AND WALKER, J.: The effects of adenosine triphosphate and adenosine diphosphate on transmission at the rat and frog neuromuscular junctions. Br. J. Pharmacol. **54:** 312–218, 1975.
221. ROSENTHAL, J.: Post-tetanic potentiation at the neuromuscular junction of the frog. J. Physiol. (Lond.) **203:** 121–133, 1969.
222. ROSSEINSKY, D. R.: Electrode potentials and hydration energies. Theories and correlations. Chem. Rev. **65:** 467–490, 1965.
223. ROTSHENKER, S., ERULKAR, S. D., AND RAHAMIMOFF, R.: Reduction in the frequency of miniature end-plate potentials by nerve stimulation in low calcium solutions. Brain Res. **101:** 362–365, 1976.
224. ROTSHENKER, S., AND RAHAMIMOFF, R.: Neuromuscular synapse: Stochastic properties of spontaneous release of transmitter. Science **170:** 648–649, 1970.
225. RUBIN, R. P.: Calcium and the Secretory Process, pp. 189, Plenum Press, New York, 1974.
226. RUBIN, R. P., WEISS, G. B., AND PUTNEY, J. W. JR.: Calcium in Biological Systems, Plenum Publishing Corp., New York, 1985.
227. SANCHEZ, ARMASS, S., NACHSHEN, D. A., AND BLAUSTEIN, M. P.: Efflux of Ca, Sr, Ba and Mn from nerve terminals. Proc. Soc. Neurosci. Abstr. **8:** 834, 1982.
228. SATOH, E., ASAI, F., ITOH, K., NISHIMURA, M., AND URAKAWA, N.: Mechanism of cadmium-induced blockade of neuromuscular transmission. Eur. J. Pharmacol. **77:** 251–257, 1982.
229. SCHILD, H. O.: pA, a new scale for the measurement of drug antagonism. Br. J. Pharmacol. **2:** 186–206, 1947.
230. SCHLESSINGER, J.: Mobilities of cell-membrane proteins: How are they modulated by the cytoskeleton? Trends Neurosci. **6:** 360–363, 1983.
231. SCHULMAN, H.: Calcium-dependent protein phosphorylation. *In* Cyclic Nucleotides I, Handbook of Experimental Pharmacology, ed. by J. A. NATHANSON, and J. W. KEBABIAN, pp. 425–478, Springer Verlag, Berlin, 1982.
232. SCHWEITZER, E. S., AND KELLY, R. B.: ATP release from cholinergic synapses. Proc. Soc. Neurosci. **8:** 493, 1982.
233. SEGEL, I. H.: Enzyme Kinetics, pp. 957, Wiley, New York, 1975.
234. SILINSKY, E. M.: On the association between transmitter secretion and the release of adenine nucleotides from mammalian motor nerve terminals. J. Physiol. (Lond.) **247:** 145–162, 1975.
235. SILINSKY, E. M.: Can barium support the release of acetylcholine by nerve impulses? Br. J. Pharmacol. **59:** 215–217, 1977.
236. SILINSKY, E. M.: An estimate of the equilibrium dissociation constant for calcium as an *antagonist* of evoked acetylcholine release: Implications for excitation-secretion coupling. Br. J. Pharmacol. **61:** 691–693, 1977.
237. SILINSKY, E. M.: On the role of barium in supporting the asynchronous release of acetylcholine quanta by motor nerve impulses. J. Physiol. (Lond.) **274:** 157–171, 1978.
238. SILINSKY, E. M.: Enhancement by an antagonist of transmitter release from frog motor nerve terminals. Br. J. Pharmacol. **63:** 485–493, 1978.
239. SILINSKY, E. M.: Evidence for specific adenosine receptors at cholinergic nerve endings. Br. J. Pharmacol. **71:** 191–194, 1980.
240. SILINSKY, E. M.: On the calcium receptor that mediates depolarization-secretion coupling at cholinergic motor nerve terminals. Br. J. Pharmacol. **73:** 413–429, 1981.
241. SILINSKY, E. M.: Properties of calcium receptors that initiate depolarization-secretion coupling. Fed Proc. **41:** 2172–2180, 1982.
242. SILINSKY, E. M.: To an adenosine moiety. Trends Pharmacol. Sci. **4:** 494, 1983.
243. SILINSKY, E. M.: On the mechanism by which adenosine receptor activation inhibits the release of acetylcholine from motor nerve endings. J. Physiol. (Lond.) **346:** 243–256, 1984.
244. SILINSKY, E. M.: Calcium and transmitter release: Modulation by adenosine derivatives. *In* Calcium in Biological Systems, ed. by R. P. RUBIN, G. B. WEISS, AND J. W. PUTNEY, JR., Chap. 13, pp. 109–119, Plenum Press, New York, 1985.
245. SILINSKY, E. M.: Processes by which purines inhibit transmitter release. *In* Purines: Pharmacological and Physiological Roles. ed. by T. W. STONE, Macmillan Press Ltd., London, in press, 1985.
245a. SILINSKY, E. M.: Inhibition of transmitter release by adenosine: Are calcium currents depressed or are the intracellular effects of calcium impaired? Trends Pharmacol. Sci. **6:** in press, 1985.
246. SILINSKY, E. M., AND GINSBORG, B. L.: Inhibition of acetylcholine release from preganglionic frog nerves by ATP but not adenosine. Nature (Lond.) **305:** 327–328, 1983.
247. SILINSKY, E. M., AND HUBBARD, J. I.: Release of ATP from rat motor nerve terminals. Nature (Lond.) **243:** 404–405, 1973.
248. SILINSKY, E. M., AND MELLOW, A. M.: The relationship between strontium and other divalent cations in the process of transmitter release from

cholinergic nerve endings. *In* Handbook of Stable Strontium, ed. by S. Skoryna, pp. 263–285, Plenum Press,New York, 1981.
249. SILINSKY, E. M., MELLOW, A. M., AND PHILLIPS, T. E.: Conventional calcium channel mediates asynchronous acetylcholine release by motor nerve impulses. Nature (Lond.) **270:** 528–530, 1977.
250. STATHAM, H. E., AND DUNCAN, C. J.: The action of ionophores at the frog neuromuscular junction. Life Sci. **17:** 1401–1406, 1975.
251. STEIN, R. B.: Nerve and Muscle: Membranes, Cells and Systems, pp. 265, Plenum Press, New York, 1980.
252. STEPHENSON, R. P.: A modification of receptor theory. Br. J. Pharmacol. **11:** 379–393, 1956.
253. STEPHENSON, R. P., AND BARLOW, R. B.: Concepts of drug action, quantitative pharmacology, and biological assay. *In* A Companion to Medical Studies, ed. by R. PASSMORE, and J. S. ROBSON, pp. 1–19, Blackwell, Oxford, 1970.
254. STEVENS, C. F.: The neuron. Sci. Am. **241:** 54–65, 1979.
255. STOCKBRIDGE, N., AND MOORE, J. W.: Dynamics of intracellular calcium and its possible relationship to phasic transmitter release and facilitation at the frog neuromuscular junction. J. Neurosci. **4:** 803–811, 1984.
256. STOCKBRIDGE, N., AND MOORE, J. W.: Calmodulin implicated in transmission at frog neuromuscular junction. Personal communication, J. W. Moore.
257. TAKEUCHI, A.: The long-lasting depression in neuromuscular transmission of frog. Jpn. J. Physiol. **8:** 102–113, 1958.
257a. TAUC, L.: Nonvesicular release of neurotransmitter. Physiol. Rev. **62:** 857–893, 1982.
258. TAYLOR, H. S.: A Treatise on Physical Chemistry, 2nd ed., pp. 1074, Macmillan, London, 1931.
259. THESLEFF, S., AND MOLGO, J.: A new type of transmitter release at the neuromuscular junction. Neuroscience **9:** 1–8, 1983.
260. THIES, R. E.: Neuromuscular depression and the apparent depletion of transmitter in mammalian muscle. J. Neurophysiol. **28:** 427–442, 1965.
261. THRON, C. D.: On the analysis of pharmacological experiments in terms of an allosteric receptor model. Mol. Pharmacol. **9:** 1–9, 1973.
262. VAN DER KLOOT, W., AND KITA, H.: The possible role of fixed membrane surface charges in acetylcholine release at the frog neuromuscular junction. J. Memb. Biol. **14:** 365–382, 1973.
263. VAN DER KLOOT, W., AND LATTA, R.: How elevated extracellular Ca^{2+} inhibits quantal acetylcholine release at frog neuromuscular junctions in high K^+. Pflügers Arch. Eur. J. Physiol. **397:** 85–89, 1983.
264. VAN ROSSUM, J. M.: Limitations of molecular pharmacology. Adv. Drug. Res. **3:** 189–234, 1966.
265. VYSKOCIL, F., NIKOLSKY, E., AND EDWARDS, C.: An analysis of the mechanisms underlying the non-quantal release of acetylcholine at the mouse neuromuscular junction. Neuroscience **9:** 429–436, 1983.
266. WAUD, D.: Pharmacological receptors. Pharmacol. Rev. **20:** 49–88, 1968.
267. WEAKLY, J. N.: The action of cobalt ions on neuromuscular transmission in the frog. J. Physiol. (Lond.) **234:** 597–612, 1973.
268. WEINREICH, D.: Ionic mechanisms of post-tetanic potentiation at the neuromuscular junction of the frog. J. Physiol. (Lond.) **212:** 431–446, 1971.
269. WEISS, G. B.: Cellular pharmacology of lanthanum. Annu. Rev. Pharmacol. **659:** 343–354, 1974.
270. WERMAN, R.: The number of receptors for calcium ions at nerve terminals of one endplate. Comp. Gen. Pharmacol. **2:** 129–137, 1971.
271. WERNIG, A.: Estimates of statistical release parameters from crayfish and frog neuromuscular junctions. J. Physiol. (Lond.) **244:** 207–221, 1975.
271a. WHITTAKER, V. P.: Biophysical and biochemical studies of isolated cholinergic vesicles from *Torpedo marmorata*. Fed. Proc. **41:** 2759–2764, 1982.
272. WHITTAKER, V. P., DOWDALL, M. J., AND BOYNE, A. F.: The storage and release of acetylcholine from cholinergic nerve terminals: Recent results with non-mammalian preparations. Biochem. Soc. Symp. **36:** 49–68, 1972.
273. WILLIAMS, R. J. P.: Calcium ions: Their ligands and their functions. Biochem. Soc. Symp. **39:** 133–138, 1974.
274. YOUNKIN, S. G.: An analysis of the role of calcium in facilitation at the frog neuromuscular junction. J. Physiol. (Lond.) **237:** 1–14, 1974.
275. ZENGEL, J. E., AND MAGLEBY, K. L.: Differential effects of Ba^{2+}, Sr^{2+}, and Ca^{2+} on stimulation-induced changes in transmitter release at the frog neuromuscular junction. J. Gen. Physiol. **76:** 175–211, 1980.
276. ZENGEL, J. E., AND MAGLEBY, K. L.: Changes in miniature endplate potential frequency during repetitive nerve stimulation in the presence of Ca^{2+}, Ba^{2+}, and Sr^{2+} at the frog neuromuscular junction. J. Gen. Physiol. **77:** 503–529, 1981.
277. ZENGEL, J. E., AND MAGLEBY, K. L.: Augmentation and facilitation of transmitter release. *A quantitative description at the frog neuromuscular junction.* J. Gen. Physiol. **80:** 583–611, 1982.
278. ZENGEL, J. E., MAGLEBY, K. L., HORN, J. P., MCAFEE, D. A., AND YAROWSKY, P. J.: Facilitation, augmentation, and potentiation of synaptic transmission at the superior cervical ganglion of the rabbit. J. Gen. Physiol. **76:** 213–231, 1980.
279. ZIMMERBERG, J., COHEN, F. S., AND FINKELSTEIN, A.: Fusion of phospholipid vesicles with planar phospholipid bilayer membranes. I. Discharge of vesicular contents across the planar membrane. J. Gen. Physiol. **75:** 241–250, 1980.
280. ZIMMERBERG, J., COHEN, F. S., AND FINKELSTEIN, A.: Micromolar Ca^{2+} stimulates fusion of lipid vesicles with planar bilayers containing a calcium-binding protein. Science **210:** 906–908, 1980.
281. ZIMMERMAN, N. H.: Vesicle recycling and transmitter release. Neuroscience **4:** 1773–1804, 1979.
282. ZUCKER, R. S.: Changes in the statistics of transmitter release during facilitation. J. Physiol. (Lond.) **229:** 787–810, 1973.